Title

Engineering chimeric antigen receptors to overcome the immunosuppressive solid tumor microenvironment

Author

Hou, Andrew J

Publication Date

2022

Peer reviewed|Thesis/dissertation

UNIVERSITY OF CALIFORNIA

Los Angeles

Engineering chimeric antigen receptors to overcome the immunosuppressive solid tumor microenvironment

A dissertation submitted in partial satisfaction of the

requirements for the degree Doctor of Philosophy

in Chemical and Biomolecular Engineering

by

Andrew J. Hou

2022

ABSTRACT OF THE DISSERTATION

Engineering chimeric antigen receptors to overcome the immunosuppressive solid tumor microenvironment

by

Andrew J. Hou

Doctor of Philosophy in Chemical and Biomolecular Engineering

University of California, Los Angeles, 2022

Professor Yvonne Y. Chen, Chair

Adoptive T-cell therapy is a cancer treatment strategy where T cells from a cancer patient are harvested, modified *ex vivo* to target tumor cells, and subsequently reinfused back into the patient's body. Although remarkably successful against blood-based B-cell malignancies, efficacy has been limited against solid tumors, in large part due to the immunosuppressive tumor microenvironment (TME). Among the many inhibitory factors in the TME, transforming growth factor-beta (TGF-β) plays a prominent role in suppressing anti-tumor immunity through both direct inhibition of T-cell cytotoxicity, as well as recruitment and polarization of immunosuppressive cell types such as myeloid-derived suppressor cells and regulatory T cells. We therefore hypothesized that T-cell function in the solid TME could be potentiated by pairing tumor-targeting CARs with TGF-β CARs that program T-cell activation, rather than inhibition, in the presence of TGF-β. We first verified that TGF-β CAR expression is neither counterproductive to cytotoxic T-cell function, nor does it pose a significant risk of toxicity. Pairing TGF-β CARs with tumor-specific TCRs or CARs did not significantly enhance therapeutic outcomes of adoptive T-cell transfer in preclinical models of melanoma and prostate cancer, warranting further engineering efforts. In models of

glioblastoma, however, single-chain bispecific CAR-T cells targeting TGF-β and tumor antigen were not only more resistant to tumor-mediated dysfunction, but also remodeled the immune-cell composition of the tumor microenvironment to potentiate anti-tumor immunity.

The dissertation of Andrew J. Hou is approved.

Roger S. Lo

Robert M. Prins

Yi Tang

Yvonne Y. Chen, Committee Chair

University of California, Los Angeles

2022

TABLE OF CONTENTS

LIST OF FIGURES

LIST OF SUPPLEMENTAL FIGURES AND TABLES

ACKNOWLEDGMENTS

First, I would like to thank my advisor, Dr. Yvonne Chen, for her consistent and unrelenting mentorship over the last six years. One of her favorite things to tell her students is to “squeeze the data,” and I think she takes the same approach to her mentorship, in the sense that she does everything in her power to maximize our potential. Most of the time, it’s not pleasant, but looking back it is amazing to see how much she has helped me grow. A lesser PI could not have transformed a clueless bioengineer into a routine mouse neurosurgeon (among other things), and the skills and confidence I have in myself as a scientist today are in large part thanks to her rigorous training; for that, I am truly grateful.

I would like to thank the members of my committee, Drs. Rob Prins, Roger Lo, and Yi Tang for their time, input, and feedback. Dr. Rob Prins has been instrumental in providing tools, resources, and know-how to facilitate the progress of my project; whether it be through transfer of Pmel-I mice for our studies in melanoma models, or helping us get started with our GBM research, much of my work was made possible with help and support from Dr. Prins and his lab.

I’ve had a great experience with the collaborative research environment here at UCLA. I thank the members of the UCLA Flow Cytometry Core: Zoran Galic, Miriam Guemes, Begonya Comin-Anduix for the technical assistance in our CyTOF studies, and Iris Williams and Min Zhou for their assistance with hours of cell sorting. I thank the staff of UCLA DLAM for their assistance with animal husbandry: especially Miguel Campos and Karla Pineda whose friendly faces in the early hours of the morning made the CHS 3V vivarium a slightly more cheerful place. Besides the Prins lab, the members of the Nathanson lab, particularly Chris Tse, have been a tremendous help to us when we first started our GBM research. The Ribas lab, our friendly neighbors in CHS South Tower, have been so helpful for us in sharing protocols, and sometimes reagents and consumables in times of shortage.

This thesis project was built upon a strong foundation laid by Dr. ZeNan Chang and Michael Lorenzini, who covered several different lines of investigation that saved me a lot of trouble. Mandy Shafer was a tremendous help in managing the multitude of mice that my studies involved. Dr. Benji Uy and Ryan Shih have been amazing teammates that helped carry me to the finish line, and I know the project is in good hands.

I am extremely grateful for all the members of the Chen lab, past and present. To be surrounded by such dedicated, intelligent, and considerate colleagues has been one of the saving graces amidst the grind of academic research, and I am lucky to call many of you my friends.

The previous graduate student alumni: Drs. ZeNan Chang, Eugenia Zah, Patrick Ho, Meng-yin Lin, and Ximin Chen were excellent mentors and role models to me in learning how to navigate the rigors of the Chen lab. Dr. Ximin Chen has been of particular help to me in providing wise and valuable insights as I start to plan out life after the Chen lab. The PhD students that I leave behind: Amy Hong, Justin Clubb, Tora Gao, and Ryan Shih have been great friends and labmates, and their curiosity, suggestions, and feedback have inspired me to do better science. I have no doubt each one will find success in their thesis projects and beyond. I am especially grateful to two of our lab's recent alumni, who have become my close friends. Brenda Ji, our honorary grad student, has carried the team on her back in so many ways, and life in the lab would be much more difficult if not for her kindness, patience, and dedication. Dr. Laurence Chen bore the burden of his PhD journey alongside mine. I don't think anyone else on this earth could relate to me as closely as Laurence did over the past six years, and I can't imagine life in the lab without his friendship and brotherhood.

Throughout these past six years, my wonderful friends and family have kept me sane and reminded me that there's more to life than mice and failed experiments. A big thanks goes to a man who straddles the line between friends and family. Just six months apart, I grew up with my cousin, Ben Fan, and along the way I also got to call him my best friend. He has been my most consistent, reliable friend through the years and the laughs we've shared, even in the midst of

adversity, have made life much more bearable. My sister Janice has, perhaps involuntarily, served as an example for me. I take after her in a lot of ways, and there is a lot of comfort in knowing that she has blazed the trail before me. Finally, I'd like to thank the strongest person that I know: my mom. She is my rock, and for all the times that I wanted to quit, she held me up unwaveringly. Your unconditional love and belief in me has carried me to where I am today, and no matter how high I climb, I will never stop looking up to you.

Chapter 1 includes excerpts and figures adapted from a published review: Hou, A.J., Chen, L.C., Chen, Y.Y. “Navigating CAR-T cells through the solid-tumor microenvironment” *Nature Reviews Drug Discovery* 2021; 20: 531-550. The published work was co-authored with Laurence Chen, who contributed equally to the writing of the review.

Chapter 2 includes excerpts from a published Open Access article: Hou, A.J., Chang, Z.L., *et al.* “TGF-β–responsive CAR-T cells promote anti-tumor immune function” *Bioengineering and Translational Medicine* 2018; 3: 75-86.

Data in chapter 4 have been incorporated into a manuscript (pending submission). Benjamin Uy and Ryan Shih are co-authors who contributed to data collection and analysis, and manuscript preparation.

VITA

Education

University of California, Los Angeles *08/2016 – Present*
- PhD candidate, Department of Chemical and Biomolecular Engineering
- Advisor: Yvonne Chen

California Institute of Technology *09/2012 – 06/2016*
- B.S. with Honors, Bioengineering; GPA 3.9

Research

Graduate Student Researcher *08/2016 – 06/2022*
University of California, Los Angeles, Los Angeles, CA
- PI: Yvonne Chen
- Engineering CAR-T cells to overcome the immunosuppressive tumor microenvironment

Research Intern *07/2019 – 09/2019*
A2 Biotherapeutics, Agoura Hills, CA
- Characterizing novel constructs for enhanced CAR-T–cell function

Undergraduate Researcher (Rose Hills SURF Scholar) *03/2015 – 06/2016*
California Institute of Technology, Pasadena, CA
- PI: Niles Pierce
- Engineering conditional CRISPR interference in *E. coli*

Undergraduate Researcher (Rose Hills SURF Scholar) *02/2014 – 11/2014*
California Institute of Technology, Pasadena, CA
- PI: Richard Murray
- Implementation of non-endogenous quorum sensing systems in *E. coli*
- Combinatorial promoter characterization in cell-free expression system
- Done as part of Caltech iGEM team

Publications and Presentations

† = co-first authors

Hou, A.J. and Chen, Y.Y. (2021). "Programming Novel Cancer Therapeutics: Design Principles for Chimeric Antigen Receptors" In Protein Engineering (eds H. Zhao, S.Y. Lee, J. Nielsen and G. Stephanopoulos). https://doi.org/10.1002/9783527815128.ch14

Chen, L.C.†, Hou, A.J.†, Chen, Y.Y. "Getting better mileage with logically primed CARs" *Med* 2021; 2: 785-787.

Hou, A.J.†, Chen, L.C.†, Chen, Y.Y. "Navigating CAR-T cells through the solid-tumor microenvironment" *Nature Reviews Drug Discovery* 2021; 20: 531-550.

Jayaramana, J., Mellody, M.P., Hou, A.J., *et al.* "CAR-T design: Elements and their synergistic function" *EBioMedicine* 2020; https://doi.org/10.1016/j.ebiom.2020.102931

Chang, Z.L.†, Hou, A.J.†, Chen, Y.Y. "Engineering primary T cells with chimeric antigen receptors for rewired responses to soluble ligands" *Nature Protocols* 2020; https://doi.org/10.1038/s41596-020-0294-8.

Hou, A.J.†, Chang, Z.L.†, *et al.* "TGF-β–responsive CAR-T cells promote anti-tumor immune function" *Bioengineering and Translational Medicine* 2018; 3: 75-86.

Hou, A.J. (September 2019). *Characterization of a transforming growth factor-β–responsive chimeric antigen receptor for anti-tumor immunity*. Oral Presentation, UCLA NIH Biotechnology Training in Biomedical Sciences and Engineering Annual Symposium, Los Angeles, CA.

Hou, A.J.†*, Chang, Z.L.†, *et al.* (March 2019). *Characterization of a transforming growth factor-β–responsive chimeric antigen receptor for anti-tumor immunity.* Poster, EBRC Spring Retreat, Boston, MA.

Hou, A.J. (August 2018). *Function of a TGF-β–responsive CAR in regulatory T cells*. Oral Presentation, UCLA NIH Biotechnology Training in Biomedical Sciences and Engineering Annual Symposium, Los Angeles, CA.

Honors and Awards

Graduate

- UCLA Dissertation Year Fellowship (January 2021 – January 2022)
- UCLA MIMG Schering Award (June 2020 – July 2021)
- UCLA NIH Biotechnology Training Grant (2017 – 2019)
- NSF Graduate Research Fellowship – Honorable Mention (2017)
- UCLA Graduate Dean's Scholar Award (2016)

Undergraduate

- Rose Hills Foundation Scholarship (2013 – 2016)
- Rose Hills Foundation Summer Undergraduate Research Fellowship (2014, 2015)
- iGEM Giant Jamboree: Bronze Medal (2014)
- Tau Beta Pi Engineering Honor Society (2015 – present)

Teaching

Teaching Assistant: ChE103 (Separation Processes) *04/2018 – 06/2018*
04/2019 – 06/2019

- Led discussion sections
- Wrote and graded homework problems

Chegg Textbook Solutions Author *03/2013 – 09/2013*

- Wrote step-by-step solution guides for textbook problems
- Authored solutions for *Intermediate Algebra* (Kaufmann) and *Practice of Statistics in the Life Sciences* (Baldi and Moore

CHAPTER 1. The challenge of combatting the solid tumor microenvironment with adoptive T-cell therapy

Adoptive T-cell therapy has demonstrated remarkable potential to treat advanced cancers. In this novel treatment paradigm, primary human T cells are genetically modified to express tumor-specific receptors — typically either a chimeric antigen receptor (CAR) or T-cell receptor (TCR) — which enable the engineered T cells to mount a tumor-specific immune response when infused into the patient.

CARs are synthetic receptors that are comprised of extracellular ligand-binding domains fused to intracellular co-stimulatory and activation domains (**Figure 1.1**). First-generation CARs

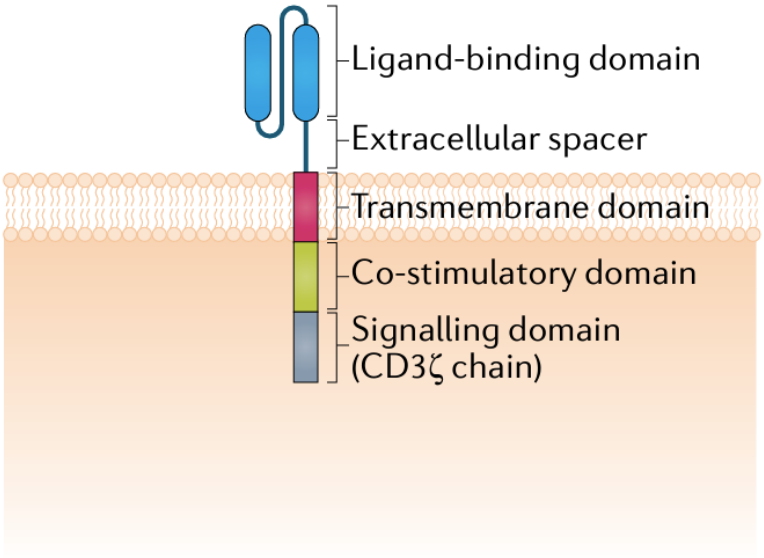

Figure 1.1 CARs are synthetic modular receptors with programmable antigen recognition. Chimeric antigen receptors (CARs) — from N terminus to C terminus — include a ligand- binding domain (typically an scFv), extracellular spacer, transmembrane domain and intracellular signalling domains consisting of one or two co- stimulatory domains (typically CD28 or 4-1BB) for second- and third- generation CARs, respectively, and an activation domain (typically CD3ζ). Target specificity can be programmed by incorporating different ligand- binding domains.

lack co-stimulatory signaling domains and have limited efficacy due to insufficient signaling strength and durability; thus, second-generation CARs and onwards incorporate one or more co-stimulatory domains to enhance and sustain T-cell activation signaling[1–4]. CARs can be built to

target a variety of tumor antigens due to their structural modularity, providing a readily adaptable platform for treatment of many types of cancers. In the case of CD19-targeting CAR-T cells — which was the first gene-therapy product to be approved by the U.S. Food and Drug Administration — patients with relapsed or refractory B-cell malignancies achieved complete remission rates of up to 90%[5]. Despite promising outcomes against hematological tumors, adoptive T-cell therapy has been much less effective against solid tumors, which comprise the vast majority of cancers. Compared to liquid tumors, solid tumors pose unique challenges. First, high antigen heterogeneity provides solid tumors with an effective mechanism of escape from CAR-T cells, which typically encode specificity towards a single antigen target and are thus unable to recognize all tumor cells. On the other hand, broadening T-cell specificity towards multiple antigens increases the risk of on-target, off-tumor toxicity. Second, solid tumors are often surrounded by physical barriers such as collagen-rich stroma that effectively prevent T-cell infiltration. In addition to physical barriers, T cells must also confront highly immunosuppressive tumor microenvironments (TME) whose cellular, molecular, and metabolic profiles ultimately lead to T-cell exhaustion and dysfunction (**Figure 1.2**). CAR-T cells so far have been inadequately equipped to surmount these additional obstacles posed by solid tumors.

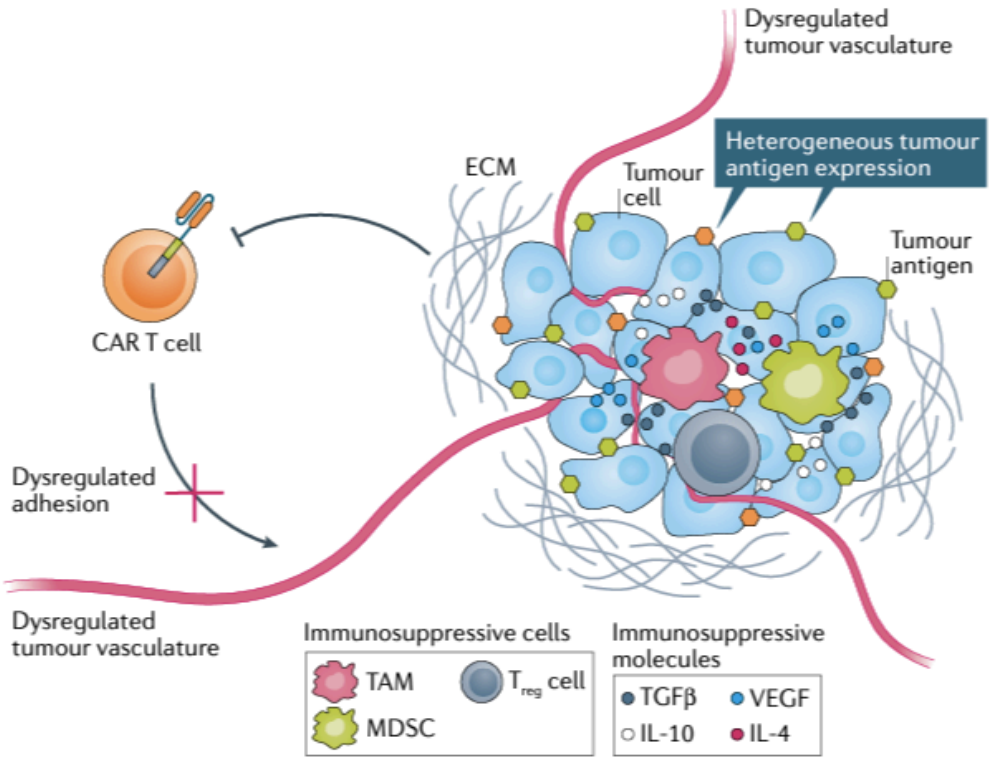

Figure 1.2 T cell-extrinsic factors limiting treatment efficacy against solid tumours. Adoptively transferred T cells are limited in their ability to infiltrate, target and kill tumour cells. Barriers to infiltration include tumour vasculature with downregulated expression of adhesion molecules necessary for T-cell extravasation from the endothelium into tumours, as well as a dense, fibrotic network of extracellular matrix (ECM) proteins that hinders T-cell motility. Heterogeneous antigen expression poses a further challenge for CAR- T cells, where cytolysis is dependent on target- antigen recognition. Finally, the presence of immunosuppressive cell types and immunosuppressive cytokines—which are produced by and can polarize or attract suppressor cells—can dampen the anti-tumour function of infiltrating CAR T cells. For instance, suppressor cells such as regulatory T cells (Treg cells) can produce transforming growth factor-β (TGF-β), which can inhibit T cell cytotoxicity through various mechanisms such as downregulation of granzymes and increased ECM deposition. TGF-β also promotes further polarization of $CD4^+$ T cells into Treg cells and can induce a more suppressive phenotype in myeloid cells. Suppressive myeloid cells in the TME include tumour- associated macrophages (TAMs) and myeloid- derived suppressive cells (MDSCs), which can inhibit T cell function through upregulated expression of the inhibitory ligand programmed cell death 1 ligand 1 (PD-L1), as well as secretion of inhibitory cytokines such as TGF-β and IL-10.

Immune cells and soluble factors mediate immune suppression in the TME

The tumor microenvironment is populated with suppressive cell types — such as regulatory T cells (Treg cells), myeloid-derived suppressor cells (MDSCs), and tumor-associated macrophages (TAMs) — that promote immune tolerance. The chemokine and cytokine expression profile of the TME not only acts to exclude cytotoxic T cells, but also preferentially recruits immune suppressor cells from the periphery, and can polarize existing immune cells at

the tumor site towards an immunosuppressive phenotype. Cytokines typically overexpressed in the solid TME include transforming growth factor-beta (TGF-β), vascular endothelial growth factor (VEGF), interleukin (IL)-4, and IL-10, which can both directly inhibit T-cell function and promote accumulation of suppressive immune cells. The recruited suppressor cells can also produce immunosuppressive cytokines themselves, reinforcing the tolerogenic state of the TME[6–8].

Current strategies to combat immune suppression in the solid TME

Given the prevalence of inhibitory cell types in the solid TME, there has been much interest in developing immunotherapies that target these suppressor cells. In particular, there is a growing appreciation for the role of suppressive myeloid cells — most notably TAMs and MDSCs, which consist of a heterogenous mix of different cell states — in the solid-tumor milieu[6]. Specific therapeutic interventions targeting the myeloid compartment include inhibition of colony stimulating factor 1 receptor (CSF1R), which depletes TAMs, and has primarily been studied in combination with either chemotherapy or checkpoint blockade[9]. A previously unappreciated role of myeloid cells in shaping responses to immunotherapy was highlighted by a recent study that demonstrated that targeted genetic ablation of PD-1 on myeloid cells inhibited tumor growth more effectively than ablation of PD-1 expression on T cells, owing to decreased differentiation of myeloid progenitors into MDSCs, unleashing a more potent anti-tumor T-cell response[10].

The therapeutic benefit of combining adoptive T-cell transfer with targeting of tumor-associated myeloid cells has been less well-characterized. In a murine pancreatic ductal adenocarcinoma (PDAC) model, administering an agonistic CD40-targeting mAb, which activates myeloid cells, can reprogram tumor-associated myeloid cells towards a more inflammatory, M1-like phenotype. When combined with adoptive T-cell therapy, this approach yielded greater anti-tumor efficacy than myeloid-cell depletion by administering a CSF1R-targeting mAb[11]. Another novel cell-based approach leveraged the overexpression of NKG2D ligands on MDSCs in the TME. Although endogenous NK cells, which express NKG2D receptors, are capable of eliminating

MDSCs that express NKG2D ligands, suppressive factors in the TME such as TGF-β downregulate endogenous NKG2D receptor expression in NK cells. NK cells were therefore engineered to express a NKG2D CAR, which maintains high surface expression levels even in the presence of TGF-β. NK cells expressing NKG2D CARs selectively targeted MDSCs, and when administered in combination with disialoganglioside (GD2)-targeted CAR T cells, resulted in enhanced tumor control in a neuroblastoma xenograft model[12].

Besides myeloid cells, Treg cells are also a major contributor to the immunosuppressive TME, and are of particular concern in applications in which cytokine boosting of anti-tumor T-cell function may be desired. Specifically, IL-2 can potently stimulate effector T-cell function, but because Treg cells overexpress the IL-2 receptor alpha chain (IL-2Rα), IL-2 administration can lead to the counterproductive consequence of preferentially expanding suppressive Treg cells. To more selectively stimulate effector T cells, recent engineering efforts have produced IL-2 variants that preferentially bind IL-2Rβ over IL-2Rα[13,14]. A similar approach to selectively stimulate anti-tumor T cells over Treg cells relies on an engineered orthogonal IL-2 (orthoIL-2) and IL-2Rβ (orthoIL-2Rβ) ligand/receptor pair[15]. T cells expressing the orthogonal IL-2Rβ are selectively stimulated by orthogonal IL-2, which does not interact with either endogenous T cells or Treg cells. This orthogonal ligand/receptor system enables highly selective stimulation of adoptively transferred engineered T cells, minimizing both the risk of toxicity by excessive stimulation of host T cells and the risk of potential outgrowth of Treg cells.

In contrast to the approach of directly targeting suppressive cell populations of interest, “armored” CAR-T cells have been engineered to secrete pro-inflammatory cytokines such as IL-12[16,17], IL-18[18,19], and IL-23[20], which can favorably shape the TME for enhanced anti-tumor immunity. CAR-T cells secreting either IL-12 or IL-18 can recruit inflammatory M1 macrophages to the TME, and autocrine IL-12 or IL-18 signaling in CAR-T cells enhances interferon-gamma (IFN-γ) secretion, which can inhibit Treg proliferation, thereby protecting T cells from Treg cell-mediated suppression[16–19]. IL-23, which promotes T-cell proliferation, consists of a p19 and p40

subunit, in which only the p19 subunit is upregulated by T cells upon activation. Engineering T cells to only express the p40 subunit results in reconstitution of functional IL-23 only upon T-cell activation, which can minimize potential toxicity that might otherwise be observed with constitutive IL-23 expression[20]. Additionally, this strategy enhanced the anti-tumor function of CAR T cells in multiple syngeneic and xenograft tumor models, with superior efficacy compared to CAR T cells expressing IL-18[20].

CAR-T cells can also be equipped with synthetic receptors that redirect the inhibitory PD-1/PD-L1 axis and the tumor necrosis factor receptor superfamily member TNFRSF6 (also known as FAS) and its ligand TNFL6 (also known as FASL) signaling axis[21–24]. In a xenograft tumor model of pleural mesothelioma, in which high levels of PD-L1 expressed on tumor cells dampened anti-tumor function of mesothelin-targeted CAR-T cells, co-expression of a PD-1 DNR enhanced CAR-T cell function both *in vitro* and *in vivo*[21]. Expression of a PD-1 DNR provided an additional advantage over systemic co-administration of a PD-1 inhibitor, which required repeated doses in order to achieve a favorable therapeutic outcome[21]. Alternatively, switch receptors consisting of a fusion between the PD-1 ectodomain and CD28 endodomain can enhance anti-tumor function of CAR T cells in multiple solid tumor xenograft models[22,23]. CD28 signaling through the PD-1/CD28 receptor was necessary to achieve optimal control over tumor burden[23]. Similarly, in syngeneic tumor models, expression of a FAS DNR in either CAR- or TCR-engineered T cells protected T cells from FASL-induced apoptosis, leading to increased *in vivo* persistence and enhanced tumor eradication[24].

TGF-β plays a pivotal role in the tumor microenvironment

TGF-β is an inhibitory factor of particular interest because of its central role in the TME. TGF-β interacts broadly with immune cells to promote tumor tolerance. Besides enforcing an immunosuppressive niche through recruitment and polarization of Tregs, MDSCs, and TAMs[25,26] — which produce TGF-β themselves — TGF-β also directly inhibits cytotoxic T cell[27–32] and NK

cell[33,34] function, and suppresses dendritic cell (DC) maturation[35,36]. In addition to its inhibitory effects on immune cells, TGF-β also promotes tumor progression, driving more invasive phenotypes by inducing epithelial-to-mesenchymal transition and promoting tumor angiogenesis[37–39]. TGF-β has also been shown to maintain self-renewing cancer stem cell populations which are often associated with resistance to therapy[40–42]. TGF-β can also act on stromal cells, such as cancer-associated fibroblasts, to induce aberrant secretion of extracellular matrix proteins[43,44], which act as a physical barrier to protect the solid tumor parenchyma from immune infiltrates.

In light of the multiple suppressive elements in the TME that are dependent on TGF-β, there is much interest in TGF-β–blocking immunotherapies. Systemic administration of TGF-β inhibitors, however, have raised concerns of toxicity[45–48]. An alternate approach is to engineer TGF-β–resistant, tumor-specific T cells, with previously reported strategies including expression of a TGF-β dominant-negative receptor (DNR) [49–53] or a TGF-β receptor (TGF-βR)/4-1BB chimera[54,55], as well as CRISPR-mediated knockout of the endogenous TGF-βRII[56,57]. Toxicity is limited in these therapies due to the fact that inhibition of TGF-β signaling would occur primarily in the engineered T cells themselves. Although receptors such as the TGF-β DNR, which is a truncated form of TGF-βRII that lacks the cytoplasmic signaling domain, may also inhibit TGF-β signaling in neighboring cells by binding TGF-β and limiting its bioavailability, this effect is localized to the tumor site, minimizing the risk of toxicities incurred at healthy tissue sites where TGF-β signaling is crucial for homeostasis. Knockout of TGF-βRII in engineered T cells should pose even less risk of toxicity as inhibition of TGF-β signaling would occur only in gene-edited cells, but efficacy of this approach is limited by the inability to sequester TGF-β and inhibit its signaling in neighboring cells in the TME.

Among these strategies, the TGF-β DNR has been most widely tested in clinical applications[53]. We hypothesize, however, that therapeutic efficacy can be further enhanced by engineering T cells to not only resist TGF-β signaling, but also reprogram TGF-β into an

immunostimulant. Potentiating T-cell effector functions in the TGF-β–rich solid TME would have the additional benefit of inducing bystander effects that can stimulate an inflammatory response in neighboring, endogenous immune cells, which is of particular importance given the prominent role of suppressive immune cells in establishing tumor tolerance. Previous work in our lab has demonstrated that CARs can be engineered to respond to TGF-β[58]. Such TGF-β–responsive CARs both inhibit endogenous TGF-β signaling by outcompeting endogenous TGF-β receptors for ligand binding, and transduce T-cell activating signals upon TGF-β binding, leading to proliferation and inflammatory cytokine production. Notably, TGF-β CAR activation does not trigger T-cell cytotoxicity, and therefore acts as a companion receptor to be paired with a tumor-reactive CAR or TCR to augment anti-tumor immunity.

In this dissertation, we address potential risks of arming T cells with TGF-β–responsive CARs for anti-tumor applications, including potential expansion of contaminating Tregs, blunting of cytotoxic payload delivery, and systemic toxicity. We next assessed the ability of the TGF-β CAR to enhance the therapeutic efficacy of tumor-specific T cells using different receptor pairing configurations in different tumor models, and demonstrate that single-chain bispecific CAR-T cells responsive to IL-13Rα2 and TGF-β can program robust anti-tumor immunity in models of glioblastoma multiforme (GBM).

References

1. Sadelain, M., Brentjens, R. & Rivière, I. The Basic Principles of Chimeric Antigen Receptor Design. *Cancer Discov.* **3**, 388–398 (2013).

2. Finney, H. M., Lawson, A. D. G., Bebbington, C. R. & Weir, A. N. C. Chimeric Receptors Providing Both Primary and Costimulatory Signaling in T Cells from a Single Gene Product. *J. Immunol.* **161**, 2791–2797 (1998).

3. Finney, H. M., Akbar, A. N. & Lawson, A. D. G. Activation of Resting Human Primary T Cells with Chimeric Receptors: Costimulation from CD28, Inducible Costimulator, CD134, and CD137 in Series with Signals from the TCRζ Chain. *J. Immunol.* **172**, 104–113 (2004).

4. Imai, C. *et al.* Chimeric receptors with 4-1BB signaling capacity provoke potent cytotoxicity against acute lymphoblastic leukemia. *Leukemia* **18**, 676–684 (2004).

5. Maude, S. L. *et al.* Chimeric Antigen Receptor T Cells for Sustained Remissions in Leukemia. *N. Engl. J. Med.* **371**, 1507–1517 (2014).

6. Gabrilovich, D. I., Ostrand-Rosenberg, S. & Bronte, V. Coordinated regulation of myeloid cells by tumours. *Nat. Rev. Immunol.* **12**, 253–268 (2012).

7. Quail, D. F. & Joyce, J. A. Microenvironmental regulation of tumor progression and metastasis. *Nat. Med.* **19**, 1423–1437 (2013).

8. Binnewies, M. *et al.* Understanding the tumor immune microenvironment (TIME) for effective therapy. *Nat. Med.* **24**, 541–550 (2018).

9. Cassetta, L. & Kitamura, T. Targeting Tumor-Associated Macrophages as a Potential Strategy to Enhance the Response to Immune Checkpoint Inhibitors. *Front. Cell Dev. Biol.* **6**, (2018).

10. Strauss, L. *et al.* Targeted deletion of PD-1 in myeloid cells induces antitumor immunity. *Sci. Immunol.* **5**, (2020).

11. Stromnes, I. M. *et al.* Differential Effects of Depleting versus Programming Tumor-Associated Macrophages on Engineered T Cells in Pancreatic Ductal Adenocarcinoma. *Cancer Immunol. Res.* **7**, 977–989 (2019).

12. Parihar, R. *et al.* NK Cells Expressing a Chimeric Activating Receptor Eliminate MDSCs and Rescue Impaired CAR-T Cell Activity against Solid Tumors. *Cancer Immunol. Res.* **7**, 363–375 (2019).

13. Parisi, G. *et al.* Persistence of adoptively transferred T cells with a kinetically engineered IL-2 receptor agonist. *Nat. Commun.* **11**, 660 (2020).

14. Sun, Z. *et al.* A next-generation tumor-targeting IL-2 preferentially promotes tumor-infiltrating CD8 + T-cell response and effective tumor control. *Nat. Commun.* **10**, 3874 (2019).

15. Sockolosky, J. T. *et al.* Selective targeting of engineered T cells using orthogonal IL-2 cytokine-receptor complexes. *Science* **359**, 1037–1042 (2018).

16. Chmielewski, M., Kopecky, C., Hombach, A. A. & Abken, H. IL-12 Release by Engineered T Cells Expressing Chimeric Antigen Receptors Can Effectively Muster an Antigen-Independent Macrophage Response on Tumor Cells That Have Shut Down Tumor Antigen Expression. *Cancer Res.* **71**, 5697–5706 (2011).

17. Pegram, H. J. *et al.* Tumor-targeted T cells modified to secrete IL-12 eradicate systemic tumors without need for prior conditioning. *Blood* **119**, 4133–4141 (2012).

18. Hu, B. *et al.* Augmentation of Antitumor Immunity by Human and Mouse CAR T Cells Secreting IL-18. *Cell Rep.* **20**, 3025–3033 (2017).

19. Avanzi, M. P. *et al.* Engineered Tumor-Targeted T Cells Mediate Enhanced Anti-Tumor Efficacy Both Directly and through Activation of the Endogenous Immune System. *Cell Rep.* **23**, 2130–2141 (2018).

20. Ma, X. *et al.* Interleukin-23 engineering improves CAR T cell function in solid tumors. *Nat. Biotechnol.* **38**, 448–459 (2020).

21. Cherkassky, L. *et al.* Human CAR T cells with cell-intrinsic PD-1 checkpoint blockade resist tumor-mediated inhibition. *J. Clin. Invest.* **126**, 3130–3144.

22. Prosser, M. E., Brown, C. E., Shami, A. F., Forman, S. J. & Jensen, M. C. Tumor PD-L1 co-stimulates primary human CD8(+) cytotoxic T cells modified to express a PD1:CD28 chimeric receptor. *Mol. Immunol.* **51**, 263–272 (2012).

23. Liu, X. *et al.* A chimeric switch-receptor targeting PD1 augments the efficacy of second generation CAR T-Cells in advanced solid tumors. *Cancer Res.* **76**, 1578–1590 (2016).

24. Yamamoto, T. N. *et al.* T cells genetically engineered to overcome death signaling enhance adoptive cancer immunotherapy. *J. Clin. Invest.* **129**, 1551–1565 (2019).

25. Flavell, R. A., Sanjabi, S., Wrzesinski, S. H. & Licona-Limón, P. The polarization of immune cells in the tumour environment by TGF-β. *Nat. Rev. Immunol.* **10**, 554–567 (2010).

26. Pickup, M., Novitskiy, S. & Moses, H. L. The roles of TGFβ in the tumour microenvironment. *Nat. Rev. Cancer* **13**, 788–799 (2013).

27. Lin, J. T., Martin, S. L., Xia, L. & Gorham, J. D. TGF-beta 1 uses distinct mechanisms to inhibit IFN-gamma expression in CD4+ T cells at priming and at recall: differential involvement of Stat4 and T-bet. *J. Immunol.* **174**, 5950–5958 (2005).

28. Chen, M.-L. *et al.* Regulatory T cells suppress tumor-specific CD8 T cell cytotoxicity through TGF-β signals in vivo. *Proc. Natl. Acad. Sci.* **102**, 419–424 (2005).

29. Thomas, D. A. & Massagué, J. TGF-β directly targets cytotoxic T cell functions during tumor evasion of immune surveillance. *Cancer Cell* **8**, 369–380 (2005).

30. Park, B. V. *et al.* TGFβ1-Mediated SMAD3 Enhances PD-1 Expression on Antigen-Specific T Cells in Cancer. *Cancer Discov.* **6**, 1366–1381 (2016).

31. Gunderson, A. J. *et al.* TGFβ suppresses CD8+ T cell expression of CXCR3 and tumor trafficking. *Nat. Commun.* **11**, 1749 (2020).

32. Bao, S., Jiang, X., Jin, S., Tu, P. & Lu, J. TGF-β1 Induces Immune Escape by Enhancing PD-1 and CTLA-4 Expression on T Lymphocytes in Hepatocellular Carcinoma. *Front. Oncol.* **11**, (2021).

33. Rook, A. H. *et al.* Effects of transforming growth factor beta on the functions of natural killer cells: depressed cytolytic activity and blunting of interferon responsiveness. *J. Immunol.* **136**, 3916–3920 (1986).

34. Viel, S. *et al.* TGF-β inhibits the activation and functions of NK cells by repressing the mTOR pathway. *Sci. Signal.* **9**, ra19–ra19 (2016).

35. Ghiringhelli, F. *et al.* Tumor cells convert immature myeloid dendritic cells into TGF-β–secreting cells inducing CD4+CD25+ regulatory T cell proliferation. *J. Exp. Med.* **202**, 919–929 (2005).

36. Fricke, I. & Gabrilovich, D. I. Dendritic Cells and Tumor Microenvironment: A Dangerous Liaison. *Immunol. Invest.* **35**, 459–483 (2006).

37. Yu, Q. & Stamenkovic, I. Cell surface-localized matrix metalloproteinase-9 proteolytically activates TGF-β and promotes tumor invasion and angiogenesis. *Genes Dev.* **14**, 163–176 (2000).

38. Xu, J., Lamouille, S. & Derynck, R. TGF-β-induced epithelial to mesenchymal transition. *Cell Res.* **19**, 156–172 (2009).

39. Batlle, R. *et al.* Regulation of tumor angiogenesis and mesenchymal–endothelial transition by p38α through TGF-β and JNK signaling. *Nat. Commun.* **10**, 3071 (2019).

40. Peñuelas, S. *et al.* TGF-β Increases Glioma-Initiating Cell Self-Renewal through the Induction of LIF in Human Glioblastoma. *Cancer Cell* **15**, 315–327 (2009).

41. Ikushima, H. *et al.* Autocrine TGF-β Signaling Maintains Tumorigenicity of Glioma-Initiating Cells through Sry-Related HMG-Box Factors. *Cell Stem Cell* **5**, 504–514 (2009).

42. Liu, Z., Kuang, W., Zhou, Q. & Zhang, Y. TGF-β1 secreted by M2 phenotype macrophages enhances the stemness and migration of glioma cells via the SMAD2/3 signalling pathway. *Int. J. Mol. Med.* **42**, 3395–3403 (2018).

43. Tauriello, D. V. F. *et al.* TGFβ drives immune evasion in genetically reconstituted colon cancer metastasis. *Nature* **554**, 538–543 (2018).

44. Chakravarthy, A., Khan, L., Bensler, N. P., Bose, P. & De Carvalho, D. D. TGF-β-associated extracellular matrix genes link cancer-associated fibroblasts to immune evasion and immunotherapy failure. *Nat. Commun.* **9**, 4692 (2018).

45. Anderton, M. J. *et al.* Induction of heart valve lesions by small-molecule ALK5 inhibitors. *Toxicol. Pathol.* **39**, 916–924 (2011).

46. Morris, J. C. *et al.* Phase I Study of GC1008 (Fresolimumab): A Human Anti-Transforming Growth Factor-Beta (TGFβ) Monoclonal Antibody in Patients with Advanced Malignant Melanoma or Renal Cell Carcinoma. *PLOS ONE* **9**, e90353 (2014).

47. Lacouture, M. E. *et al.* Cutaneous keratoacanthomas/squamous cell carcinomas associated with neutralization of transforming growth factor β by the monoclonal antibody fresolimumab (GC1008). *Cancer Immunol. Immunother.* **64**, 437–446 (2015).

48. Mitra, M. S. *et al.* A Potent Pan-TGFβ Neutralizing Monoclonal Antibody Elicits Cardiovascular Toxicity in Mice and Cynomolgus Monkeys. *Toxicol. Sci.* **175**, 24–34 (2020).

49. Bollard, C. M. *et al.* Adapting a transforming growth factor β–related tumor protection strategy to enhance antitumor immunity. *Blood* **99**, 3179–3187 (2002).

50. Foster, A. E. *et al.* Antitumor Activity of EBV-specific T Lymphocytes Transduced With a Dominant Negative TGF-β Receptor. *J. Immunother.* **31**, 500–505 (2008).

51. Bollard, C. M. *et al.* Tumor-Specific T-Cells Engineered to Overcome Tumor Immune Evasion Induce Clinical Responses in Patients With Relapsed Hodgkin Lymphoma. *J. Clin. Oncol.* **36**, 1128–1139 (2018).

52. Kloss, C. C. *et al.* Dominant-Negative TGF-β Receptor Enhances PSMA-Targeted Human CAR T Cell Proliferation And Augments Prostate Cancer Eradication. *Mol. Ther.* **26**, 1855–1866 (2018).

53. Narayan, V. *et al.* PSMA-targeting TGFβ-insensitive armored CAR T cells in metastatic castration-resistant prostate cancer: a phase 1 trial. *Nat. Med.* **28**, 724–734 (2022).

54. Sukumaran, S. *et al.* Enhancing the potency and specificity of engineered T cells for cancer treatment. *Cancer Discov.* CD-17-1298 (2018) doi:10.1158/2159-8290.CD-17-1298.

55. Roth, T. L. *et al.* Pooled Knockin Targeting for Genome Engineering of Cellular Immunotherapies. *Cell* **181**, 728-744.e21 (2020).

56. Tang, N. *et al.* TGF-β inhibition via CRISPR promotes the long-term efficacy of CAR T cells against solid tumors. *JCI Insight* **5**, (2020).

57. Shaim, H. *et al.* Targeting the **α**v integrin/TGF-**β** axis improves natural killer cell function against glioblastoma stem cells. *J. Clin. Invest.* **131**, (2021).

58. Chang, Z. L. *et al.* Rewiring T-cell responses to soluble factors with chimeric antigen receptors. *Nat. Chem. Biol.* **14**, 317–324 (2018).

CHAPTER 2. The TGF-β CAR is a viable and safe receptor platform for engineering anti-tumor T-cell therapies

Abstract

In light of the pivotal role of TGF-β in the TME, we hypothesized that pairing tumor-targeting receptors with TGF-β CARs, which can convert the typically immunosuppressive signals of TGF-β into immunostimulatory signals, presents a promising strategy to enhance T-cell function against solid tumors. Before evaluating the ability of TGF-β CARs to augment anti-tumor immunity, we first sought to address potential concerns that might derail their therapeutic viability, including potential expansion of a immunosuppressive Tregs, diversion of granzyme B (GrB) payloads from T cell-tumor cell synapses, and systemic toxicity. We demonstrate that (1) TGF-β CAR-transduced Tregs are neither selectively expanded nor suppressive in the presence of TGF-β, (2) TGF-β CAR activation does not depolarize the immunological synapse, and (3) TGF-β CAR-T cells are well-tolerated when administered systemically. Our findings support the use of the TGF-β CAR as a productive and safe modality to engineer more robust anti-tumor T-cell function.

Introduction

TGF-β–responsive CARs, which convert TGF-β from an immunosuppressive molecule to an immunostimulant in engineered T cells, hold potential for enhancing the efficacy of adoptive T-cell therapy against solid tumors. However, we sought to address three main concerns that would limit the utility of the TGF-β CAR as a cancer therapeutic; namely, (1) potential outgrowth of suppressive TGF-β CAR-Tregs, (2) TGF-β CAR-mediated depolarization of the immunological synapse, and (3) risk of systemic toxicity.

First, we sought to understand whether transduction of contaminating Tregs in a starting population of bulk T cells would result in selective expansion of immunosuppressive TGF-β CAR-Tregs. This was of particular concern given that activated Tregs are known to secrete TGF-β[1]. TGF-β secreted by Tregs could, in turn, activate TGF-β CAR-transduced Tregs, establishing an autocrine positive feedback loop resulting in TGF-β CAR-Treg proliferation and elevated levels of TGF-β. Since TGF-β can polarize naïve $CD4^+$ T cells into Tregs[2], buildup of TGF-β could also convert neighboring non-Treg cells into Tregs. The potential interplay between TGF-β, Tregs, and the TGF-β CAR therefore warrants a careful investigation of TGF-β CAR function in Tregs.

TGF-β CARs do not confer tumor-targeting specificity, and therefore must be paired with a tumor-targeting receptor to program anti-tumor function. Tumor-targeting receptors mediate T-cell cytotoxicity through a chain of events: (1) receptor binding to tumor antigen forms cell-cell contacts between the T-cell and tumor cell, (2) broad cytoskeletal re-modeling in T cells forms an immunological synapse at the T-cell: tumor-cell interface, and (3) lytic granules containing cytotoxic molecules such as granzyme B and perforin are polarized towards the immunological synapse, where they are delivered to tumor cells to induce apoptosis[3,4]. Since TGF-β is a soluble factor, no cell-cell contacts are formed upon TGF-β CAR engagement with ligand, but lytic granule polarization towards the receptor-ligand interface may still occur. We therefore sought to investigate whether TGF-β CAR engagement would reduce cytolytic efficiency by diverting cytotoxic payloads away from the immunological synapse formed by tumor-targeting receptors.

Although the role of TGF-β in promoting tumor progression and therapeutic resistance has been well-documented, TGF-β also plays a crucial role in maintaining healthy tissue homeostasis[5], and systemic administration of TGF-β inhibitors have raised concerns of cardiotoxicity and development of skin lesions[6–9]. Although TGF-β CAR stimulation does not initiate bystander killing, it does trigger production of inflammatory cytokines[10]. Since TGF-β is ubiquitously expressed, we wished to determine whether basal levels of TGF-β in healthy tissues would be sufficient to induce TGF-β CAR-T cell-mediated toxicity.

Here we demonstrate that TGF-β CAR expression in a highly purified population of Tregs does not promote Treg purity or trigger suppressive activity, indicating that contaminating fractions of Tregs in a TGF-β CAR-T cell product do not pose a risk of counterproductive expansion or immune suppression. Using engineered Jurkat T-cell lines, we found that the TGF-β CAR does not depolarize immunological synapses formed by CD19 CAR binding to tumor antigen. Lastly, we demonstrate that TGF-β CAR-T cells are well-tolerated when administered systemically into immunocompetent mice, with no evidence of aberrant T-cell expansion in the peripheral blood or systemic toxicity. Taken together, these results demonstrate that the TGF-β CAR is not counterproductive to anti-tumor T-cell function, and TGF-β CAR-T cells can be safely administered, supporting downstream engineering efforts using the TGF-β CAR to enhance the efficacy of adoptive T-cell therapy.

Results

TGF-β CARs do not promote expansion or suppressive function of Tregs

At present, CAR-T cell therapy is a personalized medical treatment, with unique cell products produced for each patient[11]. Although a variety of cell-manufacturing starting materials are used, including peripheral blood mononuclear cells (PBMCs), CD8-sorted cells, or cells sorted for either naïve or memory phenotypes[12–15], many manufacturing processes do not specifically deplete Treg cells. Since activated Treg cells secrete TGF-β[8], and TGF-β CAR signaling promotes

robust T-cell expansion[10], concerns arise of whether TGF-β CAR expression would inadvertently enrich Treg cells in a T-cell product, and whether TGF-β CAR-Treg cells would cause counterproductive CAR-mediated immunosuppression.

To evaluate the effect of TGF-β CAR expression specifically on Tregs, experiments were performed using FACS-sorted CD4$^+$/CD25^{hi}/CD127$^-$ cells (**Figures 2.1A, B**), which have been shown to be enriched in the Treg phenotype[16]. Interestingly, unlike non-Tregs[10], Treg cells consistently showed more efficient surface presentation of the TGF-β CAR containing a long (229-

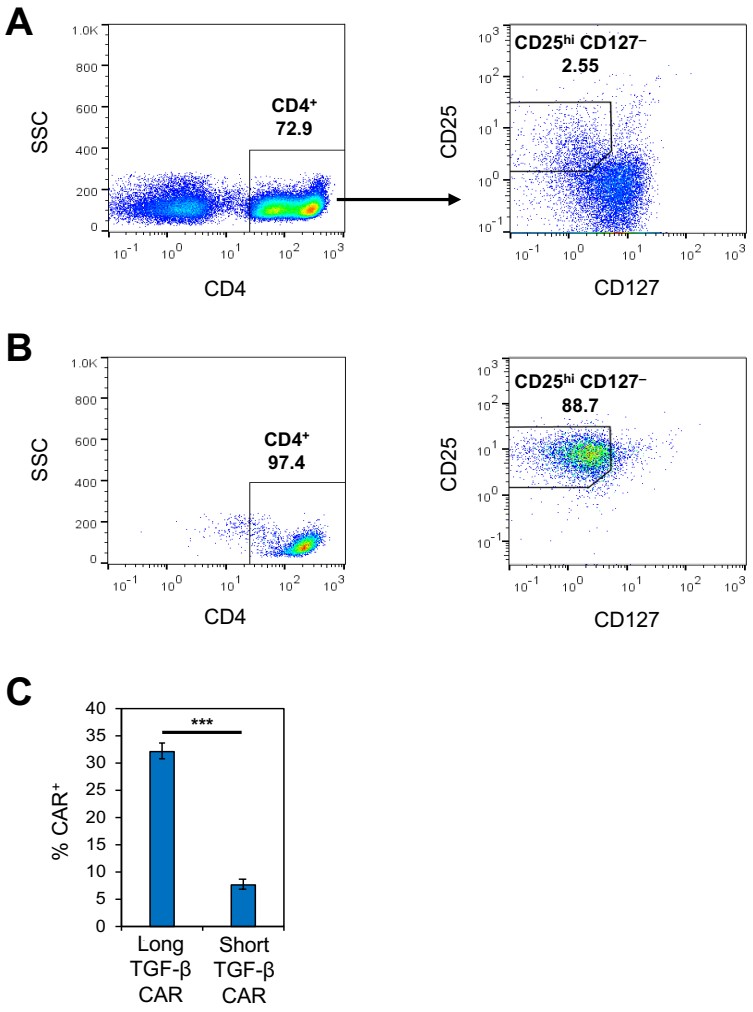

Figure 2.1 The TGF-β CAR with a long spacer exhibits more efficient surface presentation than the TGF-β CAR with a short spacer in Tregs. (a) Representative flow plots depicting gating strategy for the sorting of CD4$^+$/CD25^{hi}/CD127$^-$ Tregs. (b) Representative flow plots depicting surface marker expression of cells immediately after sorting. (c) TGF-β CAR-transduced CD4$^+$/CD25^{hi}/CD127$^-$-sorted cells were stained for surface expression of FLAG-tagged CARs. Averages of triplicates are shown, with error bars representing ± 1 SD. Statistics are calculated by a 2-tailed Student's t test. *** $p < 0.001$.

amino acid) extracellular spacer compared to an otherwise identical CAR containing a short (12-amino acid) spacer (**Figure 2.1C**). Therefore, all subsequent experiments in Treg cells were performed with the long TGF-β CAR.

The most definitive marker of Treg phenotype — FOXP3 — is an intracellular protein that cannot be used for live-cell sorting based on surface marker staining. As a result, the expanded $CD4^+/CD25^{hi}/CD127^-$-sorted cell population included a residual fraction of $FOXP3^-$ cells, regardless of whether the cells had been transduced with the TGF-β CAR (**Figure 2.2A**). The addition of TGF-β resulted in an increase in FOXP3 expression in untransduced, $CD4^+/CD25^{hi}/CD127^-$-sorted cells, confirming that TGF-β promotes the differentiation of non-Treg cells into the Treg phenotype (**Figures 2.2A, B**). In contrast, TGF-β–mediated induction of FOXP3

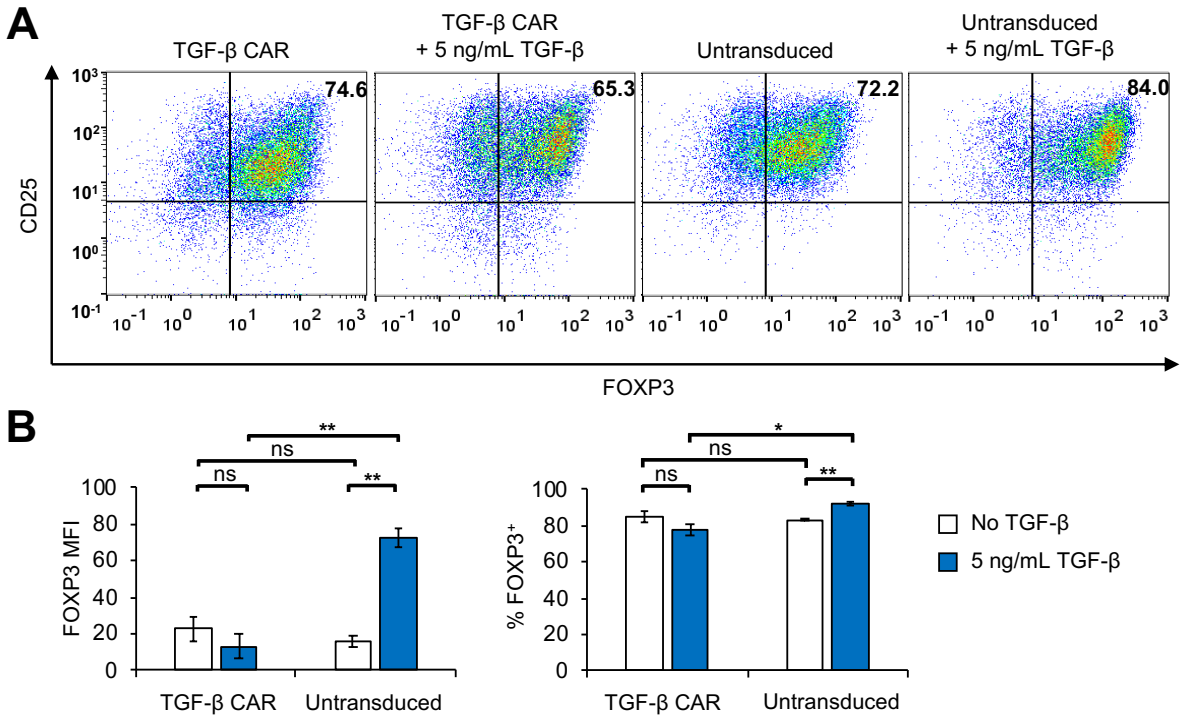

Figure 2.2 TGF-β CAR expression and stimulation does not result in preferential expansion of $FOXP3^+$ Tregs among $CD4^+/CD25^{hi}/CD127^-$-sorted cells. (a) TGF-β CAR-transduced or untransduced $CD4^+/CD25^{hi}/CD127^-$-sorted cells were expanded with Dynabeads only or Dynabeads plus 5 ng/mL TGF-β for 20 days. Shown are representative scatterplots of FOXP3 vs. CD25 expression corresponding to each transduction and expansion condition. (b) FOXP3 mean fluorescent intensity (MFI) and frequency of $FOXP3^+$ cells corresponding to each transduction and expansion condition. Averages of triplicates are shown in (b), with error bars representing ± 1 SD. Statistics are calculated by 2-tailed Student's *t* tests with the Sidak correction for multiple comparisons. * $p < 0.05$ and ** $p < 0.01$.

expression was not observed in $CD4^+/CD25^{hi}/CD127^-$-sorted cells transduced with the TGF-β CAR. These results indicate that TGF-β CAR expression does not promote preferential expansion of $FOXP3^+$ Tregs over non-Tregs. Instead, CAR expression appears to suppress the overall frequency of $FOXP3^+$ Tregs in mixed T-cell populations treated with TGF-β (**Figures 2.2A, B**), likely by preventing the differentiation of non-Treg cells into the regulatory phenotype.

We next evaluated whether Treg cells activated through TGF-β CAR signaling would exert suppressive effects on nearby effector T (Teff) cells. To ensure that $CD4^+/CD25^{hi}/CD127^-$-sorted cells contained enough Treg cells to have suppressive potential, co-cultures were set up with CFSE-labeled $CD4^+CD25^-$ Teff cells, anti-CD3, and anti-CD28, with or without TGF-β CAR-transduced $CD4^+/CD25^{hi}/CD127^-$-sorted cells (**Figure 2.3A**). In such co-cultures, anti-CD3 and anti-CD28 served to activate both Treg and Teff cells by triggering TCR signaling. CFSE dilution in Teff cells was quantified after 96 hours of co-culture, with results indicating clear suppression of Teff proliferation in the presence of $CD4^+/CD25^{hi}/CD127^-$-sorted cells (**Figure 2.3A**), confirming this population contained sufficient numbers of Treg cells to effectively suppress Teff proliferation upon TCR-mediated T-cell activation. Notably, addition of TGF-β did not enhance suppression mediated by TGF-β CAR-transduced Treg cells (**Figure 2.3A**), and TGF-β CAR-transduced Tregs were no more suppressive than untransduced Tregs (**Figure 2.3B**). These results indicate that the TGF-β CAR itself does not boost the suppressive capacity of Treg cells.

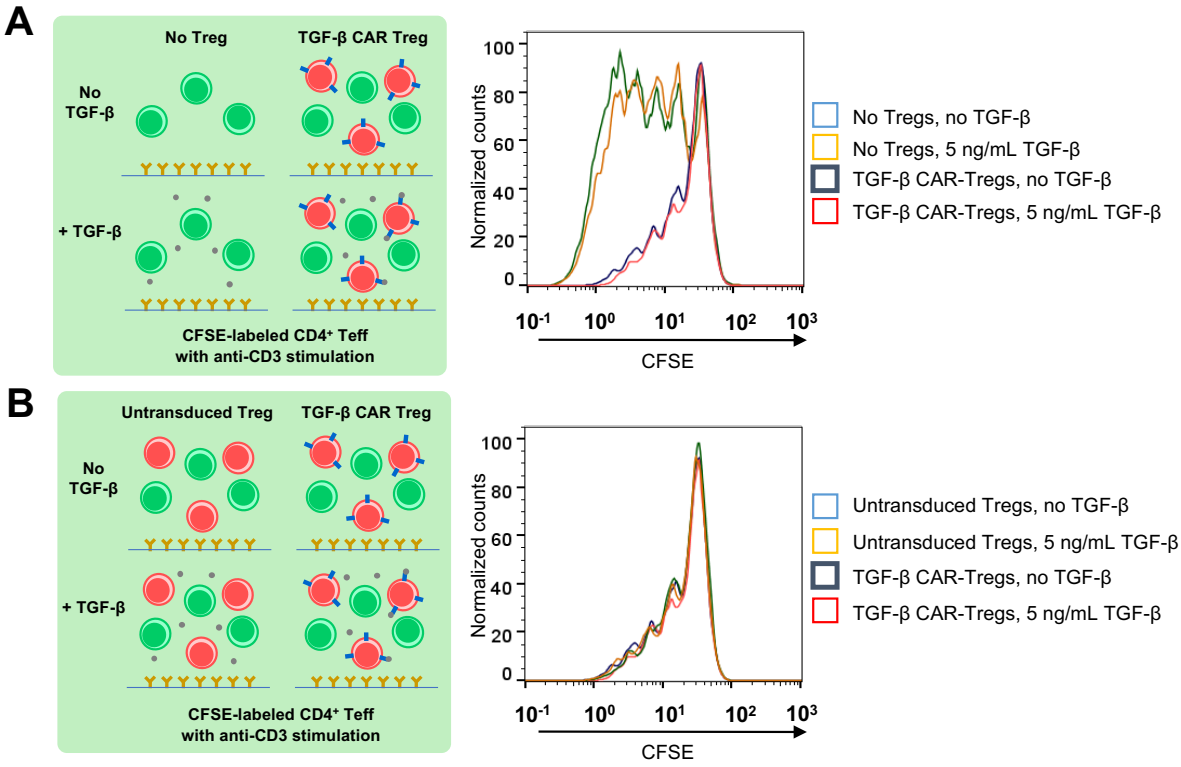

Figure 2.3 TGF-β CAR-Tregs are suppressive when stimulated through the TCR. (a) CFSE-labeled CD4$^+$ Teffs that were not previously activated in vitro were cultured in OKT3-coated wells with CD28 agonist antibody and either 0 or 5 ng/mL TGF-β, with or without the addition of TGF-β CAR-transduced CD4$^+$/CD25^{hi}/CD127$^-$-sorted cells (referred to as TGF-β CAR-Tregs) at 1:1 Treg:Teff ratio. Representative histogram overlays of CFSE dilution are shown. (b) Co-cultures were set up as described in (a), except all wells received Tregs that were either untransduced or transduced with the TGF-β CAR. Representative histogram overlays of CFSE dilution are shown.

To determine whether CAR-mediated (as opposed to TCR-mediated) Treg activation would similarly suppress CAR-Teff proliferation, a CD19 CAR was introduced into CD4$^+$ Teff cells, and co-cultures were set up with CFSE-labeled CD19 CAR-Teff cells and irradiated parental (CD19$^+$/OKT3$^-$) TM-LCL target cells, with or without CTV-labeled TGF-β CAR-transduced Treg cells (**Figure 2.4A**). In this system, the Teff and Treg cells were separately activated via their CARs by CD19 and TGF-β, respectively, thus enabling specific inquiry into the effect of CAR activation on the Treg cells' suppressive potential. CTV dilution in Tregs (**Figures 2.4B, C**) and CFSE dilution in Teffs (**Figure 2.4D**) were quantified after 72 hours of co-culture. Flow cytometry analysis revealed that TGF-β CAR-transduced Treg cells, but not untransduced Treg cells,

divided in response to TGF-β addition (**Figures 2.4B, C**), thus confirming TGF-β CAR signaling. However, this Treg population was unable to suppress Teff proliferation (**Figure 2.4D**), indicating that CAR-activated Tregs do not exert significant suppressive function on nearby Teff cells.

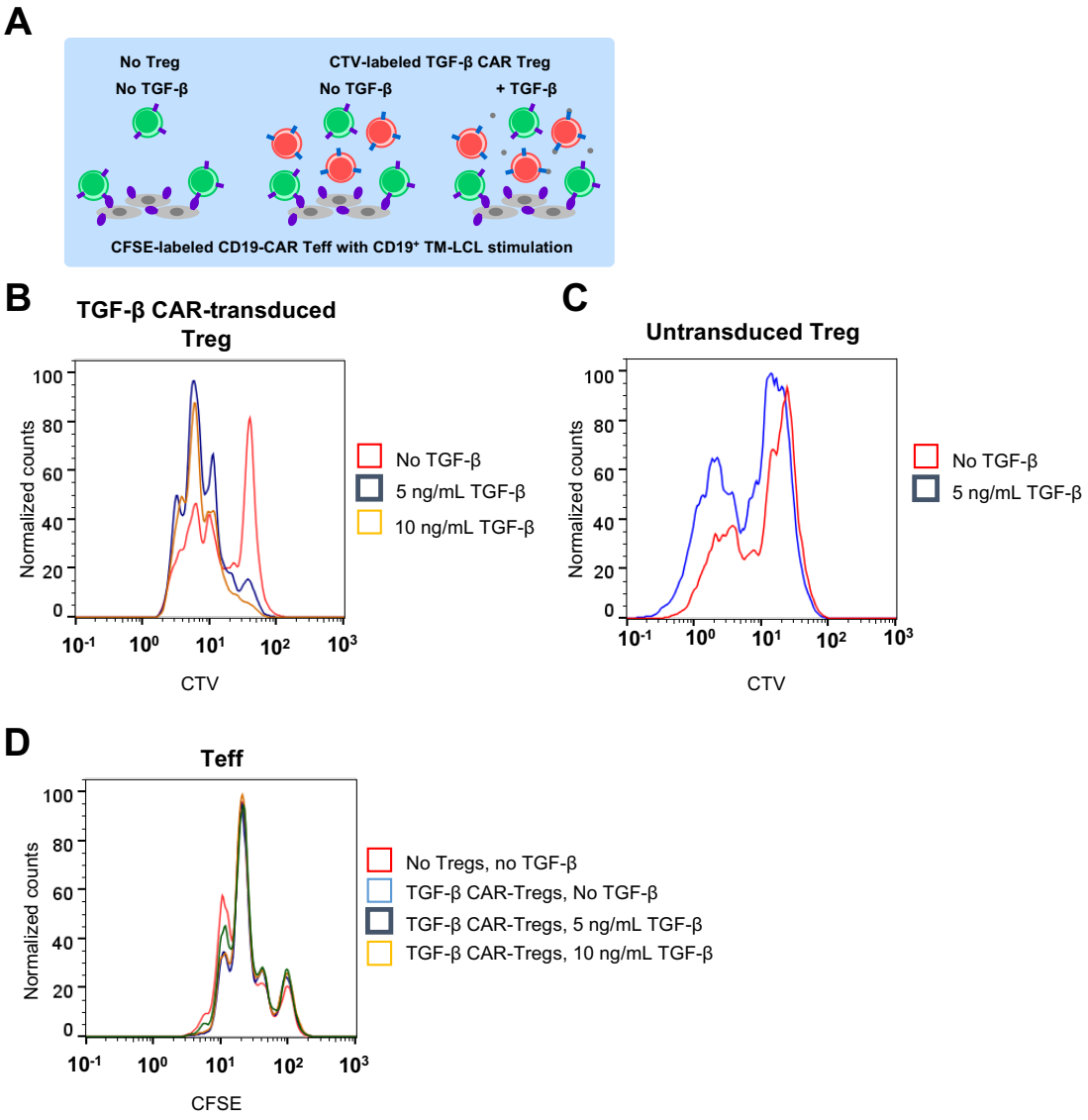

Figure 2.4 TGF-β CAR-Tregs are not suppressive when stimulated through the CAR. (a) CFSE-labeled CD19 CAR-Teffs were co-cultured with irradiated CD19+ TM-LCLs, CTV-labeled Tregs (TGF-β CAR-transduced or untransduced), and either 0, 5, or 10 ng/mL TGF-β. The co-cultures were set up at 1:2:1 Teff:TM-LCL:Treg ratio. (b) Histogram overlays of CTV dilution comparing co-cultures containing TGF-β CAR-Tregs at varying concentrations of TGF-β. (c) Histogram overlays of CTV dilution comparing co-cultures containing untransduced Tregs at varying concentratons of TGF-β. (d) Histogram overlays of CFSE dilution comparing co-cultures without Tregs and co-cultures with TGF-β CAR-transduced Tregs, at varying concentrations of TGF-β.

Taken together, these results indicate that even if the starting population for therapeutic T-cell manufacturing contains Treg cells, transduction with TGF-β CAR would not lead to the

preferential expansion of Treg cells, and the presence of any TGF-β CAR-Treg cells is unlikely to induce suppressive effects on the activity of tumor-targeting Teff cells.

TGF-β CAR expression does not blunt cytotoxic payload delivery

Previous work has demonstrated that TGF-β CAR-T cells can degranulate in response to soluble TGF-β, as evidenced by upregulation of the degranulation marker CD107a (**Supplementary Figure 2.1**; data courtesy of Dr. ZeNan Chang). We therefore sought to determine whether TGF-β CAR engagement would divert lytic granules from the immunological synapse. To investigate this, Jurkat T-cells engineered to express mCherry-labeled GrB were co-incubated with $CD19^{+}EGFP^{+}$ Raji cells, with or without TGF-β (**Figure 2.5**). Confocal microscopy images were taken to determine GrB localization patterns in Jurkat cells, with or without TGF-β present. Compared with Jurkat cells expressing a CD19 CAR alone, dual TGF-β/CD19 CAR

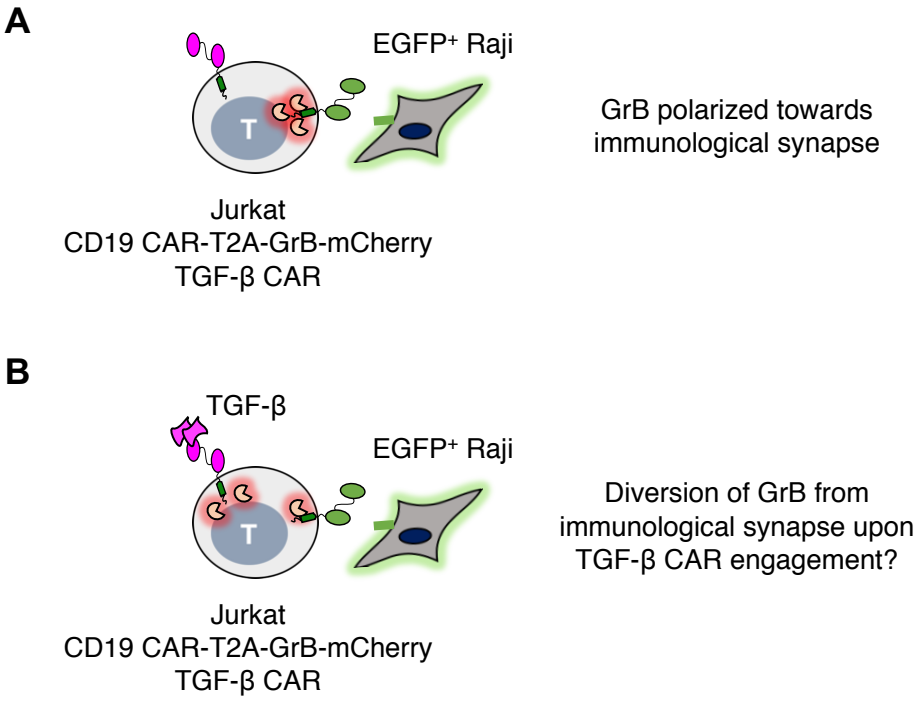

Figure 2.5 Engineered Jurkat T cells provide a model system to visualize immunological synapse formation. Jurkat T cells were engineered to co-express a CD19-targeting CAR and a TGF-β–responsive CAR, in addition to a GrB-mCherry fusion protein. Engineered Jurkat cells were co-cultured with $EGFP^{+}$ $CD19^{+}$ Raji target cells, with or without TGF-β. Localization patterns of GrB can be visualized by monitoring mCherry fluorescent signal relative to cell-cell contacts formed between Jurkat cells and $EGFP^{+}$ Raji cells.

Jurkat cells exhibited comparable GrB clustering at the interface of target-cell contacts, regardless of whether TGF-β was present (**Figure 2.6, Table 2.1**). Moreover, Jurkat cells expressing both a CD19 CAR and TGF-β CAR upregulated the degranulation marker CD107a at comparable levels compared to Jurkat cells expressing the CD19 CAR alone when challenged with $CD19^+$ Raji cells (**Figure 2.7**). Addition of TGF-β in Raji cell co-cultures did not reduce degranulation levels in

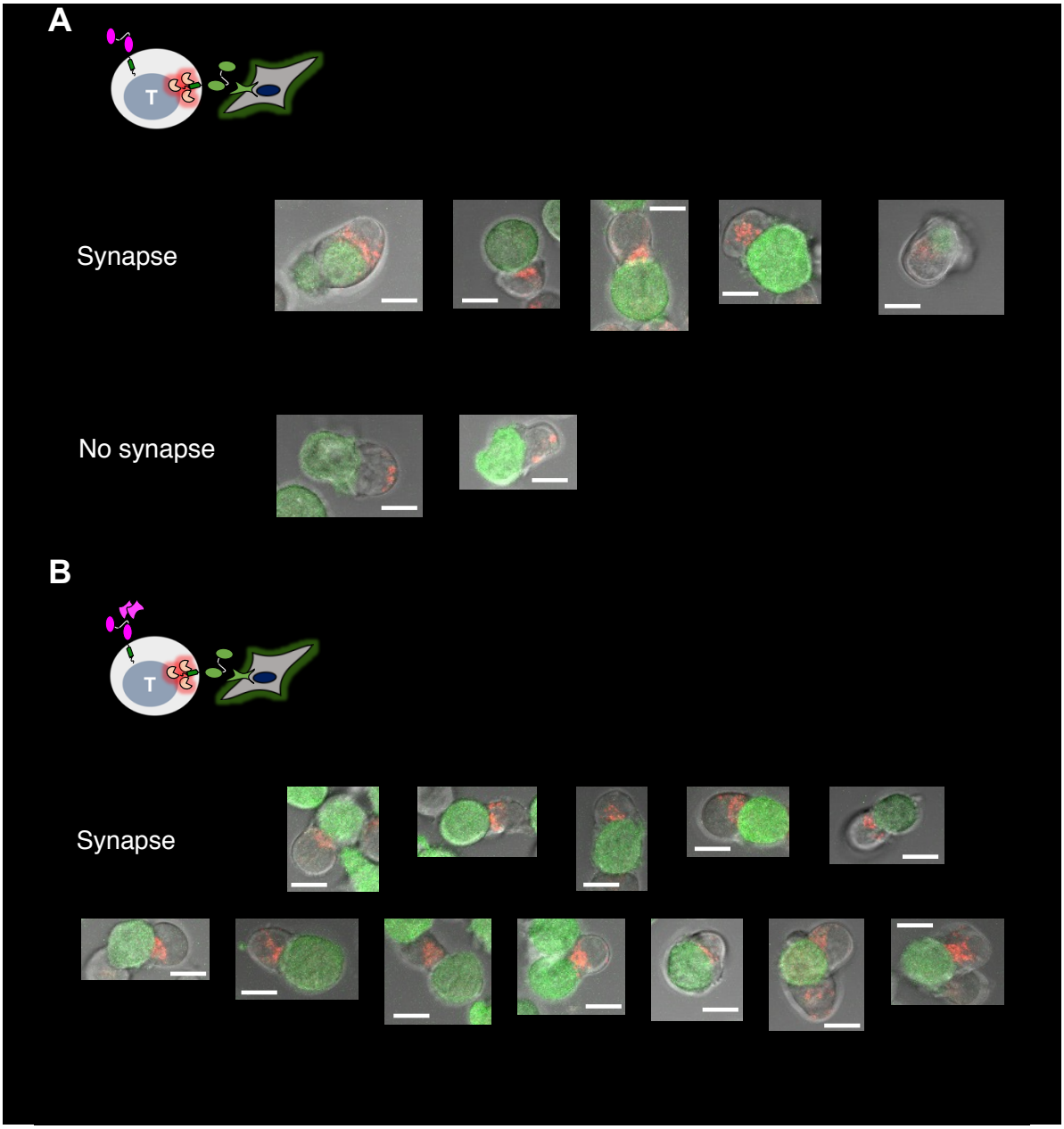

Figure 2.6 GrB polarizes towards Jurkat-Raji cell contacts. Engineered Jurkat cells as described in Figure 2.5 were co-incubated with $EGFP^+$ Raji cells. mCherry-labeled GrB molecules traffic towards the contacts formed between Jurkat and Raji cells. Scalebars denote 10 μm.

Jurkat cells co-expressing the TGF-β CAR and CD19 CAR (**Figure 2.7**). These results confirm that TGF-β CAR activation does not reduce cytotoxic efficiency by depolarization of lytic granules from the T-cell: tumor cell immunological synapse.

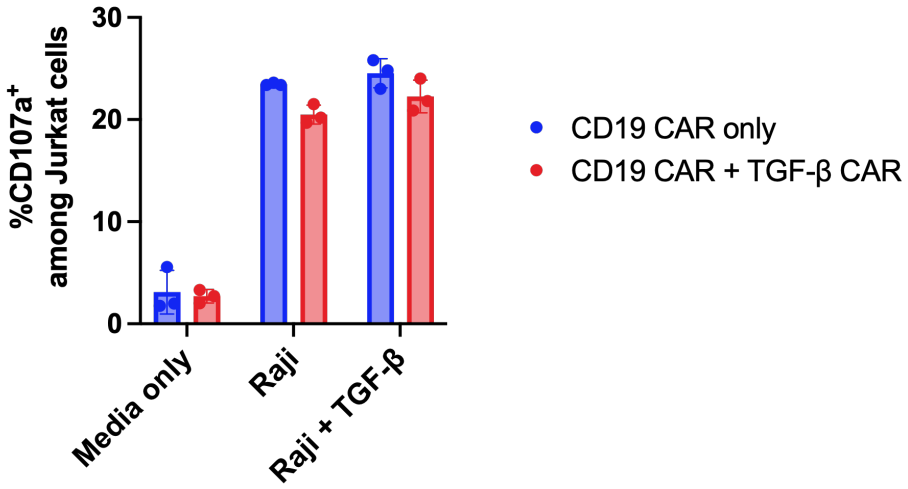

Figure 2.7 TGF-β CAR expression does not inhibit degranulation upon target cell encounter. Jurkat T cells expressing either the CD19 CAR alone or both the CD19 and TGF-β CAR were co-incubated with Raji cells. No significant differences in degranulation, as measured by CD107a expression, were observed when the CD19 CAR was expressed alone or co-expressed with the TGF-β CAR, regardless of whether TGF-β was present in co-cultures.

TGF-β CAR-T cells do not mediate systemic toxicity

Since basal levels of TGF-β are present in healthy tissue, we also assessed whether administration of TGF-β CAR-T cells might result in undesired systemic toxicities. Since concerns of toxicity are best addressed in hosts with intact immune systems, murine T cells were transduced to express a murine TGF-β CAR, consisting of murine CD28 co-stimulatory and murine CD3ζ signaling domains (**Supplementary Figure 2.2A**). Murine TGF-β CAR-T cells remained responsive to murine TGF-β *in vitro*, as evidenced by activation marker upregulation and cytokine production (**Supplementary Figure 2.2B**). Murine TGF-β CAR-T cells were then systemically administered to healthy C57BL/6 mice via intravenous injection. No gross evidence of toxicity was observed, as mouse weights remained stable over the course of one month

following adoptive cell transfer (**Figure 2.8A**). Furthermore, there was no significant expansion of $CD3^+$ T cells in peripheral blood 20 days after T-cell injection (**Figure 2.8B**). Histopathological analysis of kidney, spleen, and liver collected at time of euthanasia further corroborated the finding that TGF-β CAR-T cells do not induce systemic toxicity (**Table 2.2**).

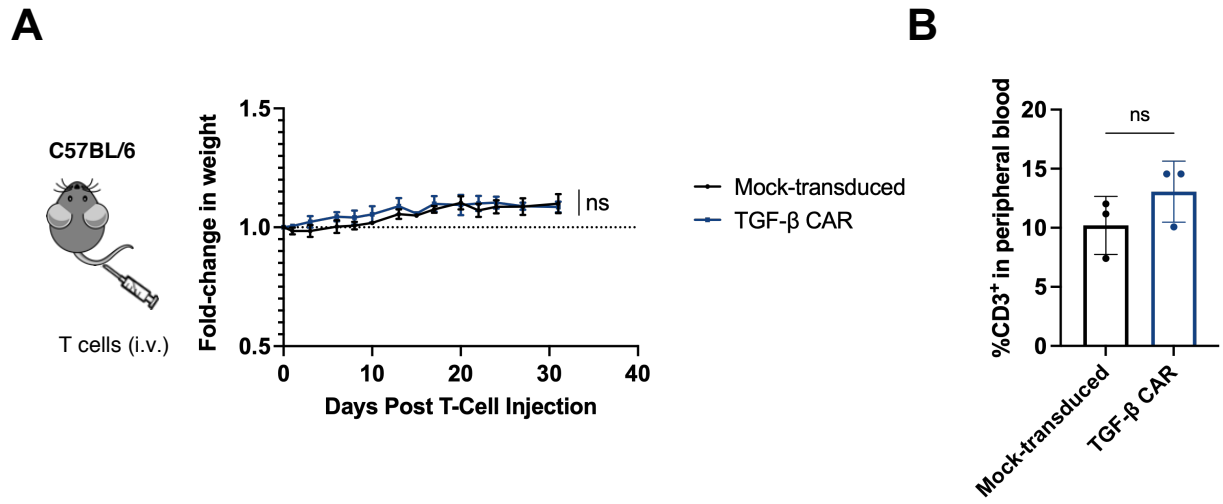

Figure 2.8 Systemic administration of TGF-β CAR-T cells is well-tolerated in immunocompetent mice. Healthy C57BL/6 mice were given an intravenous injection of TGF-β CAR-T cells. (a) Mouse weights were monitored through 30 days following CAR-T cell injection. No signs of gross toxicity were observed as mouse weights remained stable through the course of the study. Plotted are means ± standard deviations. No significant differences in weight were observed between mock-transduced and TGF-β CAR-T cell groups. (b) Retro-orbital blood was collected 20 days after T-cell injection. No significant T-cell expansion was observed as a result of TGF-β CAR-T cell injection.

Discussion

In light of lackluster responses to adoptive T-cell therapy in solid tumors, further engineering efforts are warranted to combat the immunosuppressive TME. Previous work has demonstrated that CARs can be engineered to respond to TGF-β, enabling transduced T cells to be stimulated, rather than suppressed, by TGF-β. Given the central role of TGF-β as a suppressive factor in the solid tumor milieu, we hypothesized that greater therapeutic outcomes could be achieved by equipping tumor-specific T cells with TGF-β–responsive CARs. However, we first sought to address potential concerns that might detract from the viability of the TGF-β CAR as a cancer therapeutic.

Previous work has demonstrated that TGF-β CARs with short spacers transduce more robust activation signals in conventional T cells. In regulatory T cells, short-spacer TGF-β CARs do not express efficiently on the cell surface, indicating that TGF-β CARs with short spacers may be preferable for anti-tumor applications not only due to their stronger signaling response, but also due to the minimized risk of immune suppression mediated by contaminating Tregs.

Notably, TGF-β CAR-transduced Tregs retain FOXP3 expression and remain suppressive when stimulated through the endogenous TCR, indicating that TGF-β CAR expression does not inherently alter the phenotype or function of Tregs. Rather, differences in CAR versus TCR signaling responses may be responsible for the lack of immune suppression observed when TGF-β CAR-Tregs are activated by TGF-β. These findings are also consistent with work demonstrating that Tregs expressing factor VIII-specific CARs do not suppress FVIII antibody production in mouse models of hemophilia A[17]. It has been suggested that Tregs require calibrated levels of TCR-mediated signaling to exert suppressive function, and that the more intense signaling downstream of CAR stimulation might abolish Treg suppressive function. Treg-mediated immune suppression has also been suggested to occur in a contact-dependent manner[18], and it is possible that lack of TGF-β CAR-mediated immune suppression is attributable to the lack of cell-cell contacts formed between TGF-β CAR-Tregs and neighboring Teffs.

We envision that TGF-β CARs can be paired with tumor-targeting receptors (either CARs or TCRs) to augment anti-tumor efficacy. However, a previous observation that TGF-β CAR activation triggers T-cell degranulation raised a potential concern that TGF-β CARs might divert lytic granules away from immunological synapses formed between tumor-specific T cells and target cells, thereby limiting T-cell cytotoxicity. We demonstrate, however, that TGF-β CAR stimulation does not hinder lytic granule polarization in CD19 CAR-expressing Jurkat T cells when challenged with $CD19^+$ Raji cells. Given that TGF-β is a soluble factor rather than a membrane-bound antigen, it is plausible that TGF-β CAR engagement does not transduce sufficient mechanical force to induce the broad cytoskeletal remodeling required for lytic granule polarization.

Various TGF-β inhibitors have been tested as either monotherapies or combination therapies[19–22]. One major drawback is that systemic inhibition of TGF-β signaling can be toxic, with preclinical studies reporting cardiotoxicities and skin lesions following administration of either small-molecule inhibitors or neutralizing antibodies[6–9]. Since tumor-specific T cells tend to localize at the tumor site, TGF-β CAR expression poses a minimized risk of toxicity as inhibition of TGF-β signaling would be confined to the TME. Notably, no adverse events were observed in healthy immunocompetent mice following systemic administration of T cells expressing only the TGF-β CAR and no tumor-targeting receptor, nor was there any evidence of excess T-cell expansion in the periphery. These data provide preliminary evidence that TGF-β CAR-T cells are well-tolerated. Altogether, our data demonstrate that the TGF-β CAR can be productively and safely expressed in T cells, and we therefore proceeded with downstream investigations of the TGF-β CAR–mediated enhancements to anti-tumor immunity.

Methods

DNA constructs

TGF-β–specific CARs with short and long spacers (IgG4 hinge and IgG4 hinge-CH2-CH3, respectively) were constructed as previously described[10]. The CARs contain the CD28 transmembrane domain, the CD28 cytosolic tail with GG mutations that may enhance CAR surface expression[23], and the CD3ζ cytosolic domain. The CD19-binding CARs contain the 4-1BB and CD3ζ intracellular domains and were previously described[24]. All receptors were linked by the "self-cleaving" T2A sequence to a truncated epidermal growth factor receptor (EGFRt), a non-signaling transduction marker[25].

Cell lines

TM-LCLs, an Epstein-Barr virus-transformed lymphoblastoid cell line, were gifts from Dr. Michael Jensen (Seattle Children's Research Institute). Jurkat T cells were obtained from ATCC. Cell lines were maintained in complete RPMI (RPMI-1640 (Lonza) + 10% heat-inactivated FBS (Gibco)).

Generation of CAR-expressing primary human T cells

For experiments involving Treg cells, $CD4^+$ T cells isolated as mentioned above were stained with fluorescently conjugated anti-CD4 (clone RPA-T4, BioLegend), anti-CD25 (clone BC96, BioLegend), and anti-CD127 (clone A019D5, BioLegend) antibodies, and then Treg ($CD4^+CD25^{hi}CD127^-$) and non-Treg ($CD4^+CD25^-$) fractions were enriched on a BD FACSAria II cell sorter. Treg cells were stimulated with CD3/CD28 Dynabeads at a 1:1 bead-to-cell ratio for 2 days and then transduced with lentivirus at an MOI of 5. Tregs were cultured in complete RPMI supplemented with 100 nM rapamycin and fed 300 U/mL IL-2 every 2 to 3 days. Dynabeads were removed after 10 days of culture, and cells were subsequently re-stimulated with Dynabeads at a 1:2 bead-to-cell ratio. Cells were then cultured in complete RPMI without rapamycin, and IL-2

was supplemented every 2 to 3 days. In some experiments, cultures were also supplemented with 5 ng/mL TGF-β after re-stimulation. Dynabeads were removed on day 20 or 21 of culture. Following Dynabead removal, Tregs were rested in IL-2–free medium for 24 hours prior to use in downstream experiments.

Treg suppression assays

In experiments testing TCR-mediated suppression, $CD4^+CD25^-$ Teffs that were never activated *in vitro* were stained with 1.25 μM CFSE. CFSE-labeled Teffs were seeded in OKT3-coated 96-well U-bottom plates at 5 x 10^4 cells/well with 1 μg/mL CD28 agonist antibody (clone CD28.2, BioLegend), and 0 or 5 ng/mL TGF-β. Tregs were added to each well at a 1:1 Treg:Teff ratio.

In experiments testing CAR-mediated suppression, CD19 CAR-transduced $CD4^+CD25^-$ Teffs were stained with 1.25 μM CFSE, and Tregs were stained with 1.25 μM CTV. CFSE-labeled Teffs were seeded in 96-well U-bottom plates at 5 x 10^4 cells/well with 1 x 10^5 irradiated TM-LCL cells and 0, 5, or 10 ng/mL TGF-β. CTV-labeled Tregs were added to each well at a 1:1 Treg:Teff ratio.

Confocal microscopy

Jurkat T cell lines were lentivirally transduced to express a granzyme B-mCherry fusion in addition to either a CD19 CAR alone, or a CD19 CAR and a TGF-β CAR together. Engineered Jurkat cells were co-incubated with $EGFP^+$ Raji cells in a 48-well glass-bottom plate (MatTek). TGF-β was added to media immediately prior to imaging. Z-stacks were obtained using a Zeiss LSM880 confocal microscope at 63x magnification (UCLA Broad Stem Cell Research Center).

Degranulation assay

1 x 10^5 Jurkat T cells were cultured alone or with 1 x 10^5 $EGFP^+$ Raji cells ± recombinant human TGF-β in a 96-well U-bottom plate. Cells were incubated at 37ºC for 1 hour, then anti-CD107a (Pacific Blue, BioLegend) and 1x monensin solution (BioLegend catalog no. 420701) were added to cultures and incubated at 37ºC for another 4 hours. Cells were washed in FACS buffer (PBS + 2% HI-FBS) prior to flow cytometric analysis.

Antibody staining for flow cytometry

EGFRt expression was measured by staining with biotinylated cetuximab (Eli Lilly; biotinylated in-house), followed by PE-conjugated streptavidin (Jackson ImmunoResearch catalog no. 016-110-084). CAR expression on the cell-surface was measured by staining with anti-DYKDDDDK (FLAG) tag conjugated to FITC (Miltenyi Biotec catalog no. 130-101-570). For intracellular FOXP3 staining, cells were fixed and permeabilized using the True-Nuclear Transcription Factor Buffer Set (BioLegend catalog no. 424401), and cells stained with PE-conjugated anti-FOXP3 (clone 206D, BioLegend catalog no. 320108).

To evaluate activation marker upregulation and cytokine production, murine T cells were incubated overnight in either media alone or with 10 ng/mL recombinant murine TGF-β. For activation marker staining, cells were stained with APC-conjugated anti-CD25 (clone 3C7, BioLegend catalog no. 101909). For intracellular cytokine staining, overnight cultures were supplemented with 1x brefeldin A (BioLegend catalog no. 420601) and 1x monensin solution (BioLegend catalog no. 420701). Cells were fixed with 1.5% paraformaldehyde followed by permeabilization with 100% methanol, and stained with PE-conjugated anti-mouse TNF-α (clone XMG1.2, BioLegend catalog no. 505817).

To monitor for potential expansion of TGF-β CAR-T cells in healthy immunocompetent mice, retro-orbital blood samples were treated with 1x Red Blood Cell Lysis Solution (Miltenyi Biotec), then stained with FITC-conjugated anti-mouse CD3 (clone 17A2, BioLegend catalog no. 100204).

Flow cytometry samples were run on a MACSQuant VYB flow cytometer (Miltenyi Biotec) and data were analyzed using FlowJo software (TreeStar).

Murine T-cell culture

Spleens were harvested from healthy, six- to eight-week–old C57BL/6mice. Single-cell suspensions were obtained by gentle maceration in 100-μm cell strainers placed over 50 mL Falcon tubes. $CD3^+$ T cells were enriched from bulk splenocytes using the Pan T Cell Isolation kit II, mouse (Miltenyi Biotec) following the manufacturer's protocol. Isolated T cells were activated with anti-mouse CD3/CD28 Dynabeads (Gibco) at a 1:1 bead-to-cell ratio. One day prior to transduction, 12-well non-TC–treated plates were coated overnight with 15 μg/mL RetroNectin (Takara) diluted in PBS at 4ºC. 24 hours following T-cell activation, retroviral supernatant was added to RetroNectin-coated plates and centrifuged at 2000xg for 2 hours (no brakes). Activated T cells were subsequently applied to spinoculated plates and centrifuged at 2000xg for 15 minutes (no brakes). T cells were maintained in RPMI-1640 + 10% HI-FBS + 50 μM β-mercaptoethanol. Cell cultures were supplemented with 50 U/mL human IL-2 every 2–3 days.

In vivo toxicity study

Animal studies were approved by the UCLA Animal Research Committee (ARC). C57BL/6 mice were obtained from the UCLA Department of Radiation Oncology. Healthy C57BL/6 mice were injected intravenously with either murine TGF-β CAR-T cells or mock-transduced murine T cells, at a dose of 4×10^6 total cells per mouse. On day 20 following T-cell injection, peripheral blood was collected from the retro-orbital sinus directly into tubes coated with EDTA (BD Biosciences, catalog no. 365974). Mouse weights were tracked for one month prior to euthanasia. Following euthanasia, mouse spleens, kidneys, and livers were collected and fixed in 10% neutral-buffered formalin for 24 hours. Fixed tissue samples were submitted to the Comparative

Pathology Laboratory at the University of California, Davis and analysis completed by a third-party histopathologist.

Statistical analyses

Statistical tests were performed in Excel. Two-tailed student's *t* tests with unequal variances were used to compare continuous variables between two groups, with the Sidak correction for multiple comparisons.

Supplementary Figures and Tables

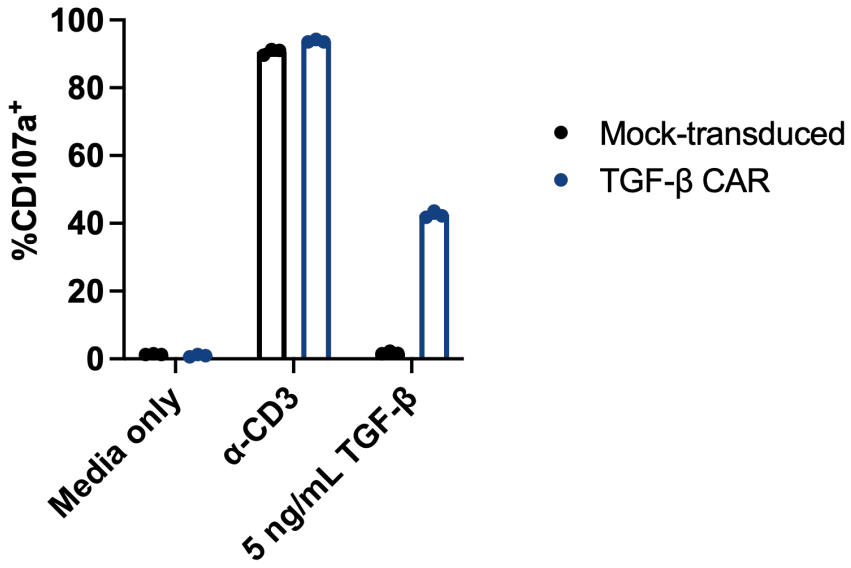

Supplementary Figure 2.1 TGF-β CAR-T cells degranulate upon CAR stimulation. Mock-transduced or TGF-β CAR-T cells were cultured either in media alone (negative control), with anti-CD3 (positive control), or 5 ng/mL TGF-β. TGF-β induces upregulation of the degranulation marker CD107a in TGF-β CAR-T cells, but not mock-transduced T cells, confirming that TGF-β CAR stimulation induces T-cell degranulation, albeit to a lesser extent compared to stimulation through the endogenous TCR. *Data courtesy of Dr. ZeNan Chang*

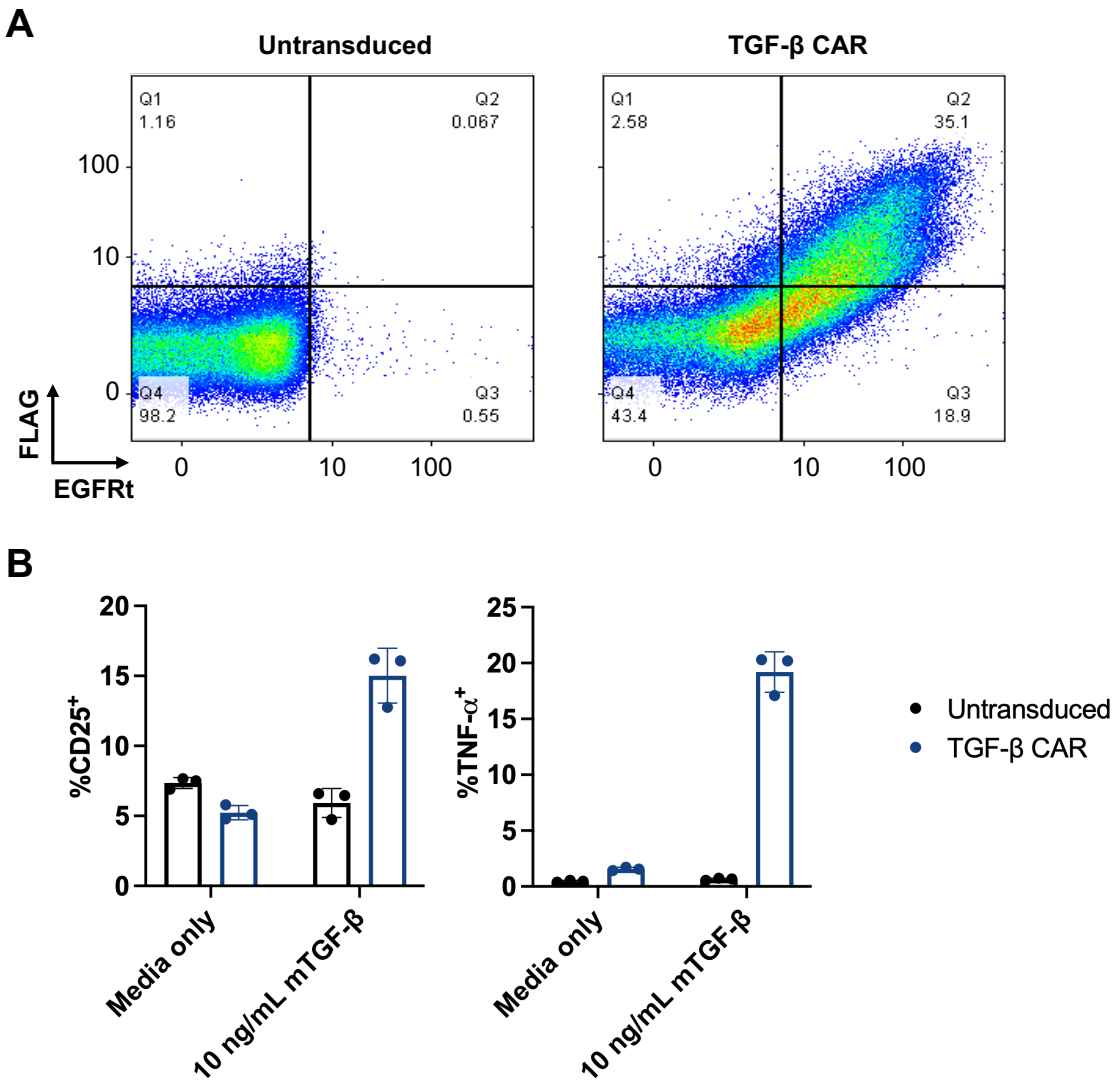

Supplementary Figure 2.2 Murine TGF-β CAR-T cells are functional. (A) Flow cytometric staining of the transduction marker EGFRt and surface CAR expression (by FLAG staining). Murine TGF-β CARs are efficiently transduced and express on the cell surface of transduced murine T cells. (B) CD25 expression (*left*) and TNF-α production (right) in untransduced or murine TGF-β CAR-T cells after culture in media alone or murine TGF-β. Murine TGF-β CAR-T cells are activated by murine TGF-β, as evidenced by CD25 upregulation and TNF-α production.

Condition	Total no. Jurkat cells imaged	No. Jurkat-Raji cell contacts observed	No. immunological synapses formed
No TGF-β	89	33	10
5 ng/mL TGF-β	90	34	13

Table 2.1 Quantification of total immunological synapses formed between Jurkat cells and Raji cells. TGF-β CAR engagement does not inhibit effective formation of immunological synapses between engineered Jurkat cells and Raji cells, as defined by localization of mCherry-GrB at the Jurkat:Raji interface.

	Mock	Mock	TGF-β CAR	TGF-β CAR
Gross Findings	NGL	NGL	Mild, diffuse pale-tan liver	NGL
Liver	Minimal, multifocal sinusoidal congestion	NA	NSF	NSF
Spleen	NSF	NSF	NSF	NSF
Kidneys	Focal perivascular lymphocytic aggregate	NSF	NSF	NSF

NGL = No gross lesions
NSF = No significant findings
NA = Not applicable, information not available

Table 2.2 Histopathological analysis of tissue samples in immunocompetent mice treated with TGF-β CAR-T cells. Liver, spleen, and kidneys were harvested from healthy immunocompetent C57BL/6 mice one month following intravenous administration of TGF-β CAR-T cells or mock-transduced T cells. Analyses were performed on fixed tissue by a third-party histopathologist, and no evidence of toxicity was observed.

References

1. Chen, M.-L. *et al.* Regulatory T cells suppress tumor-specific CD8 T cell cytotoxicity through TGF-β signals in vivo. *Proc. Natl. Acad. Sci.* **102**, 419–424 (2005).

2. Liu, V. C. *et al.* Tumor evasion of the immune system by converting CD4+CD25- T cells into CD4+CD25+ T regulatory cells: role of tumor-derived TGF-beta. *J. Immunol.* **178**, 2883–2892 (2007).

3. Huppa, J. B. & Davis, M. M. T-cell-antigen recognition and the immunological synapse. *Nat. Rev. Immunol.* **3**, 973–983 (2003).

4. Dustin, M. L. The Immunological Synapse. *Cancer Immunol. Res.* **2**, 1023–1033 (2014).

5. Siegel, P. M. & Massagué, J. Cytostatic and apoptotic actions of TGF-β in homeostasis and cancer. *Nat. Rev. Cancer* **3**, 807–820 (2003).

6. Anderton, M. J. *et al.* Induction of heart valve lesions by small-molecule ALK5 inhibitors. *Toxicol. Pathol.* **39**, 916–924 (2011).

7. Morris, J. C. *et al.* Phase I Study of GC1008 (Fresolimumab): A Human Anti-Transforming Growth Factor-Beta (TGFβ) Monoclonal Antibody in Patients with Advanced Malignant Melanoma or Renal Cell Carcinoma. *PLOS ONE* **9**, e90353 (2014).

8. Lacouture, M. E. *et al.* Cutaneous keratoacanthomas/squamous cell carcinomas associated with neutralization of transforming growth factor β by the monoclonal antibody fresolimumab (GC1008). *Cancer Immunol. Immunother.* **64**, 437–446 (2015).

9. Mitra, M. S. *et al.* A Potent Pan-TGFβ Neutralizing Monoclonal Antibody Elicits Cardiovascular Toxicity in Mice and Cynomolgus Monkeys. *Toxicol. Sci.* **175**, 24–34 (2020).

10. Chang, Z. L. *et al.* Rewiring T-cell responses to soluble factors with chimeric antigen receptors. *Nat. Chem. Biol.* **14**, 317–324 (2018).

11. Chang, Z. L. & Chen, Y. Y. CARs: Synthetic Immunoreceptors for Cancer Therapy and Beyond. *Trends Mol. Med.* **23**, 430–450 (2017).

12. Hinrichs, C. S. *et al.* Adoptively transferred effector cells derived from naïve rather than central memory CD8+ T cells mediate superior antitumor immunity. *Proc. Natl. Acad. Sci.* **106**, 17469–17474 (2009).

13. Klebanoff, C. A. *et al.* Determinants of successful CD8+ T-cell adoptive immunotherapy for large established tumors in mice. *Clin. Cancer Res.* **17**, 5343–5352 (2011).

14. Sommermeyer, D. *et al.* Chimeric antigen receptor-modified T cells derived from defined $CD8^+$ and $CD4^+$ subsets confer superior antitumor reactivity *in vivo*. *Leukemia* **30**, 492 (2016).

15. Turtle, C. J. *et al.* CD19 CAR–T cells of defined $CD4^+$:$CD8^+$ composition in adult B cell ALL patients. *J. Clin. Invest.* **126**, 2123–2138 (2016).

16. Liu, W. *et al.* CD127 expression inversely correlates with FoxP3 and suppressive function of human CD4+ T reg cells. *J. Exp. Med.* **203**, 1701–1711 (2006).

17. Nguyen, P., Moisini, I. & Geiger, T. L. Identification of a murine CD28 dileucine motif that suppresses single-chain chimeric T-cell receptor expression and function. *Blood* **102**, 4320–4325 (2003).

18. Zah, E., Lin, M.-Y., Silva-Benedict, A., Jensen, M. C. & Chen, Y. Y. T Cells Expressing CD19/CD20 Bispecific Chimeric Antigen Receptors Prevent Antigen Escape by Malignant B Cells. *Cancer Immunol. Res.* **4**, 498–508 (2016).

19. Wang, X. *et al.* A transgene-encoded cell surface polypeptide for selection, in vivo tracking, and ablation of engineered cells. *Blood* **118**, 1255–1263 (2011).

20. Rana, J. *et al.* CAR- and TRuC-redirected regulatory T cells differ in capacity to control adaptive immunity to FVIII. *Mol. Ther.* **29**, 2660–2676 (2021).

21. Nakamura, K., Kitani, A. & Strober, W. Cell contact-dependent immunosuppression by CD4(+)CD25(+) regulatory T cells is mediated by cell surface-bound transforming growth factor beta. *J. Exp. Med.* **194**, 629–644 (2001).

22. Rodon, J. *et al.* First-in-Human Dose Study of the Novel Transforming Growth Factor-β Receptor I Kinase Inhibitor LY2157299 Monohydrate in Patients with Advanced Cancer and Glioma. *Clin. Cancer Res.* **21**, 553–560 (2015).

23. Brandes, A. A. *et al.* A Phase II randomized study of galunisertib monotherapy or galunisertib plus lomustine compared with lomustine monotherapy in patients with recurrent glioblastoma. *Neuro-Oncol.* **18**, 1146–1156 (2016).

24. Faivre, S. *et al.* Novel transforming growth factor beta receptor I kinase inhibitor galunisertib (LY2157299) in advanced hepatocellular carcinoma. *Liver Int.* **39**, 1468–1477 (2019).

25. Wick, A. *et al.* Phase 1b/2a study of galunisertib, a small molecule inhibitor of transforming growth factor-beta receptor I, in combination with standard temozolomide-based radiochemotherapy in patients with newly diagnosed malignant glioma. *Invest. New Drugs* **38**, 1570–1579 (2020).

CHAPTER 3. Exploration of TGF-β CAR and tumor-targeting receptor pairing configurations demonstrate sub-optimal outcomes with receptor co-expression

Abstract

Although adoptive transfer of tumor-specific T cells has been remarkably effective in treating blood-based malignancies, efficacy against solid tumors has been much more limited, owing in large part to the immunosuppressive tumor microenvironment (TME). TGF-β is commonly overexpressed across several cancer types, and can orchestrate tumor tolerance by interacting with not only adoptively transferred T cells, but also endogenous immune cells. In light of the pivotal role of TGF-β in shaping the immunosuppressive TME, we hypothesized that better therapeutic responses to adoptive T-cell transfer against solid tumors could be achieved by inhibiting or reversing immunosuppressive TGF-β signaling. Since the TGF-β CAR does not direct tumor-targeting specificity, we evaluated anti-tumor function of different pairing configurations with tumor-specific receptors. In models of murine melanoma and human prostate cancer, we observed sub-optimal therapeutic outcomes when the TGF-β CAR is co-expressed with either a tumor-specific TCR or CAR, and instead provide support for more focused engineering efforts to develop single-chain, bispecific CARs responsive to tumor antigen and TGF-β.

Introduction

In light of our findings in support of the TGF-β CAR as a viable and safe receptor platform, we sought to evaluate its ability to enhance the efficacy of adoptively transferred tumor-specific T cells in solid tumor models. Since the TGF-β CAR does not direct tumor-cell killing, optimal anti-tumor function requires the TGF-β CAR to be paired with either a tumor-specific TCR or CAR. We therefore explored the effect of different modes of receptor pairing on anti-tumor function.

We first studied paired expression of the TGF-β CAR with a tumor-targeting TCR in the widely used B16-F10 murine melanoma model. Pmel-I T cells, which can be isolated from transgenic mice whose T cells all express a TCR specific for the gp100 antigen expressed by melanoma cells, are typically ineffective in adoptive transfer studies against tumor-bearing mice, and often require either combination with other immunotherapies or further engineering strategies[1–5], including expression of a TGF-β DNR[6], in order to achieve adequate control over tumor outgrowth. When paired with the pmel-I TCR, we considered whether a TGF-β chimeric co-stimulatory receptor (CCR) which lacks the CD3ζ signaling chain, would confer greater enhancements to therapeutic efficacy compared to a TGF-β CAR.

Due to MHC restriction, pmel-I T cells are homogeneously $CD8^+$. Others have reported, however, that adoptive transfer of a mixed population of $CD8^+$ and $CD4^+$ T cells results in better survival outcomes[7]. The presence of $CD4^+$ T cells may be particularly important for optimal function of the TGF-β CAR, which triggers cytokine production but not tumor-cell killing. In addition, tumor cells are known to downregulate MHC expression, allowing them to escape TCR-mediated killing. In light of these potential drawbacks of pairing the TGF-β CAR with a tumor-specific TCR, we next investigated whether the TGF-β CAR would be more effectively paired with a tumor-specific CAR, which is not MHC-restricted. To do this, we utilized a human prostate cancer model, pairing the TGF-β CAR with a prostate cancer maturation antigen (PSMA)-targeting CAR. PSMA is a clinically relevant target for prostate cancer immunotherapies, as studies have demonstrated overexpression of PSMA to be a specific marker of malignant tumor

with limited expression in healthy tissue outside of the prostate[8–10], but PSMA CAR-T cells have demonstrated limited efficacy in clinical trials[11]. TGF-β has been shown to limit the immunogenicity of prostate cancer and drive disease progression, with poor prognoses in patients with high levels of TGF-β[12,13]. TGF-β signaling inhibition is therefore a promising strategy to enhance the efficacy of PSMA-targeted therapies, and in fact, preclinical studies have demonstrated that TGF-β DNR expression potentiates PSMA CAR-T cell function[11]. We therefore hypothesized that similar, if not superior, improvements to anti-tumor efficacy could be achieved by pairing TGF-β and PSMA CARs, either by receptor co-expression, or expression of a single-chain bispecific CAR whose extracellular domain encodes both a TGF-β– and PSMA-binding scFv.

Here, we demonstrate that co-expressing a TGF-β CAR with either a tumor-targeting TCR or CAR results in sub-optimal anti-tumor function in models of melanoma and prostate cancer, respectively. Our findings indicate that receptor co-expression is not a robust pairing configuration for the TGF-β CAR, and instead provide support for deeper characterization of single-chain bispecific CARs targeting tumor antigen and TGF-β.

Results

TGF-β CARs underperform when co-expressed with the melanoma-specific pmel-I TCR

To assess whether TGF-β CARs can effectively augment the therapeutic efficacy of T-cell therapeutics against solid tumors, we first assessed their anti-tumor efficacy in the highly aggressive B16-F10 melanoma model. Pmel-I T cells, were engineered to express either TGF-β CARs or CCRs, encoding either CD28 or 4-1BB co-stimulatory domains (**Figure 3.1A**). In parallel to our panel of TGF-β CARs and CCRs, we also transduced pmel-I T cells to express either a TGF-β DNR, or an scFv-less CAR, which lacks an extracellular ligand-binding domain. The latter was included as a control to assess the anti-tumor function of the pmel-I TCR alone. Transduced T cells bicistronically expressed an EGFP-firefly luciferase (ffLuc) fusion protein, enabling us to

monitor T-cell expansion and persistence *in vivo* through bioluminescent IVIS imaging. C57BL/6 mice were subcutaneously inoculated with B16-F10 melanoma cells, and treated with pmel-I T cells intravenously after lymphodepleting irradiation (**Figure 3.1B**). With the exception of the TGF-β CAR encoding the CD28 co-stimulatory domain, TGF-β CARs and CCRs conferred slightly improved control over tumor outgrowth compared to scFv-less CAR-transduced pmel-I T cells (**Figures 3.1C, D**). Consistent with lackluster anti-tumor function, pmel-I T cells expressing the CD28-based TGF-β CAR exhibited the poorest *in vivo* expansion and persistence (**Figure 3.1E**). In contrast, pmel-I T cells expressing CD28-based TGF-β CCR exhibited the greatest *in vivo* persistence, suggesting that excessive activation driven by the CD28-based TGF-β CAR hinders anti-tumor T-cell function, which can be partially rescued by removing the CD3ζ signaling domain, which should reduce TGF-β–mediated signaling strength (**Figure 3.1E**). However, pmel-I T cells expressing the TGF-β DNR exhibited the greatest control over tumor burden and produced the best survival outcomes, with good *in vivo* persistence (**Figures 3.1C–E**), demonstrating that TGF-β CARs and CCRs underperform when paired with a pmel-I TCR.

One limitation of the melanoma model tested is that pmel-1 TCR expression is restricted to $CD8^+$ T cells. However, TGF-β CAR activation triggers functions more characteristic of $CD4^+$ T cells, such as cytokine release and proliferation, but not cytotoxicity[14]. We hypothesized that the therapeutic potential of the TGF-β CAR expression may not be fully appreciated when expressed solely in $CD8^+$ T cells. We therefore sought to evaluate TGF-β CAR function when co-expressed with tumor-targeting CARs, which are not MHC-restricted and can therefore be expressed by a mixed population of $CD4^+$ and $CD8^+$ T cells. Using a tumor-specific CAR also enables exploration of different receptor architectures to program simultaneous targeting of TGF-β and tumor antigen. In particular, we wished to compare the performance of TGF-β CARs when co-expressed with a tumor-specific CAR (termed “dual CAR”), and single-chain bispecific CARs, whose extracellular

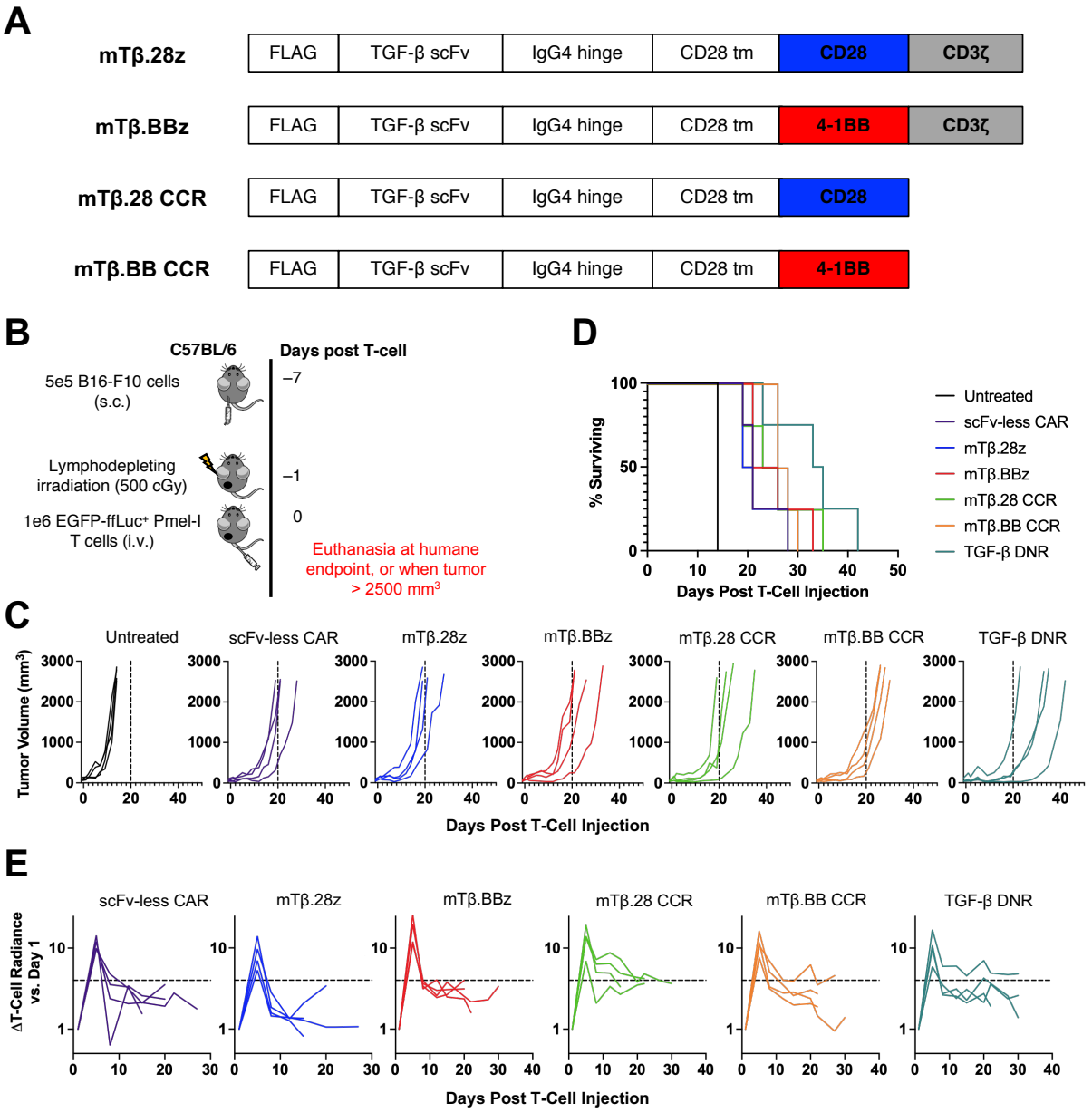

Figure 3.1 TGF-β CARs underperform in melanoma-specific pmel-I T cells. (A) Schematic of TGF-β chimeric receptor constructs tested. Briefly, either CARs (encoding CD3ζ signaling chain) or CCRs (lacking CD3ζ signaling chain) were tested. CARs and CCRs either encoded a CD28 or 4-1BB co-stimulatory domain. (B) Study schematic. C57BL/6 mice were injected subcutaneously with B16-F10 melanoma cells. Six days following tumor engraftment, mice were subjected to lymphodepleting irradiation. Engineered pmel-I T cells (with stable integration of EGFP-ffLuc) were injected intravenously the following day. Tumor burden was tracked by caliper measurement, and *in vivo* T-cell expansion and persistence was tracked by bioluminescent imaging (n = 4 mice per treatment group). (C) Tumor volumes, (D) survival curves, and (E) T-cell radiance measurements for mice treated with engineered pmel-I T cells. Each individual trace in (C) and (E) represents a single mouse, and traces end following euthanasia.

domains consist of both a tumor antigen-binding domain and a TGF-β–binding scFv (**Figure 3.2A**). Compared to dual CARs, single-chain bispecific CARs may be advantageous due to the reduced transgenic payload, facilitating viral integration into the T-cell genome[15,16].

Single-chain bispecific TGF-β/PSMA CARs outperform better than dual TGF-β/PSMA CARs

Next, we paired the TGF-β CAR with a PSMA-targeting CAR to interrogate different modes of CAR pairing. We engineered either dual or single-chain, bispecific TGF-β/PSMA CARs, and compared them against single-input PSMA CARs with or without TGF-β DNR expression. Since the single-input PSMA CAR utilizes a short extracellular spacer, the bispecific TGF-β/PSMA CAR was constructed such that the PSMA-targeting scFv (clone J591) was oriented in the membrane-proximal position and the TGF-β–targeting scFv in the membrane-distal position. Bispecific TGF-β/PSMA CARs configured in this manner enable us to control for potential differences in PSMA-targeting that may arise with changes in the distance between the PSMA-binding scFv and the cell-membrane. One potential advantage of a dual CAR configuration is the ability to program diverse T-cell signaling responses, which was exploited in our CAR designs: in the dual CAR configuration, CD28 and 4-1BB co-stimulatory domains were encoded by the TGF-β CAR and PSMA CAR, respectively; in contrast, the single-chain bispecific TGF-β/PSMA CAR encoded a shared 4-1BB co-stimulatory domain.

Both dual and bispecific TGF-β/PSMA CARs were efficiently expressed on the cell surface (**Supplementary Figure 3.1)**. However, bispecific TGF-β/PSMA CAR-T cells exhibited much weaker upregulation of the activation marker CD69 in response to TGF-β compared to dual TGF-β/PSMA CAR-T cells (**Figure 3.2B**). The dulled responsiveness of bispecific TGF-β/PSMA CARs to TGF-β *in vitro* is consistent with the observation that TGF-β CARs with a long extracellular spacer exhibit weaker signaling compared to their short spacer counterparts[14].

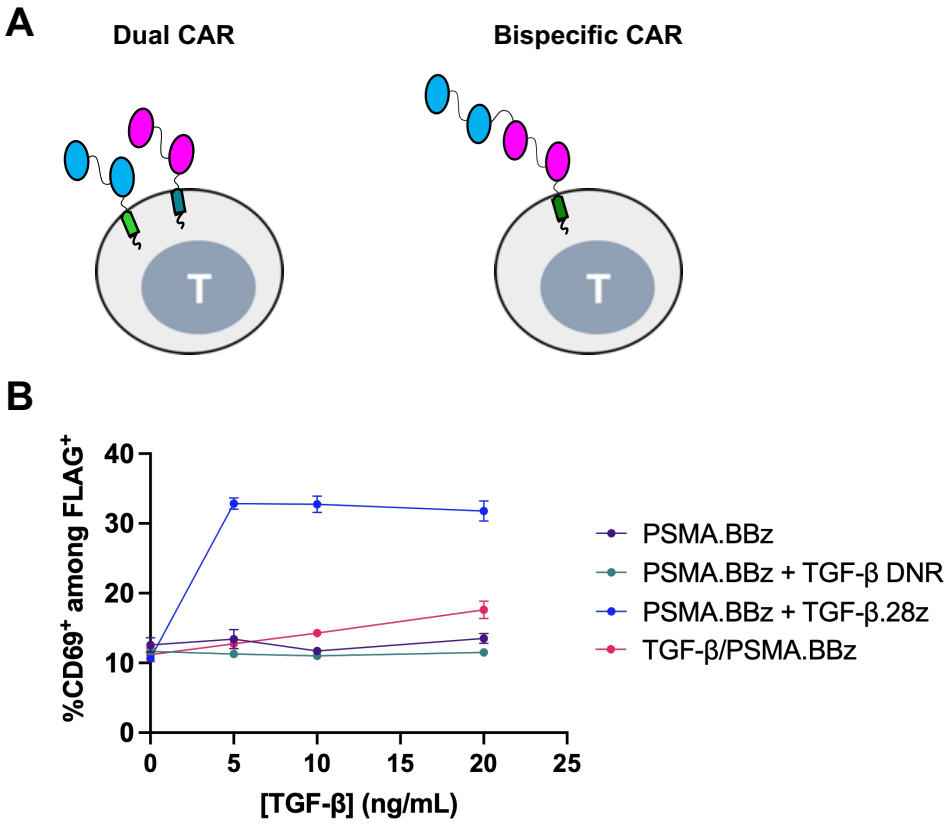

Figure 3.2 Dual TGF-β/PSMA CAR-T cells respond more strongly to TGF-β *in vitro* than bispecific TGF-β/PSMA CAR-T cells. (A) Schematic comparing dual and single-chain bispecific CAR designs. (B) CD69 expression in CAR-T cells following overnight incubation in increasing concentrations of TGF-β. While dual TGF-β/PSMA CAR-T cells strongly upregulate CD69 in the presence of TGF-β, bispecific TGF-β/PSMA CAR-T cells exhibit a weaker activation response.

We next evaluated the anti-tumor function of PSMA CAR-T cells *in vitro*. PC-3 prostate cancer cells, which naturally secrete both latent and active forms of TGF-β *in vitro* (**Supplementary Figure 3.2**), were engineered to express prostate-specific membrane antigen (PSMA), commonly overexpressed in prostate cancer cells. When co-cultured with PSMA$^+$ PC-3 tumor cells, dual and bispecific TGF-β/PSMA CAR-T cells exhibited the greatest proliferation (**Figure 3.3A**). However, PSMA CAR-T cells co-expressing the TGF-β DNR exhibited the greatest tumor-cell clearance (**Figure 3.3B**). Furthermore, whereas bispecific TGF-β/PSMA CAR-T cells and single-input PSMA CAR-T cells with and without TGF-β DNR expression continued to expand

after three rounds of challenges with PSMA^{+} PC-3 tumor cells, dual TGF-β/PSMA CAR-T cells significantly contracted following the third challenge (**Figure 3.3C**). Moreover, dual TGF-β/PSMA CAR-T cells exhibited a deficit in tumor-cell killing after four serial challenges (**Figure 3.3D**). Taken together, these findings indicate that despite greater responsiveness to TGF-β, dual TGF-β/PSMA CAR-T cells exhibit impaired anti-tumor function *in vitro*, and further studies were therefore conducted without dual TGF-β/PSMA CAR-T cells.

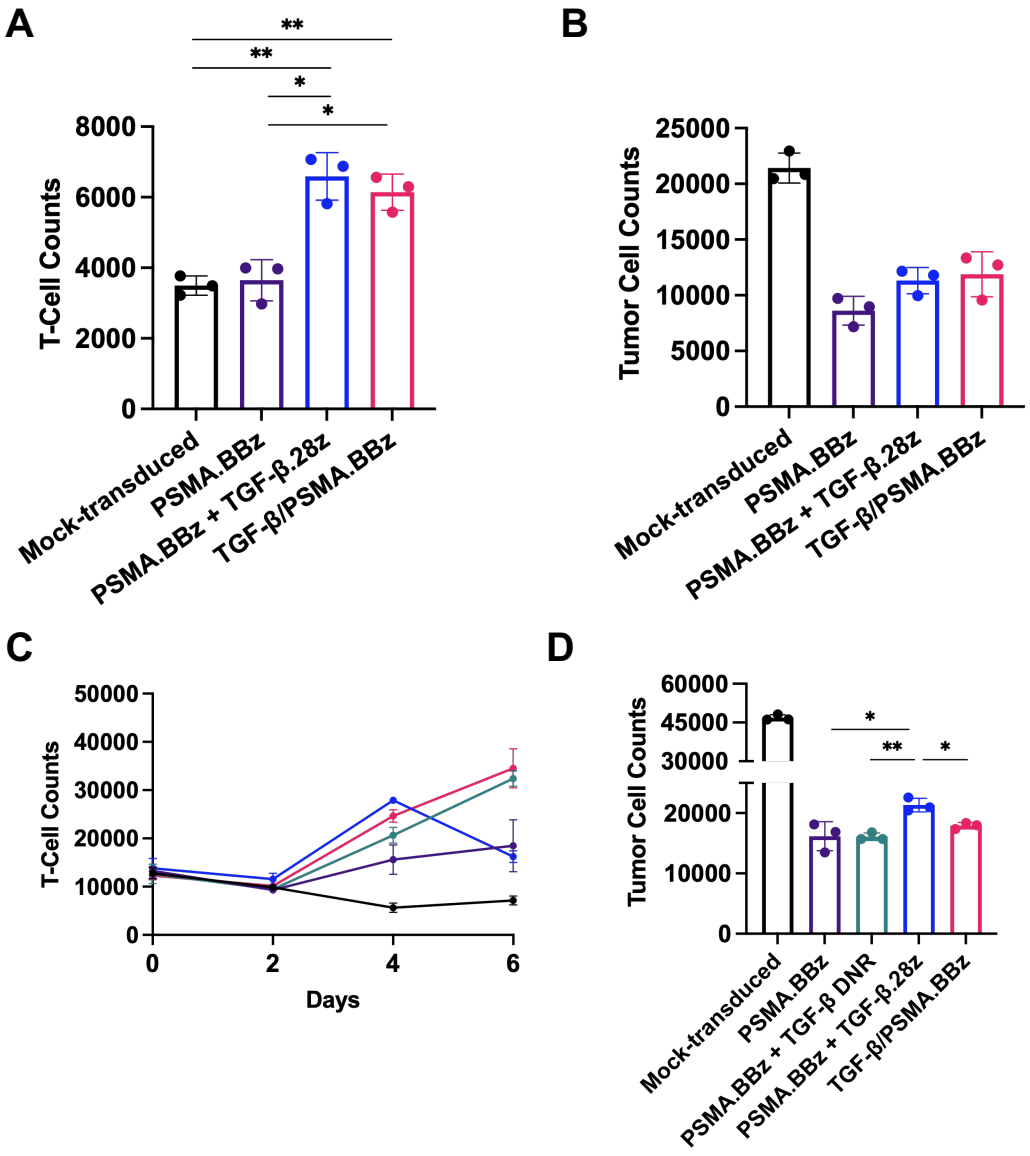

Figure 3.3 Dual TGF-β/PSMA CAR-T cells exhibit lackluster *in vitro* function. *(caption on next page)*

Figure 3.3 Dual TGF-β/PSMA CAR-T cells exhibit lackluster *in vitro* function. (A and B) PSMA$^+$ PC-3 tumor cells were co-cultured with CAR-T cells at a 1:2 E:T ratio. After four days, T-cell counts (A) and tumor cell counts (B) were measured by flow cytometry. Although dual and bispecific TGF-β/PSMA CAR-T cells exhibited superior proliferation compared to single-input PSMA CAR-T cells, no improvement over tumor-cell killing was observed. (C and D) CAR-T cells were repeatedly challenged every 2 days with PSMA$^+$ PC-3 tumor cells. T-cell counts were measured every two days (C) and tumor-cell counts were measured after four consecutive challenges (D). Despite strong early expansion, dual TGF-β/PSMA CAR-T cells exhibited a sharp contraction after the third challenge, resulting in sub-optimal tumor-cell killing following the fourth challenge.

Following *in vitro* characterization, CAR-T cell function was evaluated in a disseminated tumor model whereby PSMA$^+$ PC-3 tumors were injected intravenously, as previously reported (**Figure 3.4A**)[17,11]. In these studies, PSMA$^+$ PC-3 tumors were stably integrated to express EGFP-ffLuc, enabling us to monitor tumor progression by bioluminescent IVIS imaging. Compared to single-input PSMA CAR-T cells with or without the TGF-β DNR, bispecific TGF-β/PSMA CAR-T cells were slightly more effective at controlling tumor outgrowth, resulting in two tumor-free mice at the conclusion of the study (**Figure 3.4B**). Notably, tumor-free mice that were treated with bispecific TGF-β/PSMA CAR-T cells remained tumor-free even after a re-challenge with PSMA$^+$ PC-3 tumors (**Figures 3.4B, Supplementary Figure 3.3**). In addition, bispecific TGF-β/PSMA CAR-T cells were persistent *in vivo,* as adoptively transferred human CD45$^+$ cells were detectable in the peripheral blood of mice treated with TGF-β/PSMA CAR-T cells up to 82 days following tumor-cell injection, at comparable if not slightly higher levels compared to mice treated with PSMA CAR-T cells with or without TGF-β DNR expression (**Figure 3.4C**). Altogether, our findings demonstrate that co-expression of a TGF-β CAR with the PSMA CAR yields sub-optimal anti-tumor function compared to a single-chain bispecific TGF-β/PSMA CAR, which exhibits promising efficacy in preliminary *in vivo* studies. Despite these encouraging results, we observed spontaneous tumor regression in later studies using the same disseminated tumor model (**Supplementary Figure 3.4**), indicating that more robust, physiologically relevant models need to be developed for further study of bispecific TGF-β/PSMA CAR-T cell *in vivo* function.

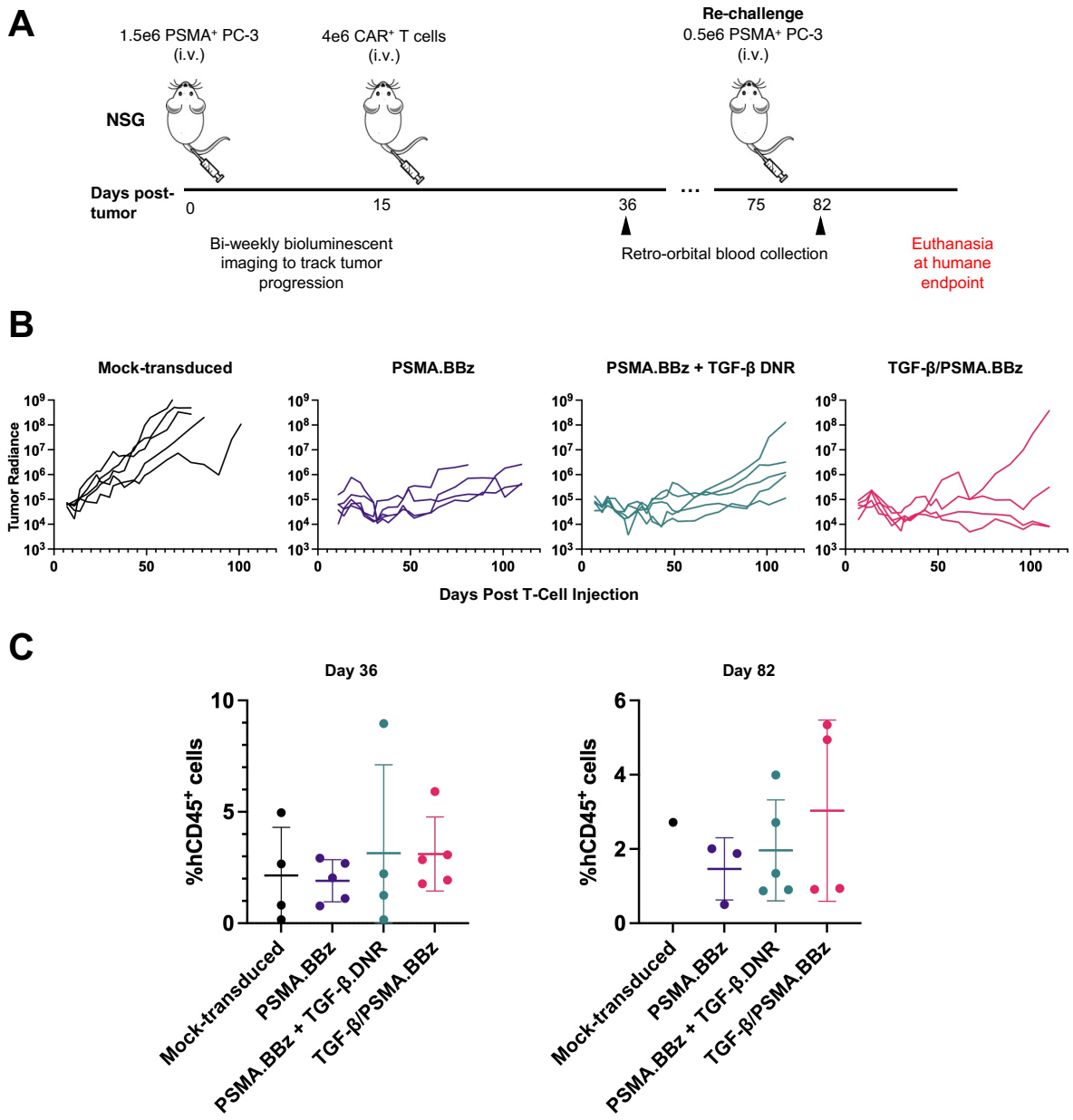

Figure 3.4 Bispecific TGF-β/PSMA CAR-T cells exhibit improved *in vivo* anti-tumor function. (A) Study schematic. PSMA$^+$ PC-3 tumor cells were injected intravenously in NSG mice. Fifteen days after tumor-cell injection, after confirming tumor engraftment, mice were treated with CAR-T cells. Tumor burden was tracked by bioluminescent imaging. Surviving mice on day 75 were re-challenged with tumor cells. Retro-orbital blood was collected on days 36 and 82 after tumor-cell injection. (n = 5 mice per treatment group) (B) Tumor radiance traces for mice treated as depicted in (A). Each individual trace represents a single mouse, and traces end following euthanasia. Mice treated with bispecific TGF-β/PSMA CAR-T cells exhibit the greatest control over tumor outgrowth over time. (C) Analysis of adoptively transferred, human CD45$^+$ cells in peripheral blood on days 36 and 82 of the study reveals good *in vivo* persistence of bispecific TGF-β/PSMA CAR-T cells.

Discussion

While work in our lab has previously demonstrated that expression of single-chain bispecific CARs targeting the multiple myeloma antigens BCMA and CS1 is more effective than co-expressing of BCMA- and CS1-targeting CARs[16], it was unclear to us whether these results were translatable when targeting both a surface-bound, tumor-associated antigen *and* a soluble factor. Here, we demonstrate that co-expressing a TGF-β CAR with either a tumor-targeting TCR or CAR results in sub-optimal anti-tumor function, providing rationale for engineering single-chain bispecific CARs targeting TGF-β and tumor antigen.

Although we speculate that the MHC-restriction imposed by the pmel-I TCR—which excludes $CD4^+$ T cells from the adoptively transferred T-cell population—contributes to the suboptimal performance of the TGF-β CAR in pmel-I T cells, further investigation is warranted to better understand whether it is indeed the case that TGF-β CARs are suboptimal when paired with tumor-targeting TCRs. A recently developed TYRP1 CAR[18] has been shown to effectively target B16-F10 melanoma, and studies pairing TGF-β CARs with TYRP1 CARs would enable a more meaningful comparison of TGF-β CAR function in the context of melanoma when paired with a non-MHC–restricted tumor-specific CAR versus an MHC-restricted TCR.

Nonetheless, co-expression of a TGF-β CAR and a PSMA CAR also results in sub-optimal anti-tumor function, indicating that the configuration of receptor pairing, rather than the type of tumor-targeting receptor used, may be the more relevant parameter dictating therapeutic outcomes. Indeed, single-chain bispecific TGF-β/PSMA CAR-T cells exhibited promising anti-tumor efficacy in preliminary studies. There may, however, exist more optimal bispecific CAR configurations, warranting a deeper exploration of possible designs. Of note, bispecific TGF-β/PSMA CARs were weakly responsive to TGF-β, likely due to the fact that the TGF-β–binding scFv was oriented distal to the cell membrane. We hypothesize that augmenting T-cell responses to TGF-β by engineering bispecific PSMA/TGF-β CARs that position the TGF-β–binding scFv in the membrane-proximal position (and the PSMA-binding scFv in the membrane-distal position)

may program even more robust anti-tumor function. It is, however, unknown whether re-orienting the PSMA-binding scFv towards the membrane-distal position in a bispecific CAR would negatively impact tumor-cell recognition and killing. Therefore, the proposed engineering efforts to optimize the bispecific TGF-β/PSMA CAR must also balance potential trade-offs in relative responses to TGF-β and tumor antigen.

It is worth noting that our preliminary *in vivo* studies using PSMA$^+$ PC-3 tumor cells did not accurately recapitulate the physiology of prostate cancer, as tumors were injected intravenously to form disseminated tumors rather than a solid tumor mass. The importance of proper tumor contextualization has been highlighted in previous work demonstrating that divergent responses to immune checkpoint blockade in prostate cancer bone metastases were observed depending on whether tumors were injected subcutaneously or intraosseously[19]. In fact, PSMA$^+$ PC-3 tumors did not always reliably engraft when injected intravenously in NSG mice, as we observed spontaneous tumor regression in control-treated mice in some studies. Therefore, further studies evaluating bispecific TGF-β/PSMA CAR-T cell function will require adoption of *in vivo* models that more faithfully recapitulate the prostate cancer TME.

Methods

Murine T-cell culture

Spleens were harvested from healthy, six- to eight-week–old Pmel-I mice. Single-cell suspensions were obtained by gentle maceration in 100-µm cell strainers placed over 50 mL Falcon tubes. $CD3^+$ T cells were enriched from bulk splenocytes using the Pan T Cell Isolation kit II, mouse (Miltenyi Biotec) following the manufacturer's protocol. Isolated pmel-I T cells were activated with anti-mouse CD3/CD28 Dynabeads (Gibco) at a 1:1 bead-to-cell ratio. One day prior to transduction, 12-well non-TC–treated plates were coated overnight with 15 µg/mL RetroNectin (Takara) diluted in PBS at 4ºC. 24 hours following T-cell activation, retroviral supernatant was added to RetroNectin-coated plates and centrifuged at 2000xg for 2 hours (no brakes). Activated T cells were subsequently applied to spinoculated plates and centrifuged at 2000xg for 15 minutes (no brakes). T cells were maintained in RPMI-1640 + 10% HI-FBS + 50 µM β-mercaptoethanol. Cell cultures were supplemented with 50 U/mL human IL-2 every 2–3 days.

Primary human T-cell culture

T cells were isolated from healthy donor whole-blood obtained from the UCLA Blood and Platelet Center. $CD3^+$ T cells were isolated using the RosetteSep $CD3^+$ T Cell Enrichment kit (STEMCELL Technologies) following the manufacturer's protocol. Isolated T cells were activated with CD3/CD28 Dynabeads (Gibco) at a 1:3 bead:cell ratio, and two rounds of retroviral transduction were performed at 48 hours and 72 hours following activation. T cells were maintained in complete RPMI (RPMI-1640 + 10% HI-FBS) and cultures were supplemented with 50 U/mL IL-2 and 1 ng/mL IL-15 every 2–3 days. Dynabeads were removed on day 7. All downstream assays were performed between day 9 and day 15 of culture.

In vitro cytotoxicity assays

For single timepoint challenges, 1.25 x 10^4 CAR-T cells were co-cultured with 2.5 x 10^4 $PSMA^+$ PC-3 cells in 96-well flat bottom plates. After four days, cells were harvested from co-cultures and counts were obtained by flow cytometry using a MACSQuant VYB.

For repeated antigen challenges, 1 x 10^4 CAR-T cells were co-cultured with 2 x 10^4 $PSMA^+$ PC-3 cells in 96-well flat-bottom plates. One set of technical replicates was set up for each re-challenge timepoint. Every two days, T cells were re-challenged with 2 x 10^4 $PSMA^+$ PC-3 tumors cells. At each timepoint, cells were harvested from co-cultures and counts were obtained using a MACSQuant VYB.

In vivo studies

All *in vivo* experiments were approved by the UCLA ARC. C57BL/6 and NSG mice were obtained from the UCLA Department of Radiation Oncology. Pmel-I mice were a generous gift from Dr. Rob Prins.

For studies with B16-F10 melanoma tumors, C57BL/6 mice were inoculated subcutaneously in the left flank with 5 x 10^5 B16-F10 cells. Tumors were measured three times per week with digital calipers, and tumor volume was calculated with the following formula: (1/2) x (Length) x $(Width)^2$. Six days after tumor-cell injection, mice were subjected to lymphodepleting irradiation (500 cGy). One day later (seven days after tumor-cell injection), mice with palpable tumors were randomized such that tumor burden was equally distributed among treatment groups, and mice were injected intravenously with 1 x 10^6 EGFP-$ffLuc^+$ pmel-I T cells. Starting on day of T-cell injection, mice were also given an intraperitoneal dose of 50000 units hIL-2 for three days. *In vivo* T-cell expansion and persistence was monitored by bioluminescent IVIS imaging. Briefly, mice were injected intraperitoneally with 3 mg D-luciferin (GoldBio) and imaged on an IVIS Lumina III LT Imaging System (Perkin Elmer). Photon flux was analyzed with LivingImage Software (Perkin Elmer). Mice were euthanized when they reached the humane endpoint, or when tumor volume exceeded 2500 mm^3.

For studies with $PSMA^+$ PC-3 tumors, NSG mice were injected intravenously with 1.5 x 10^6 $PSMA^+$ PC-3 tumor cells. Tumor burden was monitored throughout the study by bioluminescent IVIS imaging. Prior to treatment, tumor-bearing mice were randomized such that tumor burden was equally distributed among treatment groups. Fifteen days following tumor-cell injection, mice were injected intravenously with 4 x 10^6 CAR^+ T cells. Blood was collected from the retro-orbital sinus on days 36 and 82 following tumor-cell injection. On day 75 following tumor-cell injection, all surviving mice were re-challenged with an intravenous dose of 5 x 10^5 $PSMA^+$ PC-3 tumor cells. Mice were euthanized when they reached the humane endpoint.

ELISA

Cell culture supernatants were collected 24 and 48 hours after seeding 1 x 10^6 cells in 48-well plates. TGF-β concentrations in supernatant were determined using the Human TGF-β1 DuoSet ELISA kit (R&D Systems), following the manufacturer's protocol.

Flow cytometry

EGFRt expression was measured by staining with biotinylated cetuximab (Eli Lilly; biotinylated in-house), followed by PE-conjugated streptavidin (Jackson ImmunoResearch catalog no. 016-110-084). CAR expression on the cell-surface was measured by staining with anti-DYKDDDDK (FLAG) tag conjugated to APC (BioLegend catalog nos. 637308).

Activation marker upregulation in the presence of TGF-β was performed by staining human T cells with PacificBlue-conjugated anti-CD69 (clone FN50, BioLegend catalog no. 310920), and APC-conjugated anti-FLAG tag.

T-cell persistence in the peripheral blood of mice bearing disseminated $PSMA^+$ PC-3 tumors was analyzed by staining retro-orbital blood samples. Samples were treated with 1x Red Blood Cell Lysis Solution (Miltenyi Biotec), then stained with PacificBlue-conjugated anti-human

CD45 (clone HI30, BioLegend catalog no. 304029) and biotinylated cetuximab, followed by PE-conjugated streptavidin (Jackson ImmunoResearch).

Flow cytometry samples were run on a MACSQuant VYB flow cytometer (Miltenyi Biotec) and data were analyzed using FlowJo software (TreeStar).

Supplementary Figures

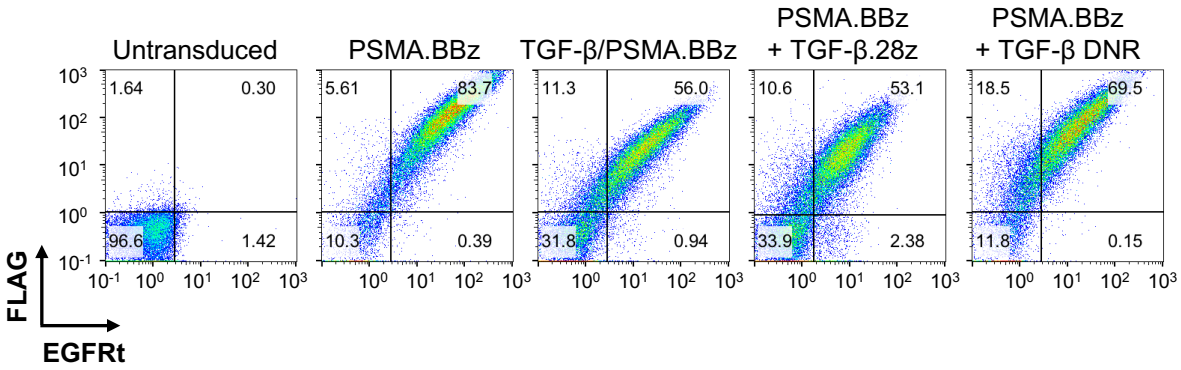

Supplementary Figure 3.1 Bispecific and dual TGF-β/PSMA CARs are efficiently expressed on the T-cell surface. Cell-surface expression of the transduction marker EGFRt and the CAR (by FLAG tag staining) was quantified by flow cytometry. Both bispecific and dual TGF-β/PSMA CARs are efficiently expressed on the cell surface of positively-transduced, EGFRt$^+$ T cells.

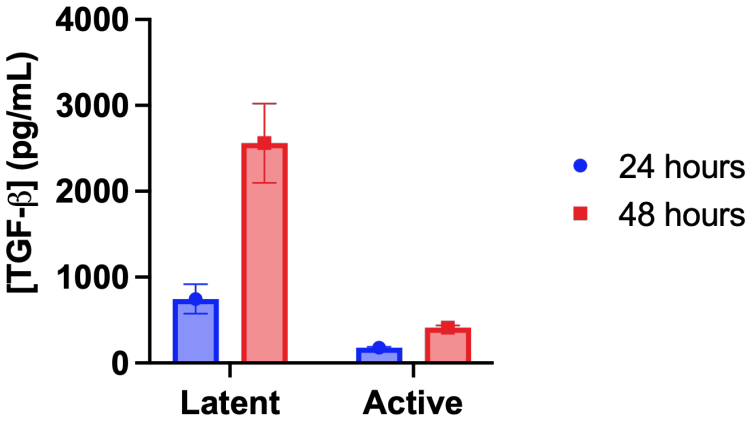

Supplementary Figure 3.2 PSMA$^+$ PC-3 tumor cells secrete TGF-β. Cell culture supernatant was collected 24 and 48 hours after seeding PSMA$^+$ PC-3 tumor cells. Both active and latent forms of TGF-β were detected by ELISA.

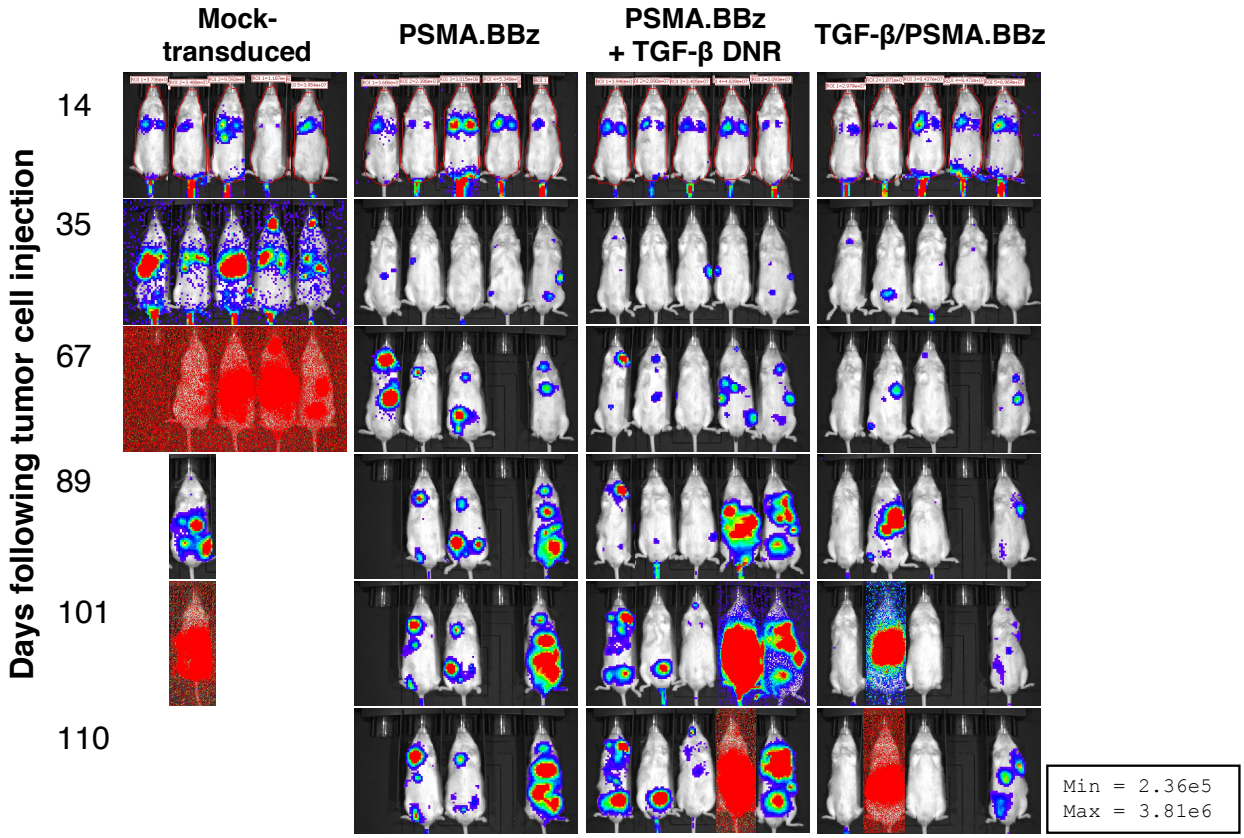

Supplementary Figure 3.3 Bioluminescent images of NSG mice bearing disseminated PSMA⁺ PC-3 xenografts. Images shown correspond to radiance traces plotted in Figure 3.4B. Bispecific TGF-β/PSMA CAR-T cells exhibit the greatest control over tumor outgrowth, resulting in complete tumor regression in 2/5 mice through 110 days following tumor-cell injection.

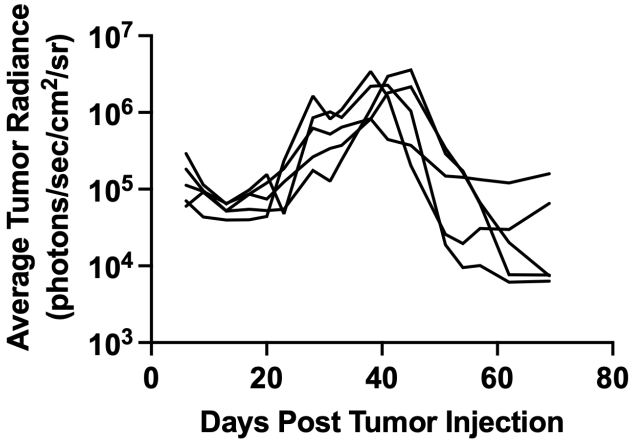

Supplementary Figure 3.4 Spontaneous rejection of disseminated PSMA⁺ PC-3 tumors in NSG mice. NSG mice were injected intravenously with PSMA⁺ PC-3 tumor cells. Mice were treated with mock-transduced T cells, and tumor burden was tracked over time by bioluminescent imaging. Despite initial tumor engraftment and progression, tumors were eventually lost.

References

1. Overwijk, W. W. *et al.* Tumor regression and autoimmunity after reversal of a functionally tolerant state of self-reactive CD8+ T cells. *J. Exp. Med.* **198**, 569–580 (2003).

2. Kerkar, S. P. *et al.* Tumor-Specific CD8+ T Cells Expressing Interleukin-12 Eradicate Established Cancers in Lymphodepleted Hosts. *Cancer Res.* **70**, 6725–6734 (2010).

3. Klebanoff, C. A. *et al.* Determinants of successful CD8+ T-cell adoptive immunotherapy for large established tumors in mice. *Clin. Cancer Res.* **17**, 5343–5352 (2011).

4. Drakes, D. J. *et al.* Optimization of T-cell Receptor–Modified T Cells for Cancer Therapy. *Cancer Immunol. Res.* **8**, 743–755 (2020).

5. Parisi, G. *et al.* Persistence of adoptively transferred T cells with a kinetically engineered IL-2 receptor agonist. *Nat. Commun.* **11**, 660 (2020).

6. Quatromoni, J. G. *et al.* T cell receptor (TCR)-transgenic CD8 lymphocytes rendered insensitive to transforming growth factor beta (TGFβ) signaling mediate superior tumor regression in an animal model of adoptive cell therapy. *J. Transl. Med.* **10**, 127 (2012).

7. Turtle, C. J. *et al.* CD19 CAR–T cells of defined $CD4^+$:$CD8^+$ composition in adult B cell ALL patients. *J. Clin. Invest.* **126**, 2123–2138 (2016).

8. Silver, D. A., Pellicer, I., Fair, W. R., Heston, W. D. & Cordon-Cardo, C. Prostate-specific membrane antigen expression in normal and malignant human tissues. *Clin. Cancer Res.* **3**, 81–85 (1997).

9. Mhawech-Fauceglia, P. *et al.* Prostate-specific membrane antigen (PSMA) protein expression in normal and neoplastic tissues and its sensitivity and specificity in prostate adenocarcinoma: an immunohistochemical study using mutiple tumour tissue microarray technique. *Histopathology* **50**, 472–483 (2007).

10. Perner, S. *et al.* Prostate-specific membrane antigen expression as a predictor of prostate cancer progression. *Hum. Pathol.* **38**, 696–701 (2007).

11. Kloss, C. C. *et al.* Dominant-Negative TGF-β Receptor Enhances PSMA-Targeted Human CAR T Cell Proliferation And Augments Prostate Cancer Eradication. *Mol. Ther.* **26**, 1855–1866 (2018).

12. Wikström, P., Stattin, P., Franck-Lissbrant, I., Damber, J.-E. & Bergh, A. Transforming growth factor β1 is associated with angiogenesis, metastasis, and poor clinical outcome in prostate cancer. *The Prostate* **37**, 19–29 (1998).

13. Matthews, E. *et al.* Down-regulation of TGF-β 1 production restores immunogenicity in prostate cancer cells. *Br. J. Cancer* **83**, 519–525 (2000).

14. Chang, Z. L. *et al.* Rewiring T-cell responses to soluble factors with chimeric antigen receptors. *Nat. Chem. Biol.* **14**, 317–324 (2018).

15. Bos, T. J., De Bruyne, E., Van Lint, S., Heirman, C. & Vanderkerken, K. Large double copy vectors are functional but show a size-dependent decline in transduction efficiency. *J. Biotechnol.* **150**, 37–40 (2010).

16. Zah, E. *et al.* Systematically optimized BCMA/CS1 bispecific CAR-T cells robustly control heterogeneous multiple myeloma. *Nat. Commun.* **11**, 1–13 (2020).

17. Kloss, C. C., Condomines, M., Cartellieri, M., Bachmann, M. & Sadelain, M. Combinatorial antigen recognition with balanced signaling promotes selective tumor eradication by engineered T cells. *Nat. Biotechnol.* **31**, 71–75 (2013).

18. CAR-Tnm cell therapy for melanoma targeting TYRP-1. https://www.cirm.ca.gov/our-progress/awards/car-tnm-cell-therapy-melanoma-targeting-tyrp-1 (2021).

19. Jiao, S. *et al.* Differences in Tumor Microenvironment Dictate T Helper Lineage Polarization and Response to Immune Checkpoint Therapy. *Cell* **179**, 1177-1190.e13 (2019).

CHAPTER 4. Bispecific CARs targeting IL-13Rα2 and TGF-β potentiate anti-tumor immunity against glioblastoma multiforme

Abstract

Glioblastoma multiforme (GBM) is one of the deadliest forms of cancer, with a median survival time of 12-15 months and no known cure to date. Although CAR-T cells targeting GBM-associated antigens such as interleukin-13 receptor subunit alpha-2 (IL-13Rα2) have been developed, clinical responses have been lackluster in large part due to the immunosuppressive tumor microenvironment (TME), which includes an abundance of inhibitory molecules such as TGF-β. To more effectively combat GBM, we engineered bispecific CARs targeting IL-13Rα2 and TGF-β, which can be used to program tumor-specific T cells that convert TGF-β from an immunosuppressant to an immunostimulant. Bispecific IL-13Rα2/TGF-β CAR-T cells confer greater therapeutic outcomes compared to single-input IL-13Rα2 CAR-T cells against both patient-derived GBM xenografts and syngeneic models of murine glioma. Importantly, bispecific IL-13Rα2/TGF-β CAR-T cells are also more effective than IL-13Rα2 CAR-T cells co-expressing a TGF-β DNR. Mechanistically, greater T-cell infiltration is observed in mouse brains following treatment with bispecific IL-13Rα2/TGF-β CAR-T cells, accompanied by a decrease in suppressive myeloid cell types. Altogether, our findings demonstrate that by reprogramming T-cell responses to TGF-β, bispecific IL-13Rα2/TGF-β CAR-T cells resist and remodel the immunosuppressive TME to drive potent anti-tumor responses in GBM.

Introduction

Glioblastoma multiforme (GBM) is the most prevalent primary brain tumor among adults, with poor patient prognoses even with aggressive treatment regimens combining chemotherapy, surgery, and radiation[1–5]. Engineering T cells to express tumor-targeting chimeric antigen receptors (CARs), which has proven to be remarkably effective against hematological malignancies[6–10], offers a tantalizing means to program *de novo* anti-tumor immunity. Several GBM-associated antigens—including interleukin-13 receptor subunit alpha-2 (IL-13Rα2), epidermal growth factor receptor variant III (EGFRvIII), the disialoganglioside GD2, the checkpoint molecule B7-H3, and human epidermal growth factor receptor 2 (HER2)—are under active clinical evaluation as targets for CAR-T cell therapies[11–15]. To date, the only patient with GBM who experienced a complete response after CAR-T cell therapy[11] received a product targeting IL-13Rα2, an antigen that is overexpressed by 58-78% of gliomas[16,17] and whose expression correlates with poor prognosis[16]. Multiple clinical trials evaluating different IL-13Rα2–targeted therapeutic modalities—ranging from CAR-T cell therapy to dendritic-cell vaccination to IL-13–conjugated toxins—have demonstrated IL-13Rα2 as a safe clinical target for malignant gliomas[11,18–21]. Nonetheless, therapeutic efficacy against GBM has been very limited thus far, with little to no improvement to overall or progression-free survival.

As with many solid tumors, a major mechanism of resistance to therapy in GBM is the highly immunosuppressive tumor microenvironment (TME)[22]. Transforming growth factor-beta (TGF-β), commonly overexpressed in a wide variety of solid tumor types, plays a prominent role in the GBM TME[23]. TGF-β can be produced not only by malignant glioma cells themselves but also by cells in the tumor stroma and plays a pivotal role in disease initiation and progression[24]. Besides maintaining tumorigenicity of glioma-initiating stem cells, promoting tumor-cell proliferation, and increasing tumor invasiveness[25–27], TGF-β also modulates immune-cell composition and function in the TME. For instance, TGF-β directly inhibits $CD8^+$ T-cell cytotoxicity and drives differentiation of naïve $CD4^+$ T cells into a regulatory phenotype[28–30]. Furthermore,

TGF-β recruits and polarizes suppressive myeloid cells such as M2-like tumor-associated macrophages (TAMs) and myeloid-derived suppressor cells (MDSCs); these cells can themselves produce TGF-β, thus effecting a positive feedback loop for maintenance of the immunosuppressive TME[31–33]. In light of its prominent role in shaping the immunosuppressive GBM microenvironment, TGF-β represents a promising therapeutic target. However, conventional strategies for blockade of TGF-β signaling, such as systemic administration of galunisertib, a small-molecule inhibitor of TGF-β receptor I (TGF-βRI), have had limited success in clinical trials[34–36]. A relative lack of immune effector cells in immunologically cold tumors such as GBM[37,38] and inefficient trafficking across the blood-brain barrier[39] may underlie the limited efficacy of TGF-β signaling blockade as a monotherapy. Furthermore, given the important functions that TGF-β plays in normal biological processes such as wound healing and angiogenesis[40], systemic administration of TGF-β signaling inhibitors raises concerns of toxicity[41,42].

In light of the programmability of cell-based immunotherapies, we sought to engineer IL-13Rα2–targeting CAR-T cells that can overcome TGF-β–mediated immune suppression. We have previously demonstrated that a TGF-β–responsive CAR can effectively convert TGF-β from an immunosuppressant into a stimulant of engineered primary human T cells[43]. Furthermore, TGF-β CAR-T cells are less prone to polarizing towards a regulatory phenotype in the presence of TGF-β and can protect neighboring tumor-specific T cells from TGF-β–mediated suppression of cytotoxicity[44]. Here, we demonstrate that when paired with an IL-13Rα2–targeting CAR, TGF-β CAR expression enhances anti-tumor immunity both by conferring resistance to TGF-β–mediated suppression in engineered T cells and by reprogramming neighboring immune cells in the TME from tolerogenic to inflammatory phenotypes.

Results

Bispecific IL-13Rα2/TGF-β CAR-T cells exhibit superior anti-tumor efficacy against patient-derived GBM neurospheres

To assess whether the TGF-β CAR can be effectively paired with a GBM-targeting CAR to enhance anti-tumor immunity, we designed a single-chain bispecific IL-13Rα2/TGF-β CAR, whose ligand-binding domain consists of the IL-13 E13Y mutein[45,46] fused to a TGF-β–specific single-chain variable fragment (scFv) (**Figure 4.1A**). The bispecific CAR, which contains 4-1BB and CD3ζ signaling domains, expresses efficiently on the cell surface of transduced primary human T cells (**Figure 4.1A**). The ability of bispecific IL-13Rα2/TGF-β CAR-T cells to recognize IL-13Rα2 was confirmed through lysis assays utilizing a panel of patient-derived GBM neurospheres expressing varying degrees of IL-13Rα2 and TGF-β (**Figure 4.1B, Supplementary Figure 4.1A, B**). IL-13Rα2 CAR-T cells (which only respond to IL-13Rα2 and are hereafter referred to as "single-input" IL-13Rα2 CAR-T cells) and T cells transduced to express an scFv-less CAR (which is identical to the IL-13Rα2/TGF-β CAR except it lacks any ligand-binding domain) were included as controls. Compared to single-input IL-13Rα2 CAR-T cells, IL-13Rα2/TGF-β CAR-T cells showed similar overall efficacy but more rapid killing kinetics against patient-derived GBM neurospheres, potentially as a result of TGF-β–mediated stimulation of bispecific IL-13Rα2/TGF-β CAR-T cells (**Figure 4.1C, D**). Efficient killing was observed against GBM with a wide range of IL-13Rα2 expression levels, including samples that were weak and heterogenous in IL-13Rα2 expression (e.g., GS013 neurospheres at 50% IL-13Rα2^{+}). However, both IL-13Rα2 and IL-13Rα2/TGF-β CAR-T cells failed to lyse GS054 neurospheres (27.8% IL-13Rα2^{+}) (**Figure 4.1C**). These results demonstrate that IL-13Rα2/TGF-β CAR-T cells can efficiently target clinically relevant tumor samples, but are unable to eliminate tumor cells with very dim or no IL-13Rα2 expression *in vitro*. This observation underscores the need to shape the GBM TME to facilitate recruitment of endogenous immune responses against a wider range of tumor antigens not targeted by the IL-13Rα2 CAR.

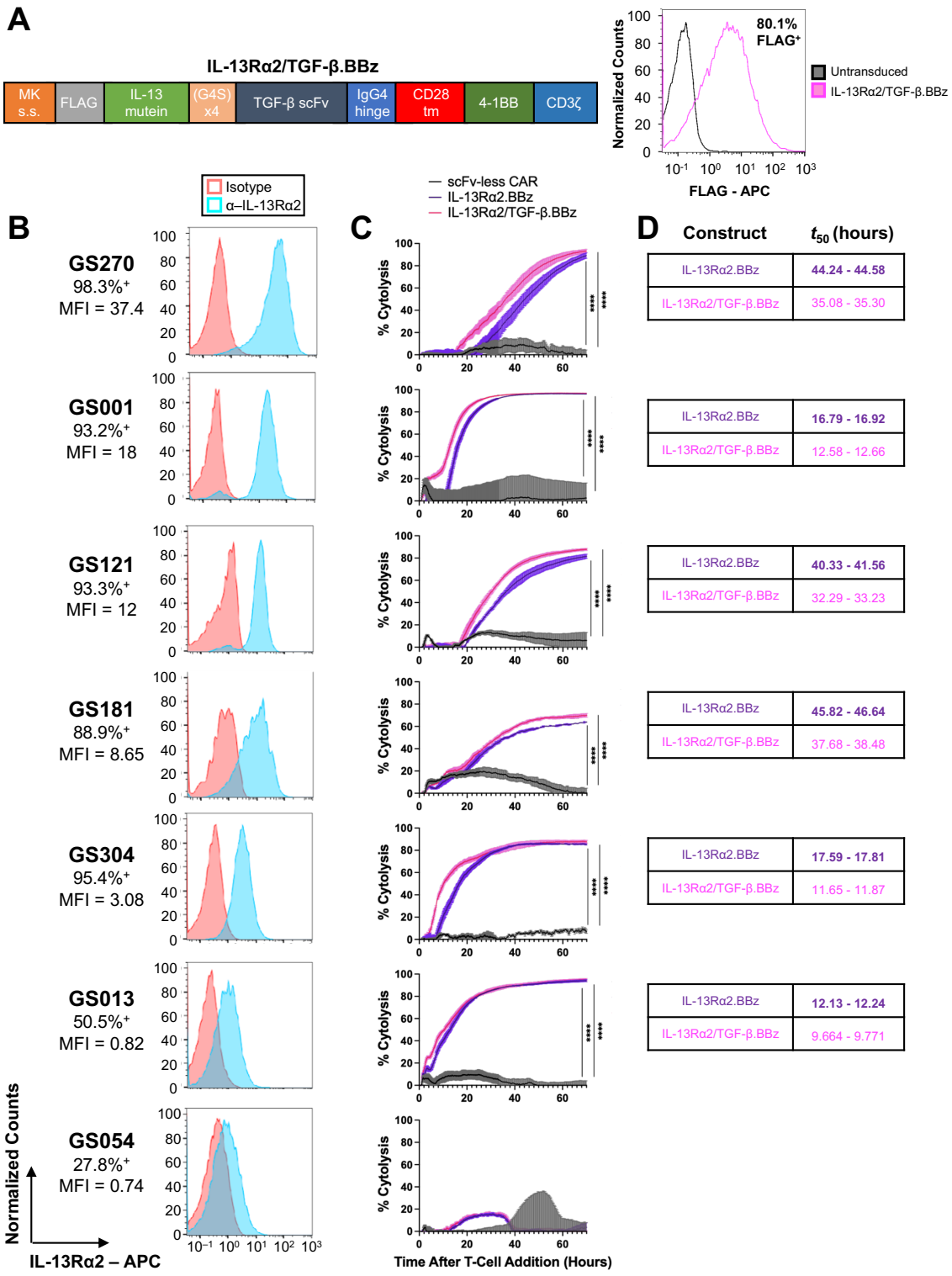

Figure 4.1 Bispecific IL-13Rα2/TGF-β CARs exhibit robust cytotoxicity *in vitro* against a panel of patient-derived neurosphere lines. *(caption continued on next page)*

Figure 4.1 *(cont)* (A) Schematic of bispecific IL-13Rα2/TGF-β CAR construct used in this study. The CAR encodes an N-terminal FLAG tag, enabling flow cytometric analysis of cell-surface CAR expression in transduced T cells. Representative histogram of bispecific IL-13Rα2/TGF-β CAR expression in human T cells via surface FLAG tag staining is shown. (B) Intraoperative samples from newly diagnosed and recurrent GBM patients at UCLA were used to establish a panel of neurosphere lines. Neurospheres were stained for surface IL-13Rα2 expression, revealing interpatient heterogeneity in IL-13Rα2 expression levels. (C) Patient-derived neurosphere lines were seeded overnight, and subsequently co-incubated with CAR-T cells at a 3:1 E:T ratio. Cytolysis was measured by xCelligence assay, revealing that bispecific IL-13Rα2/TGF-β CAR-T cells consistently lyse IL-13Rα2-expressing neurospheres with a broad range of antigen expression, with the exception of GS054, which is both weak and heterogeneous in IL-13Rα2 expression. (D) Data shown in (C) were fitted to a sigmoidal curve. Reported are 95% confidence intervals for the time to half-maximal killing (t_{50}; units in hours following addition of T cells to co-cultures). Bispecific IL-13Rα2/TGF-β CAR-T cells consistently exhibit more rapid killing kinetics compared to single-input IL-13Rα2 CAR-T cells. Pairwise comparisons of % cytolysis in (C) were performed on the last measurement value taken, and statistics computed using the two-tailed, unpaired, two-sample student's t test, with the Sidak correction for multiple corrections (****$P < 0.0001$).

We aimed to remodel the TME with the TGF-β–targeting moiety of the IL-13Rα2/TGF-β bispecific CAR, which is expected to confer three capabilities to engineered T cells: (a) inhibition of endogenous TGF-β signaling in engineered T cells through competition against endogenous TGF-β receptors for ligand binding, (b) inhibition of TGF-β signaling in nearby, endogenous immune cells by serving as a sink for TGF-β, and (c) activation of engineered T cells in the presence of TGF-β. The last capability distinguishes the TGF-β CAR from the TGF-β dominant-negative receptor (DNR), which is a truncated version of TGF-β receptor chain 2 that lacks the cytoplasmic signaling domain (**Figure 4.2A**)[47]. The DNR has been evaluated in clinical trials and has shown the ability to reduce endogenous TGF-β signaling and enhance T-cell function[48–50], but it lacks the capacity to trigger T-cell activation. Expression of the IL-13Rα2 CAR had no impact on TGF-β signaling when T cells are exposed to TGF-β1 (**Figure 4.2B**). In contrast, expression of the IL-13Rα2 CAR together with the DNR, or of the bispecific IL-13Rα2/TGF-β CAR, noticeably reduced SMAD3 phosphorylation in primary human T cells, confirming efficient inhibition of endogenous TGF-β signaling by both the bispecific CAR and the DNR. (**Figures 4.2A, B**). However, only bispecific IL-13Rα2/TGF-β CAR-T cells were activated by TGF-β as evidenced by upregulation of CD69 and CD25 (**Figure 4.2C**). Therefore, while both the bispecific IL-

13Rα2/TGF-β CAR and TGF-β DNR can block endogenous immunosuppressive TGF-β signaling, only the bispecific IL-13Rα2/TGF-β CAR converts TGF-β into an immunostimulant.

We next evaluated bispecific IL-13Rα2/TGF-β CAR-T cell function in an orthotopic model of patient-derived GBM. GS001 neurospheres, which naturally secrete TGF-β at high levels (**Supplementary Figure 4.1A**), were engineered to express firefly luciferase (ffLuc) and intracranially implanted in NSG mice. CAR-T cells were administered intratumorally once tumors were established (**Figure 4.2D**). A pilot study showed superior tumor control by bispecific IL-13Rα2/TGF-β CAR-T cells compared to T cells co-expressing the single-input IL-13Rα2 CAR and TGF-β DNR (**Supplementary Figure 4.1C**). In a larger-scale confirmatory study, bispecific IL-13Rα2/TGF-β CAR-T cells again exhibited greater control over tumor outgrowth and conferred more favorable survival outcomes compared to single-input IL-13Rα2 CAR-T cells, with or without DNR co-expression (**Figures 4.2E, F**). We noted that several mice in both studies reached humane endpoint without detectable tumor radiance signal (**Figure 4.2F; Supplementary Figure 4.1D**). Post-mortem examination of the brains of these mice showed clear abnormalities in tissue color and morphology, and immunohistochemistry (IHC) staining confirmed the presence of IL-13Rα2^{+} cells (**Supplementary Figure 4.1E**), suggesting the possibility of neurosphere differentiation upon engraftment in the brain that resulted in the loss of the luciferase transgene[51]. Taken together, these findings demonstrate that by not only blocking but also re-wiring suppressive TGF-β signaling, bispecific IL-13Rα2/TGF-β CAR-T cells exert more potent anti-tumor function compared to single-input IL-13Rα2 CAR-T cells, with or without TGF-β DNR expression.

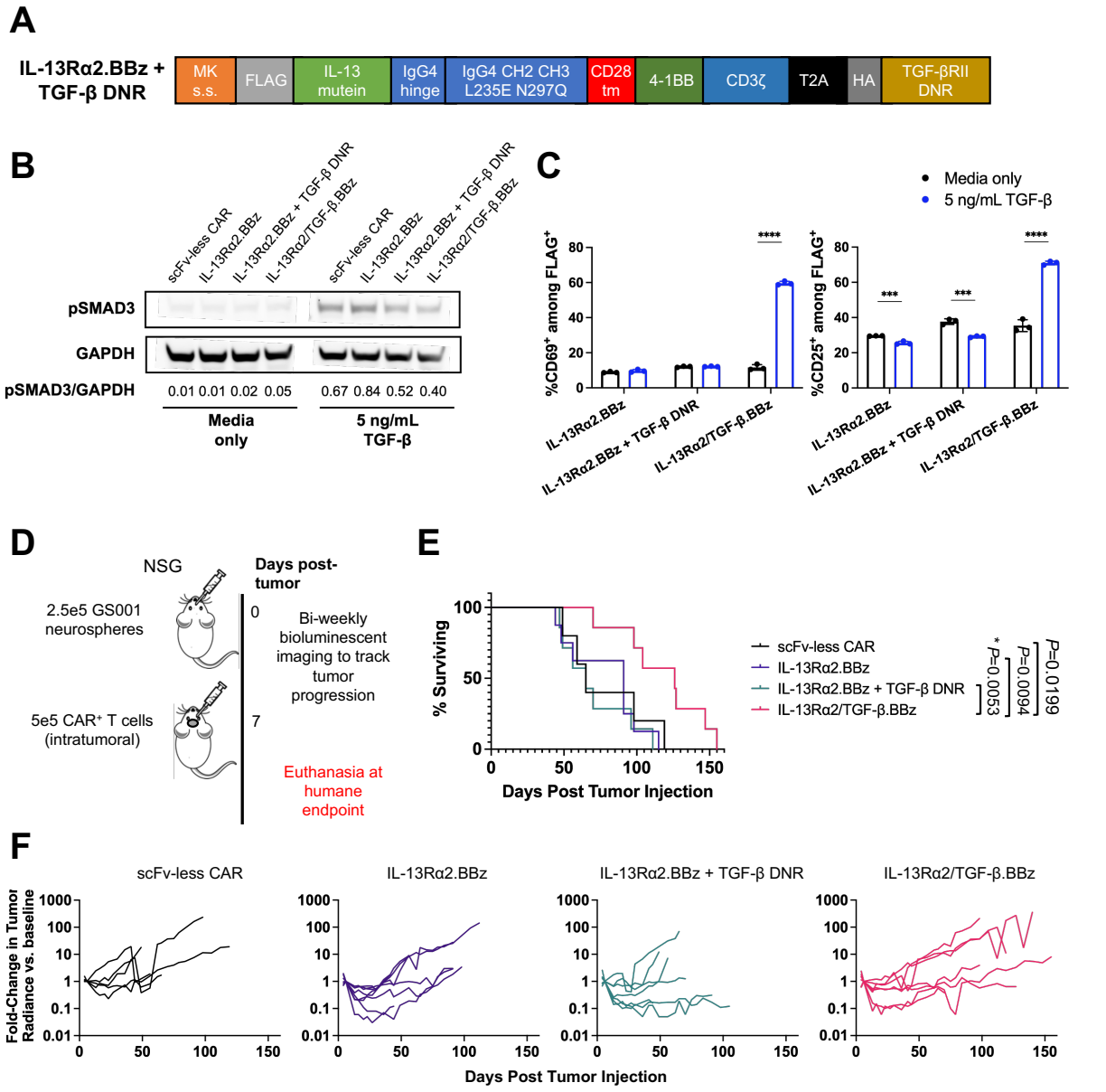

Figure 4.2 Bispecific IL-13Rα2/TGF-β CARs re-wire TGF-β signaling, resulting in superior therapeutic outcomes against orthotopically implanted xenografts. (A) Schematic of IL-13Rα2 CAR construct with bicistronic TGF-β DNR expression. (B) CAR-T cells were cultured in serum-free media, then incubated with or without TGF-β for 1 hour prior to cell lysis. Cell lysates were subsequently analyzed for phosphorylated SMAD by Western blot. Bispecific IL-13Rα2/TGF-β CAR-T cells and IL-13Rα2 CAR-T cells co-expressing the TGF-β DNR exhibit decreased SMAD phosphorylation in the presence of TGF-β compared to scFv-less or single-input IL-13Rα2 CAR-T cells, confirming blunted endogenous TGF-β signaling. (C) CAR-T cells were incubated with or without TGF-β overnight. CD69 (*left*) and CD25 (*right*) expression were measured , revealing that only bispecific IL-13Rα2/TGF-β CAR-T cells are activated in the presence of TGF-β. (D) 2.5 x 10^5 GS001 neurospheres were implanted into the right forebrains of NSG mice. Seven days following tumor-cell injection, 5 x 10^5 CAR-T cells were injected intratumorally (n = 5 for scFv-less CAR-T cell treatment group, n = 7-8 for IL-13Rα2 CAR-T cell treatment groups). Tumor burden was monitored by bioluminescent IVIS imaging, and mice were euthanized when they reached the humane endpoint.

(caption continued on next page)

Figure 4.2 *(cont)* (E) Survival curve and (F) tumor radiance traces of mice treated as depicted in (D). Each trace in (F) represents a single mouse, and traces for each mouse end following euthanasia. Bispecific IL-13Rα2/TGF-β CAR-T cells exhibit the most prolonged control over tumor outgrowth, resulting in superior survival outcomes.
Statistics in (C) were computed using the two-tailed, unpaired, two-sample student's *t* test, with the Holm-Sidak correction for multiple comparisons. Statistics in (E) were computed using the log-rank test, with Bonferroni's correction for multiple comparisons (**P* < 0.05, ***P* < 0.01, ****P* < 0.001, *****P* < 0.0001). No statistical significance was detected for pairwise comparisons not shown.

Bispecific IL-13Rα2/TGF-β CAR-T cells interact with neighboring immune suppressor cells to orchestrate anti-tumor immunity

Given the major role of TGF-β in regulation of immunosuppressive cell types such as TAMs or MDSCs, we next sought to understand how bispecific IL-13Rα2/TGF-β CAR-T cells can influence, or be influenced by, endogenous immune cells in the TME. Such an exploration requires the use of syngeneic tumor models in immunocompetent mice, which in turn requires that the CAR is functional when expressed by murine T cells and can respond to murine TGF-β. We first confirmed that the single-input TGF-β CAR responds equally robustly to human and murine TGF-β (**Supplementary Figure 4.2A**). We further observed that murine T cells expressing the TGF-β CAR robustly respond to TGF-β; in fact, the TGF-β CAR containing human 4-1BB and CD3ζ signaling domains signals more strongly than an equivalent CAR containing murine signaling domains when expressed in murine T cells (**Supplementary Figure 4.2B**). Finally, we confirmed that murine T cells expressing the bispecific IL-13Rα2/TGF-β CAR encoding human signaling domains respond to both human and murine TGF-β (**Supplementary Figure 4.2C**). Taken together, these results indicate that the human bispecific IL-13Rα2/TGF-β CAR can be directly evaluated in immunocompetent mouse models bearing syngeneic GBM tumors.

Murine CT-2A and GL261 glioma lines, which naturally secrete TGF-β (**Supplementary Figure 4.2D**), were engineered to express human IL-13Rα2 (**Supplementary Figure 4.2E**) and ffLuc. Murine T cells expressing the human bispecific IL-13Rα2/TGF-β CAR effectively lysed IL-

13Rα2^{+} target cells (**Supplementary Figure 4.2F**) and proliferated in response to antigen (**Supplementary Figure 4.2G**).

In a syngeneic glioma model, C57BL/6 mice were intracranially implanted with IL-13Rα2^{+} GL261 glioma cells and treated with either scFv-less or IL-13Rα2–targeting CAR-T cells. Bispecific IL-13Rα2/TGF-β CAR-T cells—but not single-input IL-13Rα2 CAR-T cells with or without DNR co-expression—were able to mount an observable anti-tumor response and achieve tumor clearance or delayed tumor outgrowth in a subset of animals (**Figures 4.3A, B**). However, no statistically significant difference in overall survival was detected. We next evaluated bispecific IL-13Rα2/TGF-β CAR-T cell function in the CT-2A murine glioma model (**Figure 4.3C**), which is immunologically distinct from GL261 tumors[52] and responds differently to immunotherapies [53,54]. Overall, CT-2A tumor outgrowth was better controlled by IL-13Rα2–targeting CAR-T cells when compared to GL261 tumors, and both bispecific IL-13Rα2/TGF-β CAR-T cells and IL-13Rα2 CAR-T cells co-expressing the TGF-β DNR exhibited superior anti-tumor function compared to single-input IL-13Rα2 CAR-T cells (**Figures 4.3D, E**). However, there was again no statistically significant difference in the survival of animals treated with on-target CAR-T cells. Mice treated with bispecific IL-13Rα2/TGF-β CAR-T cells and IL-13Rα2 CAR-T cells co-expressing the TGF-β DNR exhibited comparable control over tumor outgrowth in this model. However, a greater proportion of bispecific IL-13Rα2/TGF-β CAR-T cell treated mice were able to reject antigen-negative IL-13Rα2^{-} tumors upon re-challenge, suggesting that bispecific IL-13Rα2/TGF-β CAR-T cells more effectively mobilize an endogenous anti-tumor immune response (**Figures 4.3D, E**).

Failure to observe statistically significant differences in anti-tumor function between IL-13Rα2–targeting CAR-T cells may be attributed, in part, to immunogenicity of the CT-2A tumor cell line, which was engineered to express human IL-13Rα2, EGFP (derived from jellyfish), and firefly luciferase. In *ex vivo* cultures of brain-infiltrating leukocytes recovered from mice that had rejected IL-13Rα2^{+} CT-2A tumors, we found stronger IFN-γ production in response to IL-13Rα2^{+}

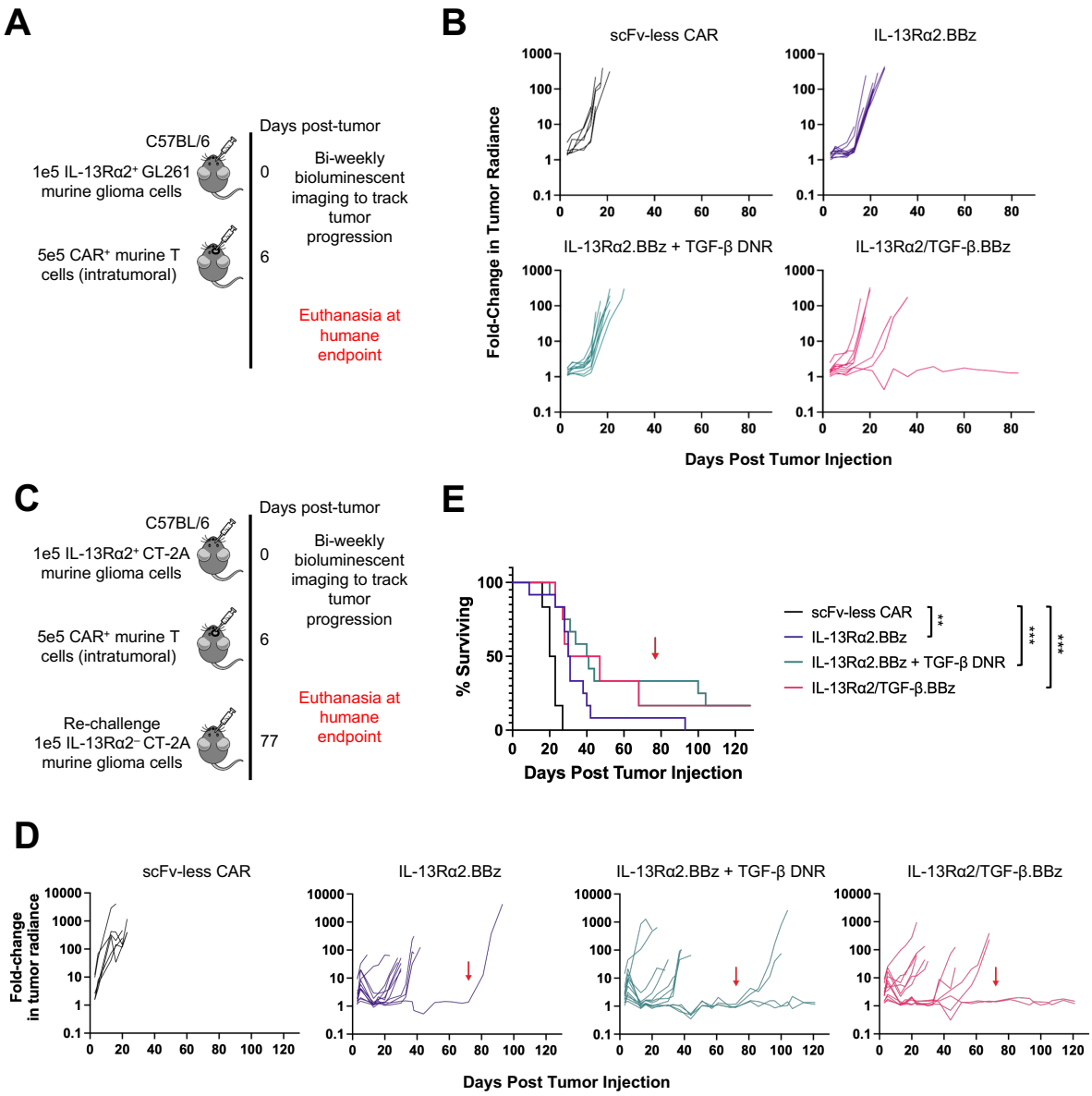

Figure 4.3 Bispecific IL-13Rα2/TGF-β CAR-T cells potentiate anti-tumor responses in syngeneic GBM models. (A) Study schematic. 1 x 10^5 IL-13Rα2$^+$ GL261 tumor cells were implanted intracranially into the right forebrains of C57BL/6 mice. Six days following tumor-cell injection, 5 x 10^5 CAR-T cells were injected intratumorally (n = 6 for scFv-less CAR-T cell treatment group, n = 10 for IL-13Rα2 CAR-T cell treatment groups). Tumor burden was monitored by bioluminescent IVIS imaging, and mice were euthanized when they reached the humane endpoint. (B) Tumor radiance traces of mice treated as depicted in (A). No anti-tumor response is observed following treatment with IL-13Rα2 CAR-T cells with or without TGF-β DNR expression, and only bispecific IL-13Rα2/TGF-β CAR-T cells are able to mount an anti-tumor response. (C) Study schematic. 1 x 10^5 IL-13Rα2$^+$ CT-2A tumor cells were implanted intracranially into the right forebrains of C57BL/6 mice. Six days following tumor-cell injection, 5 x 10^5 CAR-T cells were injected intratumorally (n = 6 for scFv-less CAR-T cell treatment group, n = 12 for IL-13Rα2 CAR-T cell treatment group). On day 77, all remaining mice were tumor-free, and re-challenged with 1 x 10^5 IL-13Rα2$^-$ CT-2A glioma cells. Tumor burden was monitored by bioluminescent IVIS imaging, and mice were euthanized when they reached the humane endpoint.
(caption continued on next page)

Figure 4.3 *(cont)* (D) Tumor radiance and (E) survival curves of mice treated as depicted in (C). Red arrow depicts timepoint of re-challenge with antigen-negative tumor cells. IL-13Rα2/TGF-β CAR-T cells and IL-13Rα2 CAR-T cells expressing the TGF-β DNR both improved anti-tumor control comparably well, but IL-13Rα2/TGF-β CAR-T cell treatment resulted in more robust protection against antigen-negative tumors. Each trace in (B) and (D) represents a single mouse, and traces for each mouse end following euthanasia. Statistics in (E) were computed using the log-rank test, with Bonferroni's correction for multiple comparisons (***P* < 0.01, ****P* < 0.001). No statistical significance was detected for pairwise comparisons not shown.

CT-2A glioma cells (which also express EGFP and ffLuc) compared to either parental or EGFP-ffLuc$^+$ CT-2A cells (**Supplementary Figure 4.3**).

To understand the influence of bispecific IL-13Rα2/TGF-β CAR-T cells on the surrounding TME, cytometry by time-of-flight (CyTOF) was performed on brain tissue collected seven days following adoptive T-cell transfer (**Figure 4.4A, Supplementary Figure 4.4A**). We noted divergent responses to IL-13Rα2 CAR-T cell treatment in the GL261 and CT-2A TMEs. Specifically, the brains of mice bearing GL261 tumors showed an enrichment of suppressive M-MDSCs and M2 TAMs after treatment with IL-13Rα2–targeting CAR-T cells, compared to treatment with scFv-less CAR-T cells (**Figure 4.4B**). In contrast, on-target CAR-T cell treatment resulted in a decrease in M-MDSC infiltration to CT-2A tumor-bearing brain, and little to no M2 TAMs were observed regardless of treatment condition (**Figure 4C**). The data shown in Figures 4.4B and 4.4C represent relative frequency of different cell populations, which does not always reflect absolute cell content. However, flow cytometric staining of CD45$^+$ cells revealed similar total numbers of brain-infiltrating leukocytes across treatment groups (**Supplementary Figure 4.4B**); thus, the observed changes in cellular frequencies correspond to an actual increase in suppressive myeloid cells in GL261-bearing brain upon on-target CAR-T cell treatment. Moreover, myeloid cells in GL261-bearing brains upregulated PD-L1 expression upon on-target CAR-T cell treatment compared to scFv-less CAR-T cell treatment, with a concomitant increase in PD-1 expression among T cells (**Figures 4.4D–F**). In contrast, on-target CAR-T cell treatment of CT-2A–bearing brains resulted in decreased PD-L1 expression among myeloid cells and decreased PD-1 expression among T cells when compared to treatment with scFv-less CAR-T cells (**Figure**

4.4D). Taken together, these results suggest GL261 tumors present a more immunosuppressive TME than CT-2A cells, consistent with the observation that GL261 is more resistant than CT-2A to CAR-T cell-mediated tumor control (**Figures 4.3B, D**).

The observation that immune cells in the GL261 TME upregulate PD-1/PD-L1 is also consistent with prior reports that GL261 is sensitive to checkpoint blockade therapy[53,55,56]. Given that TGF-β has been shown to exert immunosuppression through enhancing PD-1/PD-L1 signaling[57–59], and that GL261 cells produced higher levels of TGF-β than CT-2A cells (**Supplementary Figure 4.2D**), we next examined whether the bispecific IL-13Rα2/TGF-β CAR-T cells' ability to rewire TGF-β signaling would also affect PD-1/PD-L1 signaling in the GL261 model. Compared to the single-input IL-13Rα2 CAR-T cell group, brain tissues from the bispecific CAR-T cell-treated group showed reduced PD-L1 expression in myeloid cells and reduced PD-1 expression in T cells (**Figures 4.4D, E**). Expression of the TGF-β DNR had similar effects on PD-1 and PD-L1 expression levels, suggesting TGF-β antagonism may indeed disrupt the immunosuppressive PD-1/PD-L1 axis. Of note, T cells in mice treated with IL-13Rα2/TGF-β CAR-T cells exhibited the greatest expression levels of the effector molecule CD44, consistent with the unique ability of the IL-13Rα2/TGF-β CAR, but not the TGF-β DNR, to convert TGF-β into an immunostimulant (**Figure 4.4E**). In conjunction with low PD-1 expression, these findings demonstrate that bispecific IL-13Rα2/TGF-β CAR-T cells promote a more effector-like, and less exhausted, phenotype among brain-infiltrating T cells compared to single-input IL-13Rα2 CAR-T cells with or without DNR co-expression.

In addition, the IL-13Rα2/TGF-β CAR-T cell-treated group showed a unique increase in T-cell infiltration into the tumor-bearing brain compared to groups treated with single-input IL-13Rα2 CAR-T cells with or without the TGF-β DNR (**Figure 4.4B**). This increase in T-cell presence following bispecific CAR-T cell treatment was observed in both the GL261 and the CT-2A model (**Figures 4.4B, C**), and is consistent with the increased anti-tumor response observed in bispecific CAR-T cell-treated mice in survival studies (**Figure 4.3**). Taken together, these

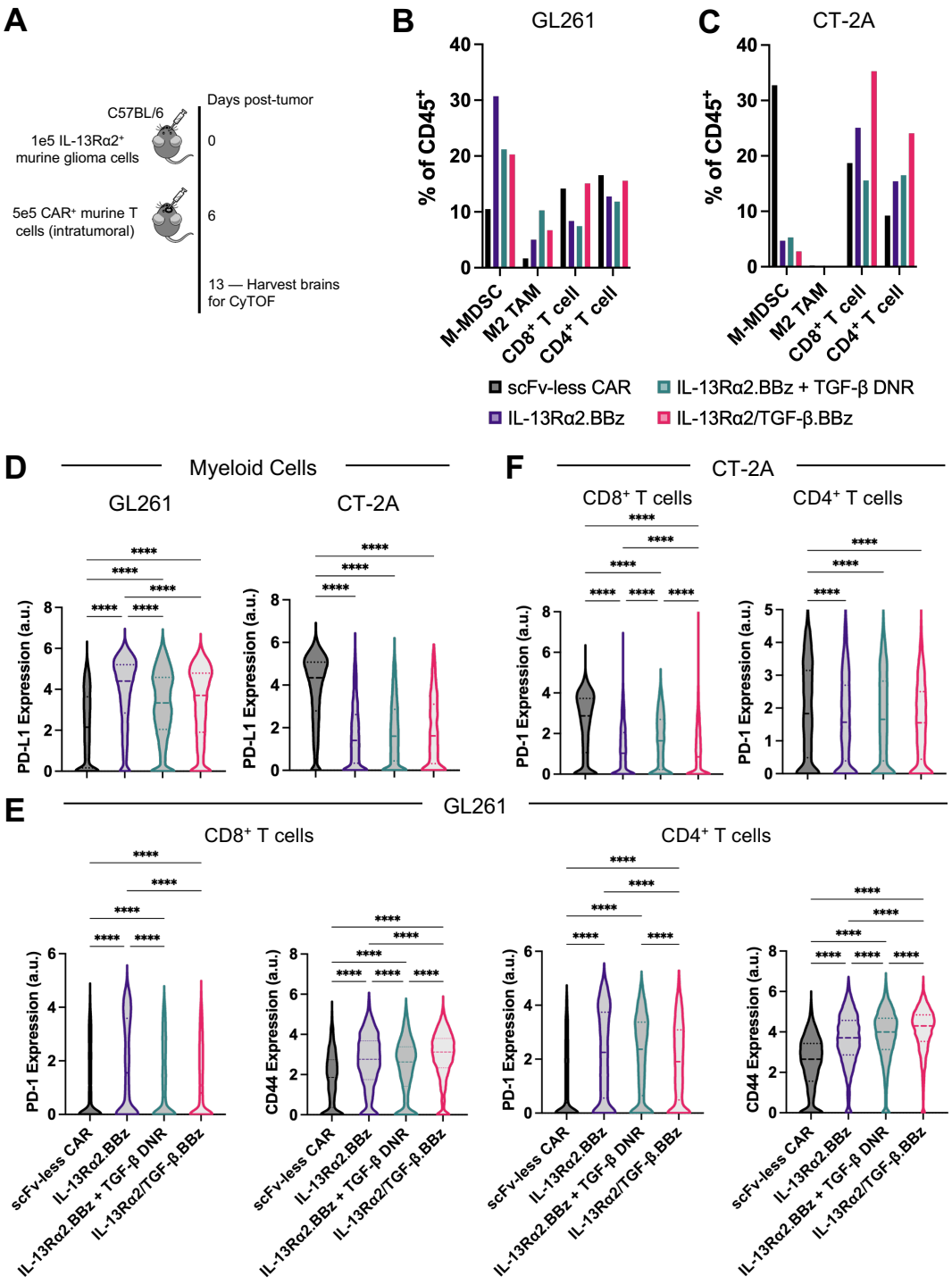

Figure 4.4 Bispecific IL-13Rα2/TGF-β CAR-T cells re-shape the TME of murine gliomas to promote anti-tumor immunity. (A) Study schematic. 1 x 10^5 IL-13Rα2$^+$ murine glioma cells (either CT-2A or GL261) were implanted intracranially into the right forebrains of C57BL/6 mice. Six days following tumor-cell injection, 5 x 10^5 CAR-T cells were injected intratumorally. On day 13 following tumor-cell injection (day 7 following T-cell injection), brains were harvested and dissociated. Brains from *n* = 4 mice per treatment group (*n* = 3 for scFv-less CAR-T cell treatment group) were pooled for CyTOF analysis of the GL261 TME. Brains from *n* = 3 mice per treatment group were pooled for CyTOF analysis of the CT-2A TME.
(caption continued on next page)

Figure 4.4 *(cont)* (B and C) (B and C) Proportions of suppressive myeloid cells (PD-L1+ macrophages, M-MDSCs, and M2 TAMs) and T cells (CD8+ and CD4+) among total brain-infiltrating leukocytes in either GL261 (B) or CT-2A (C). Among IL-13Rα2–targeting CAR-T cells, treatment with bispecific IL-13Rα2/TGF-β CAR-T cells results in the fewest total suppressive myeloid cells, and the greatest T cell infiltration in brain tissue. (D) Violin plots depicting PD-L1 expression among myeloid cells detected by CyTOF analysis of GL261 (left) and CT-2A (right) TMEs. Whereas IL-13Rα2–targeting CAR-T cells induce an upregulation of PD-L1 expression among myeloid cells in the GL261 TME, myeloid cells in the CT-2A TME exhibit lower levels of PD-L1 expression following treatment with IL-13Rα2–targeting CAR-T cells. (E) Violin plots depicting PD-1 and CD44 expression among T cells detected by CyTOF analysis of GL261 tumor-bearing brains. (F) Violin plots depicting PD-1 expression among T cells detected by CyTOF analysis of CT-2A tumor-bearing brains. Consistent with patterns of PD-L1 expression in myeloid cells following IL-13Rα2 CAR-T cell treatment, T cells exhibit higher PD-1 expression following IL-13Rα2 CAR-T cell treatment in the GL261 TME, and lower PD-1 expression following CAR-T cell treatment in the CT-2A TME. Treatment of GL261 tumor-bearing mice with either bispecific IL-13Rα2/TGF-β CAR-T cells or IL-13Rα2 CAR-T cells co-expressing the TGF-β DNR limits the PD-1/PD-L1 upregulation. In GL261 tumor-bearing mice, CD44 expression levels were highest among T cells following treatment with IL-13Rα2/TGF-β CAR-T cells. Combined with low PD-1 expression, these results suggest that T cells exhibit a greater effector-like phenotype following IL-13Rα2/TGF-β CAR-T cell treatment. Hatched lines in violin plots shown in (D) and (E) represent the 75th percentile, median, and 25th percentile of expression, in order from top to bottom. Statistics for panels (D) and (E) were computed by one-way ANOVA using Tukey's method to correct for multiple comparisons (****$P < 0.0001$).

findings demonstrate that bispecific IL-13Rα2/TGF-β CAR-T cells show superior capability to re-model the GBM TME and promote anti-tumor immunity compared to single-input IL-13Rα2 CAR-T cells with or without the TGF-β DNR.

TGF-β CAR-T cells are well-tolerated

Given reports of toxicity induced by systemic inhibition of TGF-β[41], we sought to ensure that TGF-β–responsive CAR-T cells can be well-tolerated. CAR-T cells were intracranially injected in all experiments performed in this study, a choice that was informed by preclinical and clinical evidence indicating direct CAR-T cell infusion into the central nervous system (CNS) is safe and potentially more efficacious compared to peripheral infusion[11,14,60,61]. As shown in Figures 4.2 and 4.3, animals treated with bispecific IL-13Rα2/TGF-β CAR-T cells survived for months unless they succumbed to tumor progression. When injected intratumorally in NSG mice bearing orthotopic GBM xenografts, bispecific IL-13Rα2/TGF-β CAR-T cells showed no detectable presence above background in the peripheral blood two weeks after treatment (**Figure**

4.5A). Furthermore, no evidence of toxicity was observed based on animal behavior or post-mortem dissection, and mouse weights remained stable over time (**Figure 4.5B**).

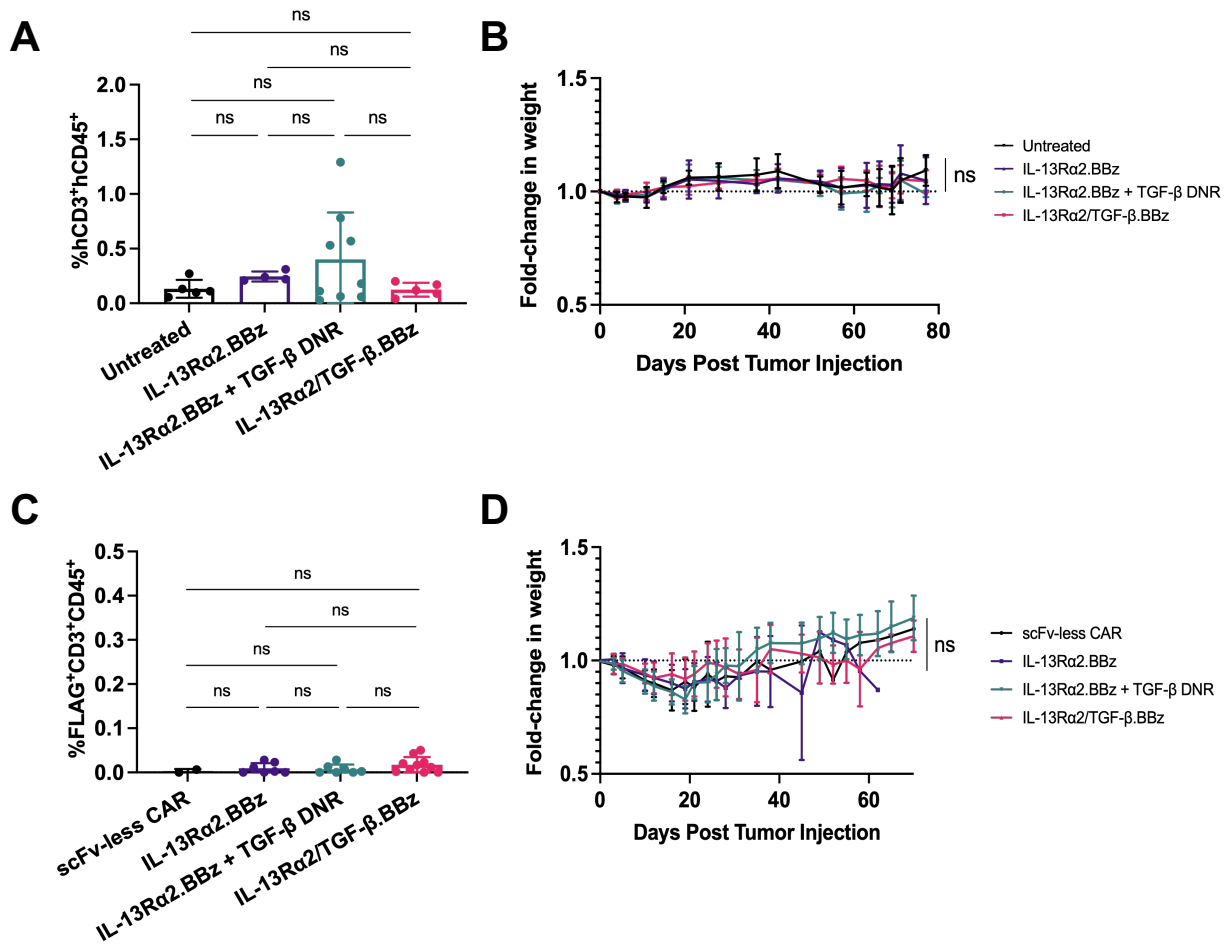

Figure 4.5 Bispecific IL-13Rα2/TGF-β CAR-T cells do not induce systemic toxicity in mouse models. (A) NSG mice were orthotopically engrafted with GS001 neurospheres and treated intratumorally with CAR-T cells, as described in Figure 4.2D. Retro-orbital blood was collected 22 days following tumor-cell injection (15 days following T-cell injection) and subsequently analyzed for presence of human T cells. Mice treated with CAR-T cells exhibited near-undetectable levels of human T cells in peripheral blood, indicating that CAR-T cells remain well-confined to the CNS following intratumoral administration. (B) Fold-change in weight relative to day 0 corresponding to NSG mice shown in (A) were tracked over time (plotted are means ± SD). No evidence of gross toxicity was observed with CAR-T cell treatment as mouse weights remained stable over time. (*n* = 4-5 for scFv-less CAR, IL-13Rα2 CAR, and IL-13Rα2/TGF-β CAR-T cell treatment groups, *n* = 9 for IL-13Rα2 CAR-T cells expressing the TGF-β DNR). (C) C57BL/6 mice were orthotopically engrafted with IL13Rα2$^+$ CT-2A gliomas and treated intratumorally with CAR-T cells, as described in Figure 4.3C. Retro-orbital blood was collected 23 days following tumor-cell injection (17 days following T-cell injection) and subsequently analyzed for presence of CAR$^+$ (i.e., FLAG$^+$) T cells. Comparable proportions of total T cells were detected in peripheral blood across all treatment groups, and no CAR$^+$ T cells were detected in the periphery, indicating that CAR-T cells remain confined to the CNS following intratumoral administration and do not escape to the periphery. (D) Weights corresponding to C57BL/6 mice shown in (C) were tracked over time (plotted are means ± SD). Changes in mouse weight did not appear to be attributable to bispecific IL-13Rα2/TGF-β CAR-T cell treatment (Supplementary Figure 4.5), indicating that bispecific IL-13Rα2/TGF-β CAR-T cells are well-tolerated in immunocompetent mice. (*n* = 7 for scFv-less CAR-T cell treatment group, *n* = 15-16 for IL-13Rα2 CAR-T cell treatment group).
Statistics in (A) and (C) were calculated using the two-tailed, unpaired, two-sample student's *t* test. Statistics in (B) and (D) were calculated by two-way ANOVA (n.s., not significant). There were no statistically significant differences detected among all pairwise comparisons.

Similarly, there was no evidence of non-disease related toxicity in the syngeneic IL-13Rα2^{+} CT-2A glioma model (**Figures 4.5C, D, Supplementary Figure 4.5**). All instances of weight reduction showed temporal correlation with tumor outgrowth, suggesting changes in weight were due to tumor burden rather than CAR-T cell administration. Together, these results demonstrate that locally administered bispecific IL-13Rα2/TGF-β CAR-T cells show no evidence of systemic toxicity.

Discussion

A major challenge in establishing effective immunotherapies in the context of GBM is the highly immunosuppressive TME. Indeed, CAR-T cells, peptide vaccines, and DC vaccines administered as single agents have largely been ineffective in clinical trials, and development of multi-pronged approaches to counter tumor-mediated immune inhibition is an area of active investigation[62]. Here, we engineer bispecific IL-13Rα2/TGF-β CARs, which compactly integrate tumor-targeting and immuno-modulatory moieties. By converting a major source of immune suppression in the TME into an immunostimulant, bispecific IL-13Rα2/TGF-β CARs can not only enhance the performance of engineered, tumor-targeting T cells, but also dampens suppressive phenotypes among brain-infiltrating immune cells. *In vitro*, bispecific IL-13Rα2/TGF-β CAR-T cells can kill neurosphere samples derived from both newly diagnosed and recurrent GBM patients, demonstrating their clinical utility. Although *in vitro* cytolytic activity is limited to tumors with relatively high IL-13Rα2 expression, our findings in syngeneic models show that IL-13Rα2/TGF-β CAR-T cells have the potential to reshape the immune-cell composition of the TME to potentiate anti-tumor responses. Robust engagement of endogenous immunity, which can drive epitope spreading—the phenomenon whereby immune recognition of tumors is extended beyond the antigen targeted by the CAR—is especially critical in light of the highly heterogeneous and immunologically cold GBM TME. Previous efforts in CAR-T cell development to address GBM antigen heterogeneity have relied on hard-coding CAR specificities against two[63] or even three target antigens[64,65]. However, such dual- or triple-targeting therapies may still be susceptible to antigen escape in the context of GBM and do not account for the immunosuppressive TME. We demonstrate that engineering CAR-T cell responsiveness to TGF-β can counter tumor-mediated immunosuppression in both engineered T cells themselves and surrounding immune cells. Previous reports have demonstrated that TGF-β blockade synergizes with radiotherapy[66,67] and PD-1/PD-L1 checkpoint blockade[59,68,69]; further investigation may reveal additional synergistic

combinations of bispecific IL-13Rα2/TGF-β CAR-T cells and other forms of immunotherapy that robustly induce epitope spreading.

Importantly, we also observed distinct patterns in the TME following treatment with bispecific IL-13Rα2/TGF-β CAR-T cells compared to IL-13Rα2 CAR-T cells co-expressing the TGF-β DNR. Although both the bispecific IL-13Rα2/TGF-β CAR and TGF-β DNR can inhibit endogenous TGF-β signaling, only the bispecific IL-13Rα2/TGF-β CAR activates T cells in the presence of TGF-β. Consequently, bispecific IL-13Rα2/TGF-β CAR-T cells—but not IL-13Rα2 CAR-T cells co-expressing the TGF-β DNR—promote T-cell infiltration and limit expansion of suppressive myeloid cells such as MDSCs and TAMs. Indeed, upregulation of suppressive, myeloid-associated molecules was also observed in metastatic castration-resistant prostate cancer patients treated with PSMA CAR-T cells co-expressing the TGF-β DNR[50]. Here, we show that remodeling of the TME to potentiate anti-tumor immunity can be more effectively achieved by not only inhibiting, but also converting immunosuppressive TGF-β signaling into a T-cell stimulant.

In our analysis of the GBM TME in immunocompetent mouse models, myeloid cells comprised the majority of tumor-infiltrating leukocytes, which is consistent with observations in human GBM patients[70]. However, given differences in murine and human immunology, studies with either *ex vivo* human GBM specimens or humanized mouse models could provide useful validation of the interactions between bispecific IL-13Rα2/TGF-β CAR-T cells and immune cells in the TME. One advantage of our study design is that cross-reactivity of the TGF-β CAR with both human and murine TGF-β enabled the use of identical CAR constructs in both xenograft and syngeneic tumor models; thus, CAR protein sequence is not a confounding factor in the interpretation of our results in syngeneic models.

Although bispecific IL-13Rα2/TGF-β CAR-T cells exhibited superior anti-tumor function in both xenograft and syngeneic tumor models, our *in vivo* studies suffered some limitations. In xenograft models using patient-derived GBM neurospheres, we observed that tumor burden did

not correlate with bioluminescent signal. In fact, brains recovered from a handful of mice which died without detectable tumor radiance exhibited abnormal features upon gross examination, and IHC staining revealed strong expression IL-13Rα2^{+}, confirming tumor outgrowth to be the cause of death. Therefore, the main criteria for evaluating CAR-T cell efficacy against xenograft tumors were survival outcomes, where bispecific IL-13Rα2/TGF-β CAR-T cells significantly increased survival in mice compared to IL-13Rα2 CAR-T cells alone or co-expressing the TGF-β DNR. In our syngeneic studies, despite stable firefly luciferase expression in murine glioma cells, we failed to observe statistically significant differences in survival between IL-13Rα2–targeting CAR-T cell treatment groups. This may be attributed, in part, to the fact that engineered murine glioma cell lines, which express human IL-13Rα2 in conjunction with other foreign proteins such as firefly luciferase, may be immunogenic. Broad immunogenicity of tumor cells may therefore obscure differences in CAR-specific anti-tumor function. Nonetheless, IL-13Rα2/TGF-β CAR-T cells exhibited better control over tumor outgrowth, as quantified by bioluminescent imaging, and produced more favorable immune-cell profiles in both GL261 and CT-2A tumor models, providing greater confidence in our findings despite lack of statistical significance.

In addition to assessing anti-tumor efficacy, we also sought to evaluate the safety of bispecific IL-13Rα2/TGF-β CAR-T cells. In both immunodeficient and immunocompetent murine hosts, there was no observable toxicity resulting from either intratumoral or intravenous administration of IL-13Rα2/TGF-β CAR-T cells. Nevertheless, approaches involving modulation of T-cell responses to TGF-β warrants caution, particularly in light of recently observed fatalities in patients treated with PSMA CAR-T cells co-expressing the TGF-β DNR[50,71]. The cause of fatality in these trials is still unresolved, but no definitive evidence links TGF-β DNR expression to the toxicity observed[50]. Moreover, previous clinical trials have demonstrated that virus-specific T cells expressing a TGF-β DNR are well-tolerated in patients through a four-year monitoring period[48], whereas patient death has previously been observed following PSMA CAR-T cell treatment[72,73]. Taken together, multiple lines of evidence suggest rewiring T-cell response to TGF-

β can be a safe and effective approach to increasing CAR-T cell function. However, incorporation of suicide genes[74–77] or high-dose steroid administration, which is common clinical practice to control cerebral edema in GBM patients[78], may still be contemplated as safeguards against unanticipated toxicity.

In addition to implementing measures to ensure patient safety, locoregional delivery of bispecific IL-13Rα2/TGF-β CAR-T cells in GBM patients should further minimize the risk of unanticipated adverse events. Indeed, in our studies, we did not detect adoptively transferred CAR-T cells in peripheral blood when administered intratumorally. In clinical trials, IL-13Rα2–targeting CAR-T cells are well-tolerated when administered intracavitarily or intraventricularly[11,18,19]. More recently, intraventricular administration of GD2 CAR-T cells in diffuse intrinsic pontine and diffuse midline glioma patients exhibited superior safety profiles compared to systemic CAR-T cell administration[14]. Taken together with these clinical observations, our study findings provide support for the clinical translation of bispecific IL-13Rα2/TGF-β CAR-T cells as a novel therapy to safely and effectively combat the immunosuppressive TME in GBM.

Methods

DNA constructs

The IL-13Rα2 CAR used in this study is a modified version of the IL-13Rα2 CAR[11] received as a generous gift from Dr. Christine Brown (City of Hope). Single-chain bispecific and CARs were constructed by isothermal assembly of DNA fragments[79]. The IL-13Rα2–binding domain was encoded by an IL-13 mutein[45,46], while the TGF-β–binding domain was encoded by a previously described scFv sequence[43]. The IL-13Rα2/TGF-β CAR encoded an IgG4 hinge extracellular spacer, a CD28 transmembrane domain (tm), 4-1BB co-stimulatory domain, and CD3ζ signaling chain. The single-input IL-13Rα2 CAR encoded an IgG4 hinge-CH2-CH3 long extracellular spacer bearing previously described L235E and N297Q mutations[80], a CD28 transmembrane domain, 4-1BB co-stimulatory domain, and CD3ζ signaling domain. In some experiments, CARs were co-expressed with a truncated epidermal growth factor receptor (EGFRt), which served as a transduction marker[81], via a "self-cleaving" T2A peptide. N-terminal FLAG tags were also encoded in order to assess surface receptor expression levels. The TGF-β DNR, which encodes the first 199 amino acids of TGFBR2, was co-expressed with the single-input IL-13Rα2 CAR via a self-cleaving P2A peptide.

Cell lines

GS001 neurospheres were derived from the patient-derived PBT106 neurosphere line, a generous gift from Dr. Christine Brown (City of Hope). PBT106 neurospheres stably expressing EGFP and ffLuc were sorted by consecutive rounds of magnetism-activated cell sorting (MACS; Miltenyi Biotec) followed by fluorescence-activated cell sorting (FACS) of positively-stained IL-13Rα2 cells to obtain GS001. FACS sorting was performed on a BD FACSAria II at the UCLA Flow Cytometry Core Facility. Intraoperative samples from both recurrent and newly diagnosed GBM patients obtained at UCLA were used to establish a panel of neurosphere lines (GS270, GS121, GS181, GS304, GS013, GS054), and were a generous gift from Dr. David Nathanson

(UCLA). All neurosphere lines were maintained in DMEM/F12 media with 15 mM HEPES, 1x serum-free B27 (Gibco), 5 µg/mL heparin (STEMCELL Technologies), and 1x GlutaMax (Gibco). Cultures were supplemented with 20 ng/mL epidermal growth factor (PeproTech) and 20 ng/mL basic fibroblast growth factor (PeproTech) every 3-4 days. For *in vitro* and *in vivo* experiments, neurospheres were dissociated into single-cell suspensions with accutase or TrypLE. CT-2A and GL261 were lentivirally transduced to express human IL-13Rα2 and ffLuc, and subsequently FACS-sorted for positively-stained IL-13Rα2 cells on a BD FACSAria II at the UCLA Flow Cytometry Core Facility. Murine glioma cells were maintained in DMEM + 10% heat-inactivated fetal bovine serum (HI-FBS). HEK 293T cells were obtained from ATCC. Phoenix-Eco cells were a generous gift from Dr. Antoni Ribas.

Retrovirus production

Retroviral supernatants for human T-cell transduction were produced by co-transfection of HEK 293T cells with plasmids encoding CAR constructs and pRD114/pHIT60 virus-packaging plasmids (gifts from Dr. Steven Feldman, National Cancer Institute), using linear polyethylenimine (PEI, 25 kDa; Polysciences). Supernatant was collected 48 hours after transfection, and cell debris removed using a 0.45 µm membrane filter.

Retroviral supernatants for murine T-cell transduction were produced by co-transfection of Phoenix-Eco cells with plasmids encoding CAR constructs and the pCL-Eco packaging plasmid (gift from Dr. Antoni Ribas, UCLA), using linear PEI. Supernatant was collected 48 hours after transfection, and cell debris removed using a 0.45 µm membrane filter.

Primary human T-cell culture

T cells were isolated from healthy donor whole-blood obtained from the UCLA Blood and Platelet Center. $CD3^+$ T cells were isolated using the RosetteSep $CD3^+$ T Cell Enrichment kit (STEMCELL Technologies) following the manufacturer's protocol. In some experiments,

naïve/memory T cells were isolated as previously described[82]. Isolated T cells were activated with CD3/CD28 Dynabeads (Gibco) at a 1:3 bead:cell ratio, and two rounds of retroviral transduction were performed at 48 hours and 72 hours following activation. T cells were maintained in complete RPMI (RPMI-1640 + 10% HI-FBS) and cultures were supplemented with 50 U/mL IL-2 and 1 ng/mL IL-15 every 2–3 days. Dynabeads were removed on day 7. All downstream assays were performed between day 9 and day 15 of culture.

Murine T-cell culture

Spleens were harvested from healthy, six- to eight-week–old C57BL/6J mice. Single-cell suspensions were obtained by gentle maceration in 70-µm cell strainers placed over 50 mL Falcon tubes. $CD3^+$ T cells were enriched from bulk splenocytes using the Pan T Cell Isolation kit II, mouse (Miltenyi Biotec) following the manufacturer's protocol. Isolated murine T cells were activated with anti-mouse CD3/CD28 Dynabeads (Gibco) at a 1:1 bead-to-cell ratio. One day prior to transduction, 12-well non-TC–treated plates were coated overnight with 15 µg/mL RetroNectin (Takara) diluted in PBS at 4°C. 24 hours following T-cell activation, retroviral supernatant was added to RetroNectin-coated plates and centrifuged at 2000xg for 2 hours (no brakes). Activated T cells were subsequently applied to spinoculated plates and centrifuged at 2000xg for 15 minutes (no brakes). T cells were maintained in RPMI-1640 + 10% HI-FBS + 50 µM β-mercaptoethanol. Cell cultures were supplemented with 50 U/mL human IL-2 every 2–3 days. Dynabeads were removed on day 5 of cell culture, and cells were used for *in vitro* and *in vivo* experiments.

In vitro killing and proliferation assays

Cytotoxic killing of tumor cells was assessed using the xCELLigence Real-Time Cell Analyzer System (Agilent Technologies). 96-well E-Plates® were coated with mouse laminin (Corning) prior to the addition of target cells. Target neurosphere lines were plated on day 0 (2 x 10^4 cells/well) in 100 µL of complete RPMI medium. After overnight tumor-cell adherence to the

well bottom, CAR-T cells were added at effector: target (E:T) ratios of 3:1 and 1:1 in complete RPMI to a final volume of 200 µL. Maximal cell release was obtained by adding 1% Triton X-100 to the wells. Cell index values (relative cell impedance) were collected over 72 hours and normalized to the maximal cell index value after addition of T cells. The percentage lysis was calculated as a proportion of the normalized cell index at a time point of interest versus the normalized cell index after effector cell plating.

To measure murine T-cell proliferation and cytotoxicity, CAR-T cells were labeled with CellTrace Yellow (CTY; ThermoFisher Scientific). 2.5 x 10^4 IL-13Rα2$^+$ CT-2A glioma cells were seeded in each well of a 96-well flat-bottom plate, and co-incubated with labeled T cells at specified effector: target (E:T) ratios, where the number of effectors was determined by CAR-positive T cell counts. After 4 days, cells were harvested as previously described[83]. T-cell counts, tumor-cell counts, and CTY dilution were assessed by flow cytometry using a MACSQuant VYB.

T-cell activation marker upregulation

1 x 10^5 human or murine T cells were seeded in 96-well flat-bottom tissue culture plates in 100 µL complete RPMI with or without recombinant human or murine TGF-β1 (PeproTech). Following overnight culture at 37ºC, cells were transferred to a 96-well U-bottom plate and activation marker expression was assessed by antibody staining and flow cytometry.

Phospho-SMAD Western blotting

To reduce background SMAD phosphorylation, primary human T cells were cultured overnight in serum-free, CTS OpTmizer media. Following overnight culture, cells were incubated at 37ºC with or without 5 ng/mL recombinant TGF-β1 (Peprotech) for 1 hour, then washed in PBS prior to cell lysis. Cell lysis and phospho-SMAD immunoblotting was performed as previously described[43].

ELISA

Cell culture supernatants were collected 24 and 48 hours after seeding 1 x 10^6 cells in 48-well plates. TGF-β concentrations in supernatant were determined using Human or Murine TGF-β1 DuoSet ELISA kits (R&D Systems) following the manufacturer's protocol.

In vivo studies

All *in vivo* experiments were approved by the UCLA Animal Research Committee (ARC). NSG and C57BL/6J mice were purchased from UCLA Department of Radiation and Oncology. For GBM xenografts, 2.5 x 10^5 GS001 neurospheres were sterotactically implanted into the right forebrains (1.5 mm lateral, 0.5 mm anterior to the bregma) of six- to eight-week–old NSG mice. 5 x 10^5 CAR-T cells were administered intratumorally seven days following tumor implantation.

For syngeneic GBM models, 1 x 10^5 glioma cells were stereotactically implanted into the right forebrains of six- to eight-week–old C57BL/6J mice. 5 x 10^5 CAR-T cells were administered intratumorally six days following tumor implantation.

Tumor burden was monitored by bioluminescent imaging. Mice were injected subcutaneously with 3 mg D-luciferin and imaged on an IVIS Lumina III LT Imaging System (Perkin Elmer). Photon flux was analyzed with LivingImage Software (Perkin Elmer). Animals were euthanized at the humane endpoint, and studies were blinded.

Antibody staining for flow cytometry

EGFRt expression was measured by staining with biotinylated cetuximab (Eli Lilly; biotinylated in-house), followed by PE-conjugated streptavidin (Jackson ImmunoResearch catalog no. 016-110-084). CAR expression on the cell-surface was measured by staining with anti-DYKDDDDK (FLAG) tag conjugated to APC or PE/Cy7 (clone L5, BioLegend catalog nos. 637308 or 637324, respectively).

Activation marker upregulation in the presence of TGF-β was performed by staining human T cells with PE-conjugated anti-human CD25 (clone BC96, BioLegend catalog no. 302606), PacificBlue-conjugated anti-CD69 (clone FN50, BioLegend catalog no. 310920), and APC-conjugated anti-FLAG tag. Activation marker upregulation in murine T cells was assessed by staining with APC-conjugated anti-mouse CD25 (clone PC61, BioLegend catalog no. 102012), PacificBlue-conjugated anti-mouse CD69 (clone H1.2F3, BioLegend catalog no. 104524), and PE/Cy7-conjugated anti-FLAG tag.

To monitor for expansion of adoptively-transferred T cells in NSG mice, retro-orbital blood samples were treated with 1x Red Blood Cell Lysis Solution (Miltenyi Biotec), then stained with PacificBlue-conjugated anti-human CD45 (clone HI30, BioLegend catalog no. 304029) and APC-conjugated anti-human CD3 (clone UCHT1, BioLegend catalog no. 300412). Peripheral blood samples collected from C57BL/6 mice were stained with stained with PE/Cy7-conjugated anti-mouse CD3 (clone 17A2, BioLegend catalog no. 100220), PacificBlue-conjugated anti-mouse CD45 (clone S18009F, BioLegend catalog no. 157212), and APC-conjugated anti-FLAG tag following red blood cell lysis.

Flow cytometry data were acquired by a MACSQuant VYB (Miltenyi Biotec). For all experiments, cells were stained, washed, and re-suspended in PBS + 2% HI-FBS. Data were analyzed and gated using FlowJo software (TreeStar).

CyTOF

Brain tumor samples were harvested from C57BL/6J mice, and single-cell suspensions obtained by gentle mechanical dissociation using the gentleMACS dissociator and Multi Tissue Dissociation kit I (Miltenyi Biotec), Debris Removal Solution (Miltenyi Biotec), and Red Blood Cell Lysis Solution (Miltenyi Biotec) following the manufacturer's protocol for dissociation of inflamed neural tissue. Single-cell suspensions were incubated with 2.5 μM monoisotopic cisplatin-194Pt (Fluidigm) at room temperature for 5 minutes, then washed with Maxpar Cell Staining Buffer

(MCSB, Fluidigm). Cells were subsequently incubated with FcR blocking reagent, mouse (Miltenyi) at room temperature for 10 minutes, then incubated with surface marker antibody cocktail at room temperature for 30 minutes. Cells were washed with MCSB, then fixed with 4% paraformaldehyde by incubation at room temperature for 10 minutes. Cells were washed with Perm-S buffer (Fluidigm) to permeabilize, and incubated with intracellular antibody cocktail at room temperature for 1 hour. Cells were washed then incubated overnight at 4°C with 200 nM iridium intercalating reagent (Fluidigm) diluted in Maxpar Fix and Perm buffer (Fluidigm). Following overnight incubation, cells were washed twice with MCSB, then twice with deionized water. Cells were re-suspended in deionized water, and run on a Helios mass cytometer (UCLA Flow Cytometry Core Facility). Data were analyzed using cytofkit2 in R.

IHC

Whole brains were fixed in 10% formalin overnight at room temperature, dehydrated in decreasing concentrations of ethanol, and embedded in paraffin by UCLA Translational Pathology Core Laboratory (TPCL). Five-micron coronal sections were cut by TPCL. Heat-induced antigen retrieval was performed using 1x Universal HIER antigen retrieval reagent (Abcam), and sections were stained with goat anti–IL-13Rα2 (R&D Systems catalog no. AF146) followed by secondary staining with donkey anti-goat IgG conjugated to AlexaFluor594 (Invitrogen catalog no. A32758). Samples were coverslipped with mounting media with DAPI (Abcam). IHC-stained sections were imaged on a Zeiss LSM880 confocal microscope at 20x magnification (UCLA Broad Stem Cell Research Center).

Statistics

All statistical tests were performed using GraphPad Prism (version 9). Sigmoidal curve fits with variable slope were performed in Prism, with the following constraints: Bottom = 0, Top = 100, and Slope > 0.

Supplementary Figures and Tables

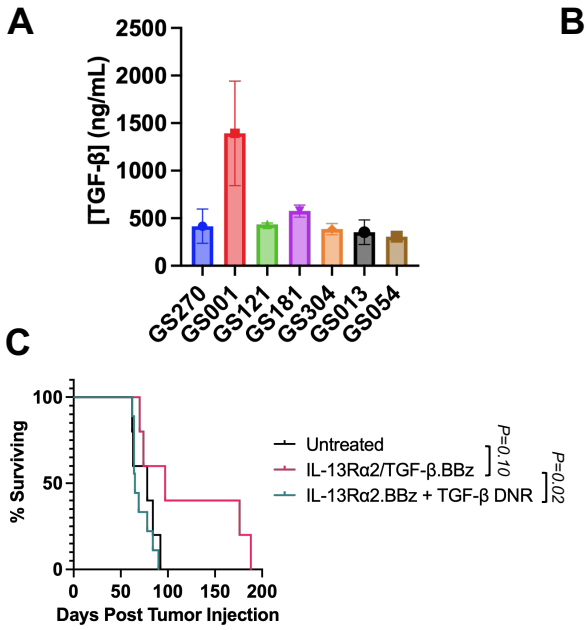

B

GS ID#	IDH status	Presentation	Modifications
270	WT	Recurrent	
001	Unknown	Unknown	Originally PBT106 from City of Hope. Transduced with EGFP-ffLuc, sorted for IL-13Rα2⁺ fraction
121	WT	Recurrent	
181	WT	Newly diagnosed	
304	WT	Recurrent	Transduced with EGFP, ffLuc
013	Mutant	Newly diagnosed	Transduced with EGFP, GLuc
054	WT	Recurrent	Transduced with EGFP, GLuc

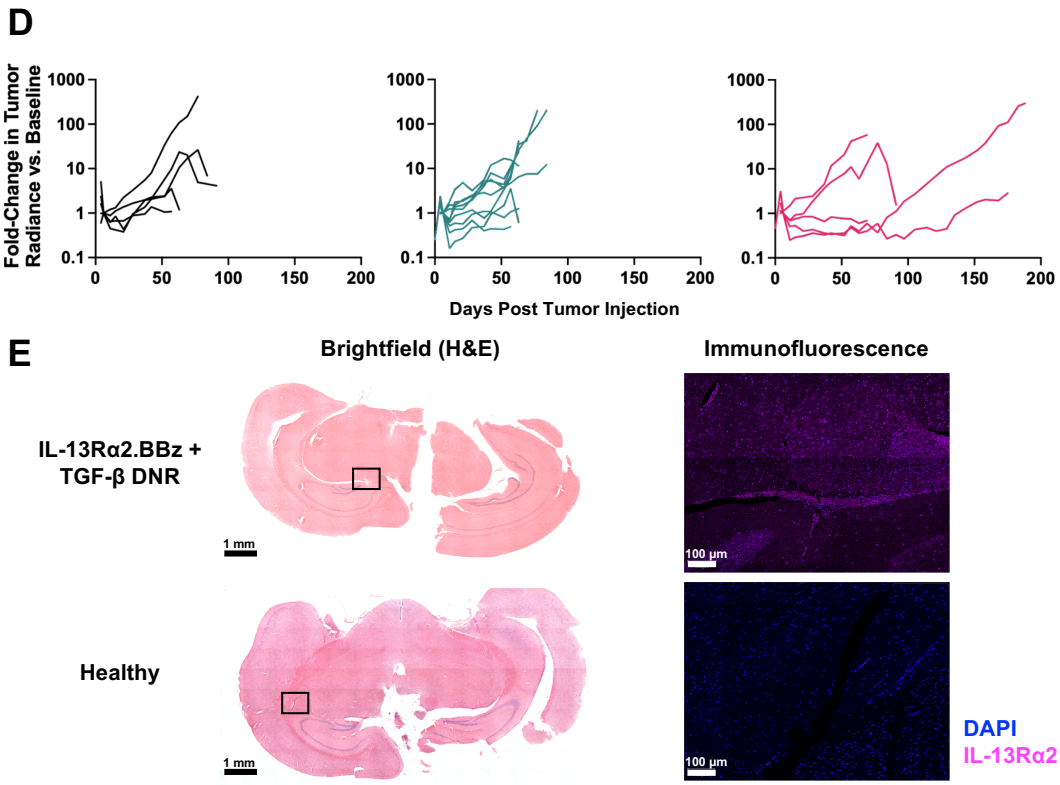

Supplementary Figure 4.1 TGF-β–mediated activation of bispecific IL-13Rα2/TGF-β CAR-T cells leads to superior therapeutic outcomes compared to IL-13Rα2 CAR-T cells co-expressing the TGF-β DNR. *(caption continued on next page)*

Supplementary Figure 4.1 *(cont)* (A) ELISA measurements of total TGF-β levels in cell culture supernatant collected from panel of GBM neurosphere lines (as shown in Figure 4.1), demonstrating that neurospheres produce TGF-β *in vitro*, with GS001 neurospheres producing the greatest amount. (B) Patient characteristics for panel of GBM neurosphere lines evaluated in Figure 4.1. (C) Survival curve and (D) tumor radiance traces of mice implanted with GS001 neurospheres and either left untreated, or otherwise treated with bispecific IL-13Rα2/TGF-β CAR-T cells or IL-13Rα2 CAR-T cells co-expressing the TGF-β DNR. Each trace in (C) represents a single mouse, and traces for each mouse end following euthanasia. These findings reveal that bispecific IL-13Rα2/TGF-β CAR-T cells exhibit superior anti-tumor efficacy compared to IL-13Rα2 CAR-T cells co-expressing the TGF-β DNR (n = 5 for scFv-less CAR and IL-13Rα2/TGF-β CAR-T cell treatment groups, n = 9 for IL-13Rα2 CAR-T cells expressing the TGF-β DNR). (E) H&E staining and IL-13Rα2 IHC staining on paraffin-embedded slides prepared from mouse treated with IL-13Rα2 CAR-T cells co-expressing the TGF-β DNR. Shown are representative slides. Mice died without detectable tumor radiance, but staining shows outgrowth of IL-13Rα2+ tumors, confirming cause of death to be tumor-related. Representative H&E and IL-13Rα2 IHC stains of healthy NSG mouse brain sections are included as negative controls. H&E images were taken at 10x magnification, immunofluorescent images were taken at 20x magnification. Scalebars represent 1 mm (*left*) and 100 μm (*right*). Boxed regions are approximate.

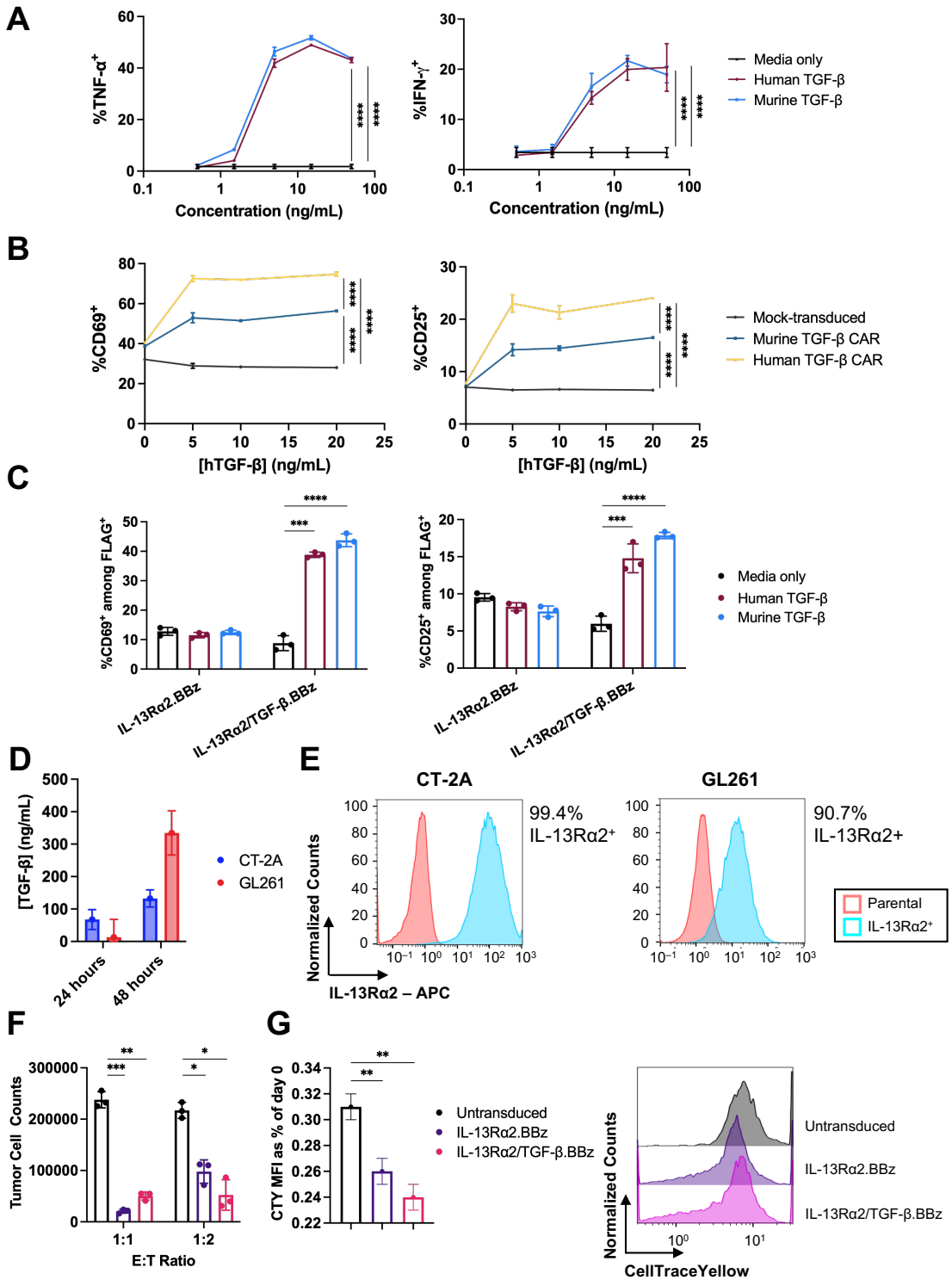

Supplementary Figure 4.2 Bispecific IL-13Rα2/TGF-β CARs cross-react with murine TGF-β and are functional in murine T cells. (A) Human PBMCs transduced to express a human TGF-β CAR were cultured in the presence of human or murine TGF-β. TNF-α (*left*) and IFN-γ (*right*) expression was measured by intracellular flow cytometry following overnight culture. Cytokine production is triggered by both murine and human forms of TGF-β, demonstrating that the TGF-β CAR is cross-reactive with murine TGF-β.

(caption continued on next page)

Supplementary Figure 4.2 *(cont)* (B) Murine T cells were transduced to express TGF-β CARs encoding either human or murine signaling domains. CAR-T cells were incubated in the presence of TGF-β overnight, then CD69 (*left*) and CD25 (*right*) expression were measured by flow cytometry. CARs with human signaling domains not only transduce activating signals in murine T cells, but also stimulate murine T cells more strongly than CARs with murine signaling domains. (C) Murine T cells transduced with CARs encoding human signaling domains were cultured in the presence of either human or murine TGF-β. CD69 (*left*) and CD25 (*right*) expression was measured by flow cytometry following overnight culture. Bispecific IL-13Rα2/TGF-β CAR-T cells, but not single-input IL-13Rα2 CAR-T cells, are activated in the presence of both human and murine TGF-β. (D) Total TGF-β levels were measured by ELISA in cell culture supernatant of IL-13Rα2$^+$ CT-2A and GL261 glioma cells, collected 24 and 48 hours after cell seeding. Both glioma lines secrete TGF-β *in vitro*. (E) IL-13Rα2 staining in CT-2A (*left*) and GL261 (*right*) tumor cells engineered to overexpress human IL-13Rα2. Parental cells are included as negative controls. (F-G) CAR-T cells were labeled with CellTraceYellow (CTY) dye and co-incubated with IL-13Rα2$^+$ CT-2A glioma cells at specified E:T ratios. Tumor cell counts (F) and CTY dye dilution in T cells (G) were measured after four days. CTY dilution in T cell following co-culture with tumor cells at a 1:1 E:T ratio are shown in (G). Dye dilution was quantified by fold-change in MFI (*left*), with representative histograms (*right*). Bispecific IL-13Rα2/TGF-β CAR-T cells kill target cells comparably well to single-input IL-13Rα2 CAR-T cells, and proliferate in response to tumor cells expressing target antigen. Statistics in (A) and (B) were computed by two-way ANOVA, with Tukey's method to correct for multiple comparisons. Statistics in (C), (F), and (G) were calculated using the two-tailed, unpaired, two-sample student's t test with the Holm-Sidak correction for multiple comparisons (**P < 0.01, ***P < 0.001, ****P < 0.0001).

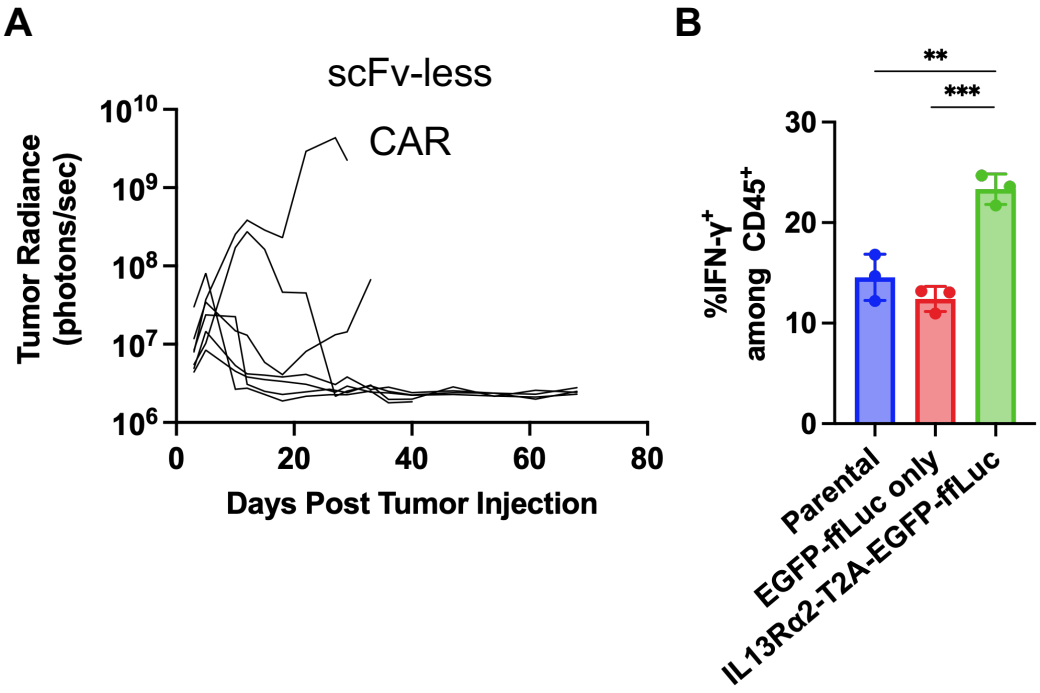

Supplementary Figure 4.3 Expression of human IL-13Rα2 in CT-2A glioma cells immunogenic.
(A) IL-13Rα2$^+$ CT-2A glioma cells were implanted in the right forebrains of C57BL/6 mice. Six days following tumor-cell injection, mice were treated intratumorally with scFv-less CAR-T cells. Tumor radiance was tracked over time, and complete tumor regression was observed in 5/7 mice. (B) Tumor-free mice in (A) were euthanized, and brain-infiltrating leukocytes isolated. Leukocytes were pooled, then co-cultured with either parental CT-2A, EGFP-ffLuc$^+$ CT-2A, or IL-13Rα2$^+$EGFP-ffLuc$^+$ CT-2A cells. IL-13Rα2$^+$ CT-2A cells triggered a stronger IFN-γ response in CD45$^+$ cells compared to parental and EGFP-ffLuc$^+$ CT-2A cells, suggesting that human IL-13Rα2 is immunogenic.
Statistics were computed using the two-tailed, unpaired, two-sample student's *t* test with the Holm-Sidak correction for multiple comparisons (** P < 0.01, *** P < 0.001).

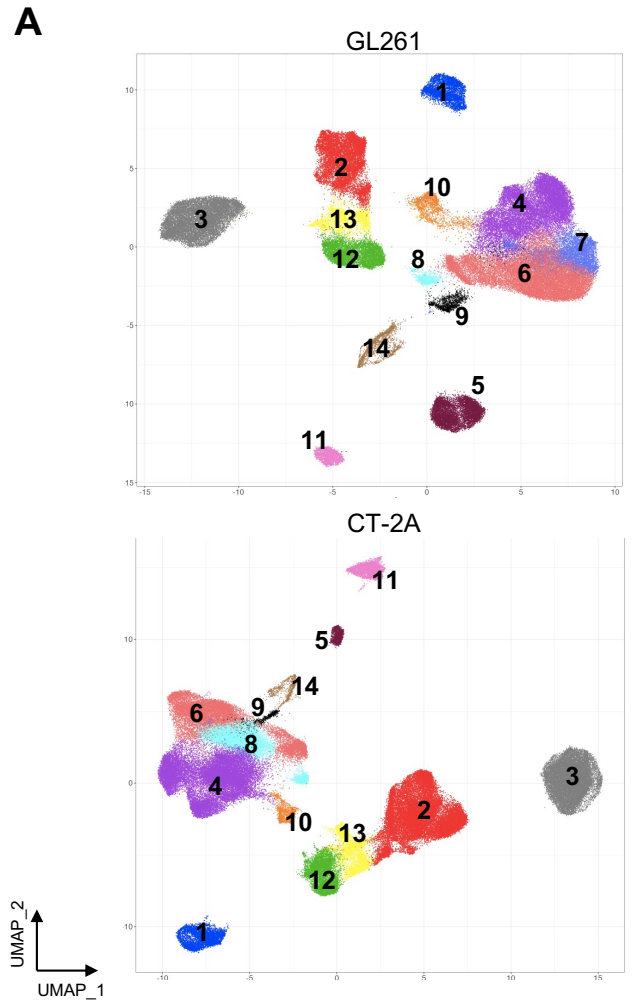

Cluster Label	Cellular Phenotype
1	B cell
2	CD8⁺ T cell
3	CD4⁺ T cell
4	DC
5	Eosinophil
6	M-MDSC
7	M2 TAM
8	PD-L1⁺ Macrophage
9	PD-L1⁻ Macrophage
10	Monocyte
11	Neutrophil
12	NK cell
13	Unknown
14	Unknown

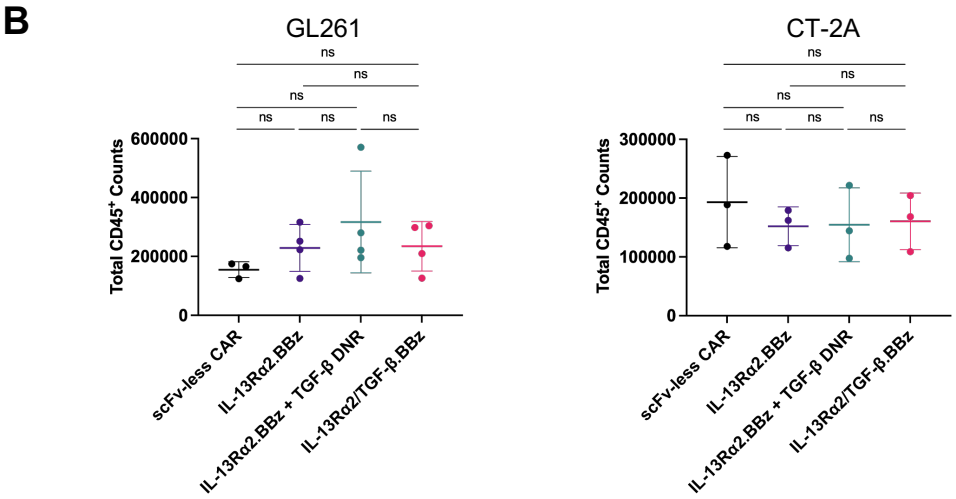

Supplementary Figure 4.4 Immune-cell types in murine gliomas, with comparable numbers of brain-infiltrating leukocytes across treatment groups. (A) UMAP projections and clusters identified from CyTOF analysis of the GL261 (*top*) and CT-2A (*bottom*) TMEs. Cellular phenotypes corresponding to each cluster label are shown on the right. (B) Flow cytometry analysis of CD45⁺ cells recovered from mouse brains reveals similar total numbers of brain-infiltrating leukocytes for each treatment group in both GL261 and CT-2A models. Statistics were calculated using the two-tailed, unpaired, two-sample student's *t* test (n.s., not significant).

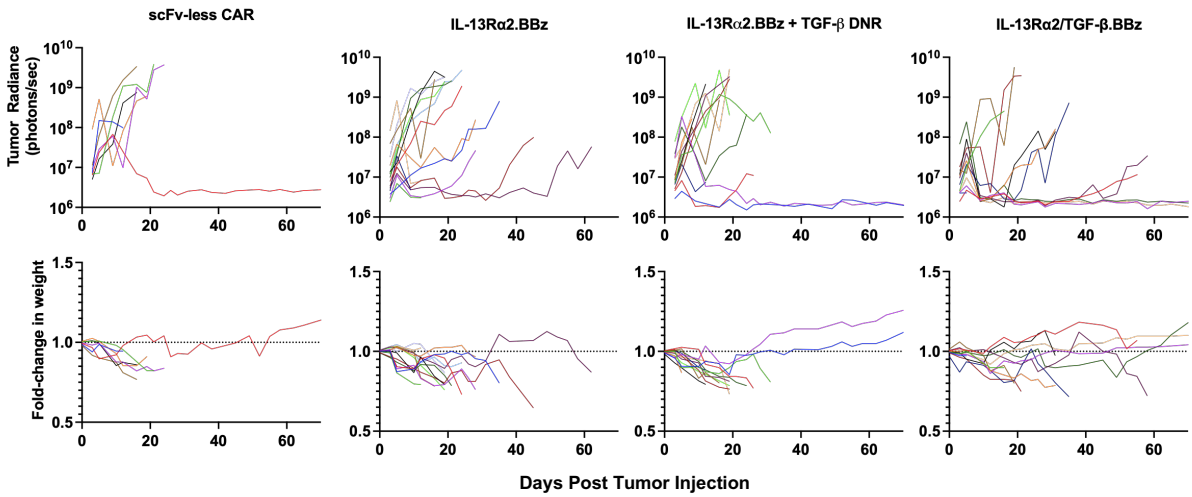

Supplementary Figure 4.5 Bispecific IL-13Rα2/TGF-β CAR-T cells do not elicit systemic toxicity in immunocompetent mice. Tumor radiance (*top*) and fold-change in mouse weights relative to one day prior to tumor-cell injection (*bottom*) are plotted for mice corresponding to each treatment group. Each individual trace represents a single mouse, and traces end following euthanasia. Data shown are from the same experiment as depicted in Figure 4.5D. Weight loss corresponded to tumor outgrowth, not CAR-T cell treatment.

References

1. Stupp, R. *et al.* Radiotherapy plus concomitant and adjuvant temozolomide for glioblastoma. *N. Engl. J. Med.* **352**, 987–996 (2005).

2. Stupp, R. *et al.* Effects of radiotherapy with concomitant and adjuvant temozolomide versus radiotherapy alone on survival in glioblastoma in a randomised phase III study: 5-year analysis of the EORTC-NCIC trial. *Lancet Oncol.* **10**, 459–466 (2009).

3. Stupp, R. *et al.* Effect of Tumor-Treating Fields Plus Maintenance Temozolomide vs Maintenance Temozolomide Alone on Survival in Patients With Glioblastoma: A Randomized Clinical Trial. *JAMA* **318**, 2306–2316 (2017).

4. Kirkpatrick, J. P., Laack, N. N., Shih, H. A. & Gondi, V. Management of GBM: a problem of local recurrence. *J. Neurooncol.* **134**, 487–493 (2017).

5. Alexander, B. M. & Cloughesy, T. F. Adult Glioblastoma. *J. Clin. Oncol.* **35**, 2402–2409 (2017).

6. Schuster, S. J. *et al.* Long-term clinical outcomes of tisagenlecleucel in patients with relapsed or refractory aggressive B-cell lymphomas (JULIET): a multicentre, open-label, single-arm, phase 2 study. *Lancet Oncol.* **22**, 1403–1415 (2021).

7. Jacobson, C. *et al.* Long-Term (≥4 Year and ≥5 Year) Overall Survival (OS) By 12- and 24-Month Event-Free Survival (EFS): An Updated Analysis of ZUMA-1, the Pivotal Study of Axicabtagene Ciloleucel (Axi-Cel) in Patients (Pts) with Refractory Large B-Cell Lymphoma (LBCL). *Blood* **138**, 1764 (2021).

8. Neelapu, S. S. *et al.* Axicabtagene ciloleucel as first-line therapy in high-risk large B-cell lymphoma: the phase 2 ZUMA-12 trial. *Nat. Med.* **28**, 735–742 (2022).

9. Berdeja, J. G. *et al.* Ciltacabtagene autoleucel, a B-cell maturation antigen-directed chimeric antigen receptor T-cell therapy in patients with relapsed or refractory multiple myeloma (CARTITUDE-1): a phase 1b/2 open-label study. *The Lancet* **398**, 314–324 (2021).

10. Abramson, J. S. *et al.* Lisocabtagene maraleucel for patients with relapsed or refractory large B-cell lymphomas (TRANSCEND NHL 001): a multicentre seamless design study. *The Lancet* **396**, 839–852 (2020).

11. Brown, C. E. *et al.* Regression of Glioblastoma after Chimeric Antigen Receptor T-Cell Therapy. *N. Engl. J. Med.* **375**, 2561–2569 (2016).

12. O'Rourke, D. M. *et al.* A single dose of peripherally infused EGFRvIII-directed CAR T cells mediates antigen loss and induces adaptive resistance in patients with recurrent glioblastoma. *Sci. Transl. Med.* **9**, (2017).

13. Ahmed, N. *et al.* HER2-Specific Chimeric Antigen Receptor–Modified Virus-Specific T Cells for Progressive Glioblastoma: A Phase 1 Dose-Escalation Trial. *JAMA Oncol.* **3**, 1094–1101 (2017).

14. Majzner, R. G. *et al.* GD2-CAR T cell therapy for H3K27M-mutated diffuse midline gliomas. *Nature* **603**, 934–941 (2022).

15. Tang, X. *et al.* Administration of B7-H3 targeted chimeric antigen receptor-T cells induce regression of glioblastoma. *Signal Transduct. Target. Ther.* **6**, 1–3 (2021).

16. Brown, C. E. *et al.* Glioma IL13Rα2 Is Associated with Mesenchymal Signature Gene Expression and Poor Patient Prognosis. *PLOS ONE* **8**, e77769 (2013).

17. Bhardwaj, R., Suzuki, A., Leland, P., Joshi, B. H. & Puri, R. K. Identification of a novel role of IL-13Rα2 in human Glioblastoma multiforme: interleukin-13 mediates signal transduction through AP-1 pathway. *J. Transl. Med.* **16**, 369 (2018).

18. Yaghoubi, S. S. *et al.* Noninvasive detection of therapeutic cytolytic T cells with 18F–FHBG PET in a patient with glioma. *Nat. Clin. Pract. Oncol.* **6**, 53–58 (2009).

19. Brown, C. E. *et al.* Bioactivity and Safety of IL13Rα2-Redirected Chimeric Antigen Receptor CD8+ T Cells in Patients with Recurrent Glioblastoma. *Clin. Cancer Res.* **21**, 4062–4072 (2015).

20. Iwami, K. *et al.* Peptide-pulsed dendritic cell vaccination targeting interleukin-13 receptor α2 chain in recurrent malignant glioma patients with HLA-A*24/A*02 allele. *Cytotherapy* **14**, 733–742 (2012).

21. Kunwar, S. *et al.* Direct Intracerebral Delivery of Cintredekin Besudotox (IL13-PE38QQR) in Recurrent Malignant Glioma: A Report by the Cintredekin Besudotox Intraparenchymal Study Group. *J. Clin. Oncol.* **25**, 837–844 (2007).

22. Hou, A. J., Chen, L. C. & Chen, Y. Y. Navigating CAR-T cells through the solid-tumour microenvironment. *Nat. Rev. Drug Discov.* **20**, 531–550 (2021).

23. Hanahan, D. & Weinberg, R. A. Hallmarks of Cancer: The Next Generation. *Cell* **144**, 646–674 (2011).

24. Han, J., Alvarez-Breckenridge, C. A., Wang, Q.-E. & Yu, J. TGF-β signaling and its targeting for glioma treatment. *Am. J. Cancer Res.* **5**, 945–955 (2015).

25. Ikushima, H. *et al.* Autocrine TGF-β Signaling Maintains Tumorigenicity of Glioma-Initiating Cells through Sry-Related HMG-Box Factors. *Cell Stem Cell* **5**, 504–514 (2009).

26. Peñuelas, S. *et al.* TGF-β Increases Glioma-Initiating Cell Self-Renewal through the Induction of LIF in Human Glioblastoma. *Cancer Cell* **15**, 315–327 (2009).

27. Bruna, A. *et al.* High TGFβ-Smad Activity Confers Poor Prognosis in Glioma Patients and Promotes Cell Proliferation Depending on the Methylation of the PDGF-B Gene. *Cancer Cell* **11**, 147–160 (2007).

28. Thomas, D. A. & Massagué, J. TGF-β directly targets cytotoxic T cell functions during tumor evasion of immune surveillance. *Cancer Cell* **8**, 369–380 (2005).

29. Flavell, R. A., Sanjabi, S., Wrzesinski, S. H. & Licona-Limón, P. The polarization of immune cells in the tumour environment by TGF-β. *Nat. Rev. Immunol.* **10**, 554–567 (2010).

30. Chen, M.-L. *et al.* Regulatory T cells suppress tumor-specific CD8 T cell cytotoxicity through TGF-β signals in vivo. *Proc. Natl. Acad. Sci.* **102**, 419–424 (2005).

31. Wu, A. *et al.* Glioma cancer stem cells induce immunosuppressive macrophages/microglia. *Neuro-Oncol.* **12**, 1113–1125 (2010).

32. Biswas, S. K. & Mantovani, A. Macrophage plasticity and interaction with lymphocyte subsets: cancer as a paradigm. *Nat. Immunol.* **11**, 889–896 (2010).

33. Gabrilovich, D. I., Ostrand-Rosenberg, S. & Bronte, V. Coordinated regulation of myeloid cells by tumours. *Nat. Rev. Immunol.* **12**, 253–268 (2012).

34. Rodon, J. *et al.* First-in-Human Dose Study of the Novel Transforming Growth Factor-β Receptor I Kinase Inhibitor LY2157299 Monohydrate in Patients with Advanced Cancer and Glioma. *Clin. Cancer Res.* **21**, 553–560 (2015).

35. Brandes, A. A. *et al.* A Phase II randomized study of galunisertib monotherapy or galunisertib plus lomustine compared with lomustine monotherapy in patients with recurrent glioblastoma. *Neuro-Oncol.* **18**, 1146–1156 (2016).

36. Wick, A. *et al.* Phase 1b/2a study of galunisertib, a small molecule inhibitor of transforming growth factor-beta receptor I, in combination with standard temozolomide-based radiochemotherapy in patients with newly diagnosed malignant glioma. *Invest. New Drugs* **38**, 1570–1579 (2020).

37. Tomaszewski, W., Sanchez-Perez, L., Gajewski, T. F. & Sampson, J. H. Brain Tumor Microenvironment and Host State: Implications for Immunotherapy. *Clin. Cancer Res.* **25**, 4202–4210 (2019).

38. Quail, D. F. & Joyce, J. A. The Microenvironmental Landscape of Brain Tumors. *Cancer Cell* **31**, 326–341 (2017).

39. Pardridge, W. M. Blood-Brain Barrier and Delivery of Protein and Gene Therapeutics to Brain. *Front. Aging Neurosci.* **11**, (2020).

40. Siegel, P. M. & Massagué, J. Cytostatic and apoptotic actions of TGF-β in homeostasis and cancer. *Nat. Rev. Cancer* **3**, 807–820 (2003).

41. Anderton, M. J. *et al.* Induction of heart valve lesions by small-molecule ALK5 inhibitors. *Toxicol. Pathol.* **39**, 916–924 (2011).

42. Lacouture, M. E. *et al.* Cutaneous keratoacanthomas/squamous cell carcinomas associated with neutralization of transforming growth factor β by the monoclonal antibody fresolimumab (GC1008). *Cancer Immunol. Immunother.* **64**, 437–446 (2015).

43. Chang, Z. L. *et al.* Rewiring T-cell responses to soluble factors with chimeric antigen receptors. *Nat. Chem. Biol.* **14**, 317–324 (2018).

44. Hou, A. J., Chang, Z. L., Lorenzini, M. H., Zah, E. & Chen, Y. Y. TGF-β–responsive CAR-T cells promote anti-tumor immune function. *Bioeng. Transl. Med.* **3**, 75–86 (2018).

45. Debinski, W., Gibo, D. M., Obiri, N. I., Kealiher, A. & Puri, R. K. Novel anti–brain tumor cytotoxins specific for cancer cells. *Nat. Biotechnol.* **16**, 449–453 (1998).

46. Debinski, W. & Thompson, J. P. Retargeting interleukin 13 for radioimmunodetection and radioimmunotherapy of human high-grade gliomas. *Clin. Cancer Res.* **5**, 3143s–3147s (1999).

47. Bollard, C. M. *et al.* Adapting a transforming growth factor β–related tumor protection strategy to enhance antitumor immunity. *Blood* **99**, 3179–3187 (2002).

48. Bollard, C. M. *et al.* Tumor-Specific T-Cells Engineered to Overcome Tumor Immune Evasion Induce Clinical Responses in Patients With Relapsed Hodgkin Lymphoma. *J. Clin. Oncol.* **36**, 1128–1139 (2018).

49. Kloss, C. C. *et al.* Dominant-Negative TGF-β Receptor Enhances PSMA-Targeted Human CAR T Cell Proliferation And Augments Prostate Cancer Eradication. *Mol. Ther.* **26**, 1855–1866 (2018).

50. Narayan, V. *et al.* PSMA-targeting TGFβ-insensitive armored CAR T cells in metastatic castration-resistant prostate cancer: a phase 1 trial. *Nat. Med.* **28**, 724–734 (2022).

51. Vroemen, M., Weidner, N. & Blesch, A. Loss of gene expression in lentivirus- and retrovirus-transduced neural progenitor cells is correlated to migration and differentiation in the adult spinal cord. *Exp. Neurol.* **195**, 127–139 (2005).

52. Khalsa, J. K. *et al.* Immune phenotyping of diverse syngeneic murine brain tumors identifies immunologically distinct types. *Nat. Commun.* **11**, 3912 (2020).

53. Liu, C. J. *et al.* Treatment of an aggressive orthotopic murine glioblastoma model with combination checkpoint blockade and a multivalent neoantigen vaccine. *Neuro-Oncol.* **22**, 1276–1288 (2020).

54. Belmans, J. *et al.* Immunotherapy with subcutaneous immunogenic autologous tumor lysate increases murine glioblastoma survival. *Sci. Rep.* **7**, 13902 (2017).

55. Genoud, V. *et al.* Responsiveness to anti-PD-1 and anti-CTLA-4 immune checkpoint blockade in SB28 and GL261 mouse glioma models. *OncoImmunology* **7**, e1501137 (2018).

56. Aslan, K. *et al.* Heterogeneity of response to immune checkpoint blockade in hypermutated experimental gliomas. *Nat. Commun.* **11**, 931 (2020).

57. Bao, S., Jiang, X., Jin, S., Tu, P. & Lu, J. TGF-β1 Induces Immune Escape by Enhancing PD-1 and CTLA-4 Expression on T Lymphocytes in Hepatocellular Carcinoma. *Front. Oncol.* **11**, (2021).

58. Trebska-McGowan, K. *et al.* The effect of TGF-β on PD-L1 expression on PDAC TAMs. *J. Clin. Oncol.* **38**, 764–764 (2020).

59. Lan, Y. *et al.* Simultaneous targeting of TGF-β/PD-L1 synergizes with radiotherapy by reprogramming the tumor microenvironment to overcome immune evasion. *Cancer Cell* **39**, 1388-1403.e10 (2021).

60. Brown, C. E. *et al.* Optimization of IL13Rα2-Targeted Chimeric Antigen Receptor T Cells for Improved Anti-tumor Efficacy against Glioblastoma. *Mol. Ther.* **26**, 31–44 (2018).

61. Theruvath, J. *et al.* Locoregionally administered B7-H3-targeted CAR T cells for treatment of atypical teratoid/rhabdoid tumors. *Nat. Med.* **26**, 712–719 (2020).

62. Bausart, M., Préat, V. & Malfanti, A. Immunotherapy for glioblastoma: the promise of combination strategies. *J. Exp. Clin. Cancer Res.* **41**, 35 (2022).

63. Hegde, M. *et al.* Tandem CAR T cells targeting HER2 and IL13Rα2 mitigate tumor antigen escape. *J. Clin. Invest.* **126**, 3036–3052.

64. Bielamowicz, K. *et al.* Trivalent CAR T cells overcome interpatient antigenic variability in glioblastoma. *Neuro-Oncol.* **20**, 506–518 (2018).

65. Choe, J. H. *et al.* SynNotch-CAR T cells overcome challenges of specificity, heterogeneity, and persistence in treating glioblastoma. *Sci. Transl. Med.* **13**, eabe7378 (2021).

66. Vanpouille-Box, C. *et al.* TGFβ Is a Master Regulator of Radiation Therapy-Induced Antitumor Immunity. *Cancer Res.* **75**, 2232–2242 (2015).

67. Hamon, P. *et al.* TGFβ receptor inhibition unleashes interferon-β production by tumor-associated macrophages and enhances radiotherapy efficacy. *J. Immunother. Cancer* **10**, e003519 (2022).

68. Tauriello, D. V. F. *et al.* TGFβ drives immune evasion in genetically reconstituted colon cancer metastasis. *Nature* **554**, 538–543 (2018).

69. Mariathasan, S. *et al.* TGFβ attenuates tumour response to PD-L1 blockade by contributing to exclusion of T cells. *Nature* **554**, 544–548 (2018).

70. Chen, Z. & Hambardzumyan, D. Immune Microenvironment in Glioblastoma Subtypes. *Front. Immunol.* **9**, (2018).

71. Exclusive: Carl June's Tmunity encounters a lethal roadblock as 2 patient deaths derail lead trial, raise red flag forcing a rethink of CAR-T for solid tumors. *Endpoints News* https://endpts.com/exclusive-carl-junes-tmunity-encounters-a-lethal-roadblock-as-2-patient-deaths-derail-lead-trial-raise-red-flag-forcing-a-rethink-of-car-t-for-solid-tumors/.

72. Poseida Therapeutics, Inc. Form 8-K. https://sec.report/Document/0001193125-20-222442/.

73. Poseida Therapeutics Announces Clinical Hold Lifted on Phase I Autologous CAR-T Study in Prostate Cancer | Poseida Therapeutics, Inc. https://investors.poseida.com/news-releases/news-release-details/poseida-therapeutics-announces-clinical-hold-lifted-phase-i/.

74. Bonini, C. *et al.* HSV-TK Gene Transfer into Donor Lymphocytes for Control of Allogeneic Graft-Versus-Leukemia. *Science* **276**, 1719–1724 (1997).

75. Berger, C., Flowers, M. E., Warren, E. H. & Riddell, S. R. Analysis of transgene-specific immune responses that limit the in vivo persistence of adoptively transferred HSV-TK–modified donor T cells after allogeneic hematopoietic cell transplantation. *Blood* **107**, 2294–2302 (2006).

76. Ciceri, F. *et al.* Infusion of suicide-gene-engineered donor lymphocytes after family haploidentical haemopoietic stem-cell transplantation for leukaemia (the TK007 trial): a non-randomised phase I–II study. *Lancet Oncol.* **10**, 489–500 (2009).

77. Di Stasi, A. *et al.* Inducible Apoptosis as a Safety Switch for Adoptive Cell Therapy. *N. Engl. J. Med.* **365**, 1673–1683 (2011).

78. Petrelli, F. *et al.* Steroids use and survival in patients with glioblastoma multiforme: a pooled analysis. *J. Neurol.* **268**, 440–447 (2021).

79. Gibson, D. G. *et al.* Enzymatic assembly of DNA molecules up to several hundred kilobases. *Nat. Methods* **6**, 343–345 (2009).

80. Jonnalagadda, M. *et al.* Chimeric Antigen Receptors With Mutated IgG4 Fc Spacer Avoid Fc Receptor Binding and Improve T Cell Persistence and Antitumor Efficacy. *Mol. Ther.* **23**, 757–768 (2015).

81. Wang, X. *et al.* A transgene-encoded cell surface polypeptide for selection, in vivo tracking, and ablation of engineered cells. *Blood* **118**, 1255–1263 (2011).

82. Zah, E. *et al.* Systematically optimized BCMA/CS1 bispecific CAR-T cells robustly control heterogeneous multiple myeloma. *Nat. Commun.* **11**, 1–13 (2020).

83. Wang, D. *et al.* In vitro tumor cell rechallenge for predictive evaluation of chimeric antigen receptor T cell antitumor function. *J. Vis. Exp.* (2019) doi:10.3791/59275.

CHAPTER 5. Future Outlook

In this dissertation, we demonstrate that the TGF-β CAR can be expressed in T cells without inducing counterproductive outgrowth of suppressive Tregs or hindering proper immunological synapse formation. In addition, TGF-β CAR-T cells are well-tolerated in murine models. These findings support the viability and safety of the TGF-β CAR as a receptor platform to enhance therapeutic efficacy of adoptive T-cell therapy. We evaluated multiple configurations pairing the TGF-β CAR with a tumor-targeting receptor, finding that co-expression of the TGF-β CAR with either a tumor-specific TCR or CAR produces sub-optimal T-cell function. In contrast, single-chain bispecific CARs can effectively pair tumor-targeting specificity with responsiveness to TGF-β. We demonstrate in multiple GBM models that bispecific IL-13Rα2/TGF-β CARs program robust anti-tumor function and in engineered T cells and promote an endogenous immune response to improve therapeutic efficacy.

Our findings leave a few outstanding questions that merit further investigation. First, although characterization of GBM tumors following adoptive cell transfer demonstrates that bispecific IL-13Rα2/TGF-β CAR-T cells can favorably remodel the TME and mobilize endogenous anti-tumor immunity, the high degree of heterogeneity in GBM tumors likely warrants exploration of combination therapies that robustly promote epitope spreading. For instance, PD-1 expression on myeloid cells has previously been shown to be a major mechanism of immune suppression against adaptive immunity in GBM[1]. Our observation that PD-L1 was strongly upregulated in myeloid cells in the GL261 TME following CAR-T cell therapy suggests that PD-1/PD-L1 checkpoint blockade may have synergistic interactions with IL-13Rα2/TGF-β CAR-T cell therapy to unleash a more potent endogenous immune response.

Much of our efforts were directed towards evaluating the efficacy of IL-13Rα2/TGF-β CAR-T cells for treatment of GBM tumors, and several aspects of our study design were influenced by considerations of clinical translatability, including use of patient-derived GBM neurospheres and

use of human IL-13Rα2/TGF-β CAR constructs in immunocompetent mouse models. However, successful translation of bispecific IL-13Rα2/TGF-β CAR-T cells for clinical applications will require more rigorous study of potential TGF-β CAR-mediated toxicities. No evidence of toxicity was observed at the CAR-T cell doses that were tested, but it is still unknown whether high CAR-T cell doses would trigger adverse events. Dose-escalation studies would provide greater insight as to whether TGF-β CAR-T cells are safe regardless of dose, or if dose limitations exist. Combined with detailed histopathological analyses of a broader array of tissues, the proposed studies would provide more compelling evidence that TGF-β–responsive CAR-T cells can be safely administered.

Although enhancements to therapeutic efficacy are only demonstrated in the context of GBM in this dissertation, from a broader perspective, single-chain bispecific CARs responsive to TGF-β and tumor antigen should be applicable to other tumor types. Indeed, preliminary studies support the *in vivo* efficacy of bispecific TGF-β/PSMA CAR-T cells, although further optimization of the bispecific CAR structure may be warranted.

In considering generalizability, one treatment parameter that may have promoted bispecific IL-13Rα2/TGF-β CAR-T cell efficacy is the route of administration. Whereas engineered T cells were administered intravenously in our melanoma and prostate cancer models, T cells were injected intratumorally in our GBM model. Others have, in fact, demonstrated that locoregional delivery of CAR-T cells confers superior therapeutic outcomes compared to systemic delivery[2,3]. Combined with the fact that TGF-β CAR-T cell activation is dependent on cell density[4], it is plausible that effective re-wiring of TGF-β signaling requires a localized dose of bispecific IL-13Rα2/TGF-β CAR-T cells. By administering CAR-T cells in a concentrated bolus directly at the tumor site, IL-13Rα2/TGF-β CAR-T cells should be able to respond more robustly to TGF-β compared to intravenous infusion, where CAR-T cells can spread throughout the circulation. This density-dependent effect may also explain why no toxicity was observed when mice were given an intravenous dose of TGF-β CAR-T cells. It is worth noting that in clinical trials, IL-13Rα2 CAR-

T cells are administered intratumorally[5], and there is a growing body of work supporting locoregional CAR-T cell delivery for other solid tumor types[6]. A more systematic understanding of how TGF-β CAR signaling is impacted by the route of T-cell administration can help guide future study design.

Lastly, a detailed study interrogating signaling processes downstream of TGF-β CAR activation and T-cell exhaustion status may help shed light on several of our findings and guide future design choices. We hypothesize that TGF-β CAR co-expression with a tumor-specific TCR or CAR results in poor anti-tumor function because excessive signaling through the TGF-β CAR may drive T cells towards pre-mature exhaustion. The fact that both TGF-β– and tumor-binding extracellular domains must share a common signaling chain in a bispecific CAR, the possibility that ligand-binding may be sterically hindered, and the observation that bispecific IL-13Rα2/TGF-β CARs are downregulated from the cell surface all suggest that single-chain bispecific CARs transduce fewer activating signals in engineered T cells over time. We propose a systematic study evaluating different bispecific versus dual CAR configurations, with varying parameters including (but not limited to) type of co-stimulatory domain and inclusion of CAR modifications shown to tune signaling strength[7,8]. Such a study would aim to establish relationships between modes of receptor pairing, downstream T-cell signaling dynamics, and T-cell dysfunction, and ultimately reveal engineering principles for future iterations of paired TGF-β– and tumor-targeting receptors.

References

1. Antonios, J. P. *et al.* Immunosuppressive tumor-infiltrating myeloid cells mediate adaptive immune resistance via a PD-1/PD-L1 mechanism in glioblastoma. *Neuro-Oncol.* **19**, 796–807 (2017).

2. Brown, C. E. *et al.* Optimization of IL13Rα2-Targeted Chimeric Antigen Receptor T Cells for Improved Anti-tumor Efficacy against Glioblastoma. *Mol. Ther.* **26**, 31–44 (2018).

3. Theruvath, J. *et al.* Locoregionally administered B7-H3-targeted CAR T cells for treatment of atypical teratoid/rhabdoid tumors. *Nat. Med.* **26**, 712–719 (2020).

4. Chang, Z. L. *et al.* Rewiring T-cell responses to soluble factors with chimeric antigen receptors. *Nat. Chem. Biol.* **14**, 317–324 (2018).

5. Brown, C. E. *et al.* Regression of Glioblastoma after Chimeric Antigen Receptor T-Cell Therapy. *N. Engl. J. Med.* **375**, 2561–2569 (2016).

6. Cherkassky, L., Hou, Z., Amador-Molina, A. & Adusumilli, P. S. Regional CAR T cell therapy: An ignition key for systemic immunity in solid tumors. *Cancer Cell* (2022) doi:10.1016/j.ccell.2022.04.006.

7. Feucht, J. *et al.* Calibration of CAR activation potential directs alternative T cell fates and therapeutic potency. *Nat. Med.* **25**, 82–88 (2019).

8. Majzner, R. G. *et al.* Tuning the Antigen Density Requirement for CAR T-cell Activity. *Cancer Discov.* **10**, 702–723 (2020).